Lehrstuhl für Luftfahrtsysteme
Technische Universität München

Integration of turbofan engines into the preliminary design of a high-capacity short-and medium-haul passenger aircraft and fuel efficiency analysis with a further developed parametric aircraft design software

David Kalwar
LS-MA 15/02

LS-SA/DA lfd Nr.	Vertraulichkeit
LS-MA 15/02	Öffentlich
Titel (und Untertitel) Integration of turbofan engines into the preliminary design of a high-capacity short-and medium-haul passenger aircraft and fuel efficiency analysis with a further developed parametric aircraft design software	Autor David Kalwar
	Betreuer 1 Niclas Randt Technische Universität München
	Betreuer 2

Daten zur Abgabe und Korrektur der Studienarbeit:

15.04.2015	12.05.2015	28.05.2015
Abgabe der Erstfassung (Datum)	Rückgabe der korrigierten Erstfassung (Datum)	Abgabe der Endversion (Datum)

Bestätigung der Einreichung der abgeschlossenen Studienarbeit durch den Betreuer:

Ort, Datum	Unterschrift des Betreuers am LLS (Niclas Randt)

Anmerkungen:

Abstract

The growth of passenger numbers in air travel implicates challenges for regions and airports with limited air and ground capacities. Environmental concerns support the need for fuel-efficient aircraft. Research by the Institute of Aircraft Design of the Technische Universität München led to the development of a turboprop-powered high capacity aircraft for operation on short and medium range routes.
The recalculation of the initial concept led to the readjustment of the ambitious requirements. The limited availability of large turboprop engines is another challenge. A turbofan-powered variant is considered feasible. Various methods for the modeling and computation of turbofan engines are integrated into a design tool and feasibility are carried out. Current generation turbofan engines are chosen to power the aircraft. The aircraft is integrated into a fuel efficiency calculation tool according to the necessary parameters and functions to carry out fuel efficiency analyses compared with existing aircraft. Finally, the design tool is integrated into an aircraft design development environment.
A two- and a four-engined turbofan variant of the aircraft are created, both proving feasible. The performance is superior to that of the turboprop aircraft, with the four-engined turbofan variant showing a 4% better fuel economy. The aircraft concept outperforms existing aircraft on short missions. On longer missions, announced long-haul aircraft can match the fuel efficiency.
The work shows the feasibility of the aircraft with both turboprop and turbofan engines. The aircraft has potential to replace current aircraft on routes with high demand and limited airport capacities while improving fuel economy.

Zusammenfassung

Das Wachstum der Passagierzahlen im Luftverkehr impliziert Herausforderungen für Regionen und Flughäfen mit limitierten Kapazitäten in der Luft und am Boden. Umweltbelange unterstützen die Notwendigkeit, sparsame Flugzeuge einzusetzen. Forschungsarbeit am Lehrstuhl für Luftfahrtsysteme der Technischen Universität München führte zur entwicklung eines Turboprop-angetriebenes Flugzeugs mit hoher Kapazität für den Betrieb auf Kurz- und Mittelstrecken.
Die Neuberechnung des ursprünglichen Konzepts führte zu einer Nachjustierung der ehrgeizigen Anforderungen. Die begrenzte Verfügbarkeit von großen Turbopropriebwerken ist eine weitere Herausforderung. Eine Turbofan-angetriebene Variante gilt als realisierbar. Verschiedene Methoden zur Modellierung und Berechnung von Turbofan-Triebwerken werden in ein Design Tool integriert und Machbarkeitsstudien für durchgeführt. Turbofan-Triebwerke aktueller Generation werden ausgewählt, das Flugzeug anzutreiben. Das Flugzeug wird Anhand der erforderlichen Parameter und Funktionen in ein Kraftstoffeffizienz-Berechnungstool integriert, um Kraftstoffeffizienzanalysen im Vergleich zu existierenden Flugzeugen durchzuführen. Schließlich wird das Design Tool in eine Flugzeugentwurfs-Entwicklungsumgebung integriert.
Eine zwei- und eine viermotorige Variante des Turbofan-Flugzeugkonzepts wird erstellt, die sich beide als machbar erweisen. Die Leistung ist besser als die der Turboprop-Flugzeuge, wobei die viermotorige Turbofan-Variante einen 4% niedrigeren Kraftstoffverbrauch zeigt. Das Flugzeug übertrifft existierenden Flugzeugen auf kurzen Strecken. Auf längeren Strecken kommen angekündigte Langstreckenflugzeuge gleichauf.
Die Arbeit beweist die Machbarkeit des Flugzeugs mit Turboprop- und Turbofan-Triebwerken. Das Flugzeug hat das Potenzial, aktuelle Flugzeuge auf Routen mit hoher Nachfrage und Flughäfen mit begrenzten Kapazitäten zu ersetzen, und dabei den Kraftstoffverbrauch zu reduzieren.

Contents

List of Figures

List of Tables

List of acronyms

ADDAM	Aircraft Design DAta Model
ADEBO	Aircraft DEsign BOx
AEO	All Engines Operative
APF	Airline Procedure File
ARC	Aerodrome Reference Code
ATC	Air Traffic Control
BADA	Base of Aircraft Data
CAS	Calibrated Airspeed
CFRP	Carbon Fibre Reinforced Plastic
EIS	Entry Into Service
ETOPS	Extended-range Twin-engine Operational Performance Standards
FAA	Federal Aviation Administration
FCECT	Fuel Consumption and Emissions Calculation Tool
HCACDT	High Capacity Aircraft Design Tool
ICAO	International Civil Aviation Organization
IDT	Integrated Design Tool
LTO	Landing and Take-Off
MTOW	Maximum Take-Off Weight
MSL	Mean Sea Level
MZFW	Maximum Zero Fuel Weight
OME	Operating Mass Empty
OPF	Operations Performance File
PAX	Passengers

PSFC	Power Specific Fuel Consumption
ROCD	Rate Of Climb or Descent
SEP	Specific Excess Power
SFC	Specific Fuel Consumption
TAS	True Airspeed
TSFC	Thrust Specific Fuel Consumption
UML	Unified Modeling Language

CHAPTER 1

Introduction

The continuous growth of passenger numbers in the air transport industry are a challenge to airlines and infrastructure as well as aircraft manufacturers (ICAO, 2013a). While the current answer to the increasing demand is the introduction of more flights on the respective route or the replacement of small single-aisle aircraft by medium sized single-aisle aircraft, the infrastructure of some airports will reach a point where no additional take-offs and landings are possible. To solve this problem, aircraft manufacturers like Airbus and Boeing invest in expanding the capacity of their current single-aisle airframes like the A320 family and the Boeing 737 (AIRBUS, 2014) (Boeing, 2014a) (Hamilton, 2014). Additional studies showed that especially in Asia, single-aisle aircraft are replaced by medium to long haul aircraft on short to medium haul routes, as aircraft with high passenger capacity designed for short to medium haul routes are not available (AIRBUS, 2014c). An answer to this demand is the announcement of the Airbus A330 regional, a version of the A330 optimized for short to medium haul routes (AIRBUS, 2013). The aircraft is supposed to have a lower Maximum Take-Off Weight (MTOW) as less fuel tanks and thus less powerful engines are needed (Hamilton, 2013).

At the Institute of Aircraft Design of the Technische Universität München, the potential benefits of a high-capacity aircraft designed for short- to medium-range routes are investigated. Iwanizki et al. have developed a concept of a turboprop-powered transport aircraft for 420 passengers with a design mission range of about 3,000 km, dubbed 'Propcraft P-420' (Iwanizki, 2014), (Iwanizki et al., 2014). Key design requirements were chosen for operation in this market. In the next step, Kügler used handbook methods to create a MATLAB-based design tool called IDT which calculates and analyzes the performance of the aircraft concept. The result of his work was a slightly altered version of the P-420, dubbed 'P-420/B', as the initial requirements could not be met (Kügler, 2014). A detailed description of the P-420 versions is given in chapter 2.

In this thesis, the integration of jet engines into the P-420 is investigated. The focus lies on the minimum necessary performance as well as the overall mission fuel consumption. On top of that, operational aspects are discussed. Furthermore, the fuel efficiency of the P-420 is analyzed and compared to existing aircraft on a variety of missions. Finally, the IDT is integrated into the ADEBO development environment of the Institute of Aircraft Design.

The thesis is divided into eight chapters with the following content:

Chapter 2 introduces the history of the development of the P-420/A and /B aircraft concepts. The IDT is introduced and analyzed. Furthermore, some drawbacks of the IDT are changed and the requirements for the following chapters of the thesis are defined.

In chapter 3, an introduction to the fundamental theory of the thesis is given for a better understanding of the theory and models that are used in this thesis. This includes the basics on point mass modeling, as this method is used for aircraft performance modeling. Moreover, the principles of jet engines is summed up, as well as the specific fuel consumption. Finally, the theory for fuel efficiency calculations and analysis are introduced.

Chapter 4 introduces the integration of jet engines into the existing P-420 aircraft concept. Advantages and disadvantages of jet engines versus turboprop engines are discussed. Necessary changes to mass estimation and aerodynamics calculation are introduced. For performance analysis, different models are integrated and analyzed. Finally, jet engines are chosen and the overall aircraft performance is analyzed.

In chapter 5, the approach to fuel efficiency analysis is explained. First, the method of comparing aircraft and the software is introduced. Then, the generation of the necessary dataset of the aircraft is explained. In a third step, the fuel economy of the different P-420 versions is compared to existing aircraft on different missions. Lastly, the results of the analysis are discussed.

In chapter 6, a sensitivity analysis of the P-420 aircraft is performed. First, the sensitivities are identified and mission characteristics defined. Finally, the results are presented and discussed.

Chapter 7 provides an overview of the implementation of the IDT into the ADEBO development environment of the Institute of Aircraft Design.

The results as well as the performance of the newly created aircraft are summed up in chapter 8. A short outlook is given on future investigations which will help to further improve the aircraft concept.

CHAPTER 2

The Propcraft P-420 aircraft concept

During the research on the environmental impact of commercial air transport at the Institute of Aircraft Design of the Technische Universität München, it was decided to investigate the performance of a high-capacity aircraft designed for the operation on short- to medium-range routes. From this idea, the concept of the P-420 was born, developed by Iwanizki et al. The P-420 is a double-deck aircraft with turboprop engines. It was designed to carry a payload of 420 PAX and 5 tons of cargo over a design range of approximately 3.500 km (Iwanizki, 2014). To analyze and validate the performance of the P-420 concept, a MATLAB-based software tool was written. The IDT was designed by Kügler and provides detailed handbook methods for aircraft design and performance calculation (Kügler, 2014). The IDT makes it possible to carry out fast and simple trade studies of the overall preliminary aircraft design. The initial P-420, now dubbed P-420/A, was analyzed and some issues were found, which resulted in its modification and creation of the P-420/B.

In this chapter a description of the P-420 concept is given as well as the specifications of the design requirements. The IDT is introduced and analyzed, leading to the modification of the P-420/B into the P-420/C. Finally, trade-studies on the P-420/C are carried out and the design requirements for the course of this thesis are set.

2.1. Development of the initial aircraft concept

The information in this section follow the summary of Iwanizki's work by Kügler (Kügler, 2014).

2.1.1. Market analysis and requirements

In order to find the right requirements and needs for the concept aircraft, Iwanizki et al. performed a profound market analysis. The analysis was based on the global market forecasts provided by the two largest aircraft manufacturers Airbus and Boeing, a flight data collection from OAG (2014) as well as the comparison of historical and existing aircraft of a similar category.

It was found that the global air transport volume is expected to grow continuously. Additionally, the need to replace current aircraft by newer generations is mostly driven by better fuel efficiency. The need for a high-capacity aircraft designed for short to medium routes was derived from the high average aircraft capacity on intra-regional routes in Asia. Also, hub-and-spoke networks in Europe and other regions support these findings, as feeder flights between some airports need large passenger capacities.

The analysis of the OAG database, which includes all worldwide scheduled flights of June 2008, showed that about 90 % of all flights (excluding long-range flights) cover distances of 3,000 km or less, with single-aisle aircraft operating most of these routes. However, a significant number of long-range aircraft were found to be operated on routes within Asia.

The technical feasibility of a high-capacity turboprop aircraft for short to medium range operations was proven with the comparison of similar aircraft such as the Canadair CL-44, Tupolev Tu-114, Lockheed L-188, and Antonov An-10 as passenger transports in addition to the Antonov An-70 and Airbus A400M as military transport aircraft. Additionally, the feasibility of turboprop engines with a power in the category of about 10 MW was proven with the examples of the Iwtschenko Progress D-27 and the Europrop International TP400.

On the basis of this research, the passenger capacity of the aircraft concept was chosen to replace roughly two units of current generation single-aisle mid-range aircraft like the Airbus A320 or Boeing 737, resulting in a passenger capacity ranging from 300 to 500 PAX. A minimum cargo of 5 tons was defined, and the design mission range set to 3,000 km to enable the aircraft to perform on 90 % of the currently operated regional flights.

The aircraft concept should be enabled to be operated in developing countries with underdeveloped airport infrastructure. This lead to the ambitious choice of the an International Civil Aviation Organization (ICAO) Aerodrome Reference Code (ARC) of 3D and an Federal Aviation Administration (FAA) Airport Index of C (ICAO, 2013b) (FAA, 2011). The ARC 3D translates into a maximum wingspan of 52 m and maximum runway field length of 1,800 m. The Airport Index C limits the fuselage length to 48.46 m. All requirements are listed in table 2.1.

2.1.2. Summary of the P-420/A concept

Based on the requirements described above, an aircraft concept called 'Propcraft P-420/A' was developed with a prospected Entry Into Service (EIS) in 2025.

Passenger capacity	300 - 500
Cargo capacity [t]	$\geq$ 5
Range of standard mission [km]	$\geq$ 3,000
ICAO Aerodrome reference code	3D
Field length [m]	1,200 - 1,800
Wing span [m]	<52
ICAO Airport Index	C
Fuselage length [m]	<48.46

Table 2.1.: Summary of requirements for the P-420/A. Source: Iwanizki et al. (2014)

The P-420/A has a conventional aircraft layout, consisting of double-deck fuselage, low-mounted wings and a tail. It is powered by four large turboprop engines with dual-rotating, pulling propellers. The wingspan with 51.65 m and the fuselage length with 47.7 m meet the minimum requirements. The aircraft concept provides a seating capacity of 420 PAX in a double-deck twin-aisle layout. Doors and emergency exits are located in a way that grants fast boarding and evacuation. A cargo deck with a maximum capacity of 16 LD3-containers is located below the main passenger deck. Figure 2.1 shows a three-view drawing of the aircraft concept.

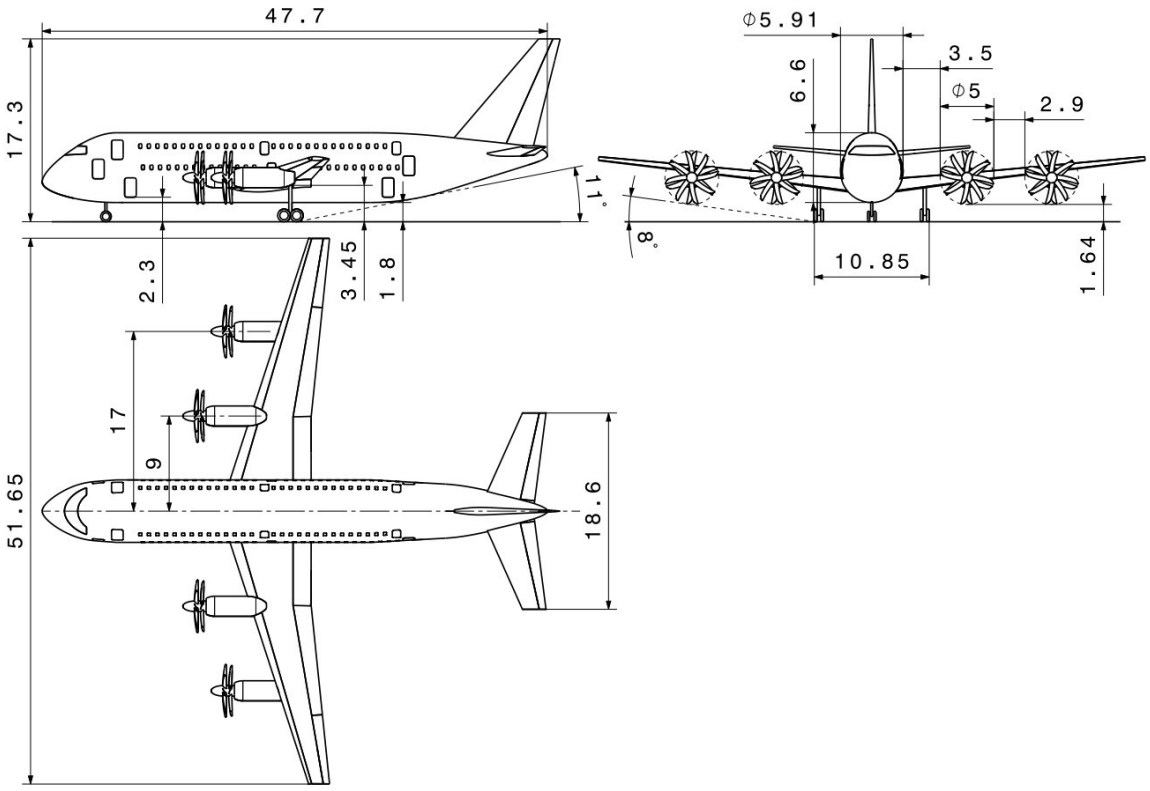

Figure 2.1.: Three-view drawing of the Propcraft P-420/A. Source: Iwanizki et al. (2014)

2.1.3. Design mission

A design mission was introduced to evaluate the performance of the P-420/A aircraft concept. The design mission, shown in figure 2.2, consists of the taxi-out, climb, cruise, descent and taxi-in phases, plus the diversion and loiter phase which is required for certification. Speeds and altitudes are set according to the performance of the aircraft.

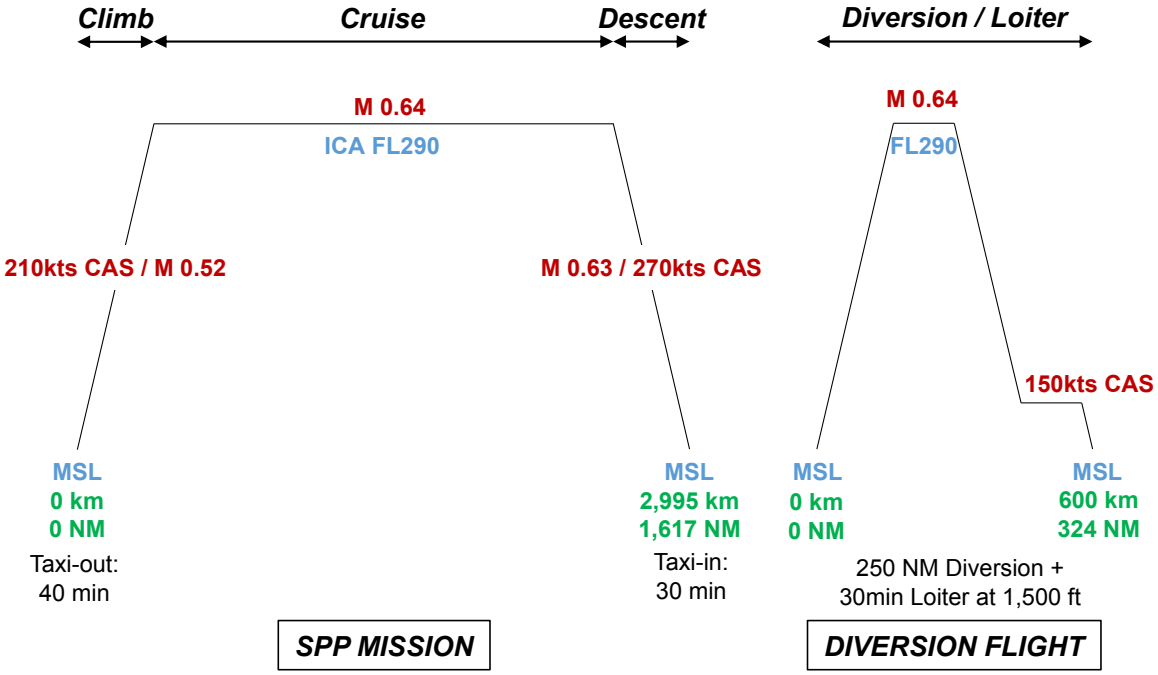

Figure 2.2.: Design mission of the Propcraft P-420/A. Source: Randt (2014a)

In addition, fuel efficiency analyses were carried out to evaluate the efficiency of the aircraft. The theoretical fuel efficiency as suggested by Randt was introduced (Randt, 2014a). The method uses the publicly available MTOW and the Maximum Zero Fuel Weight (MZFW). It is assumed that the difference between the MTOW and the MZFW equals the available fuel mass for a mission with maximum payload, including the necessary reserves. The theoretical fuel efficiency TFE is, as shown in equation 2.1, defined as the amount of fuel (in liters) divided by the maximum payload $M_{PLD,max}$ and the attainable range at maximum payload $R_{PLD,max}$. These two values are generally available for civil aircraft from their respective payload-range diagrams.

$$TFE = \frac{(MTOW - MZFW)\,/\rho_{fuel}}{M_{PLD,max} \cdot R_{PLD,max}} \tag{2.1}$$

A value of 0.212 l/t/km was calculated for the baseline P-420/A concept. Figure 2.3 shows the payload-range diagram of the concept, which could reach a range of 3,460 km at its design payload of 420 PAX and 5 tons of cargo. Additional calculations showed the feasibility of the take-off requirements limited by the ICAO ARC.

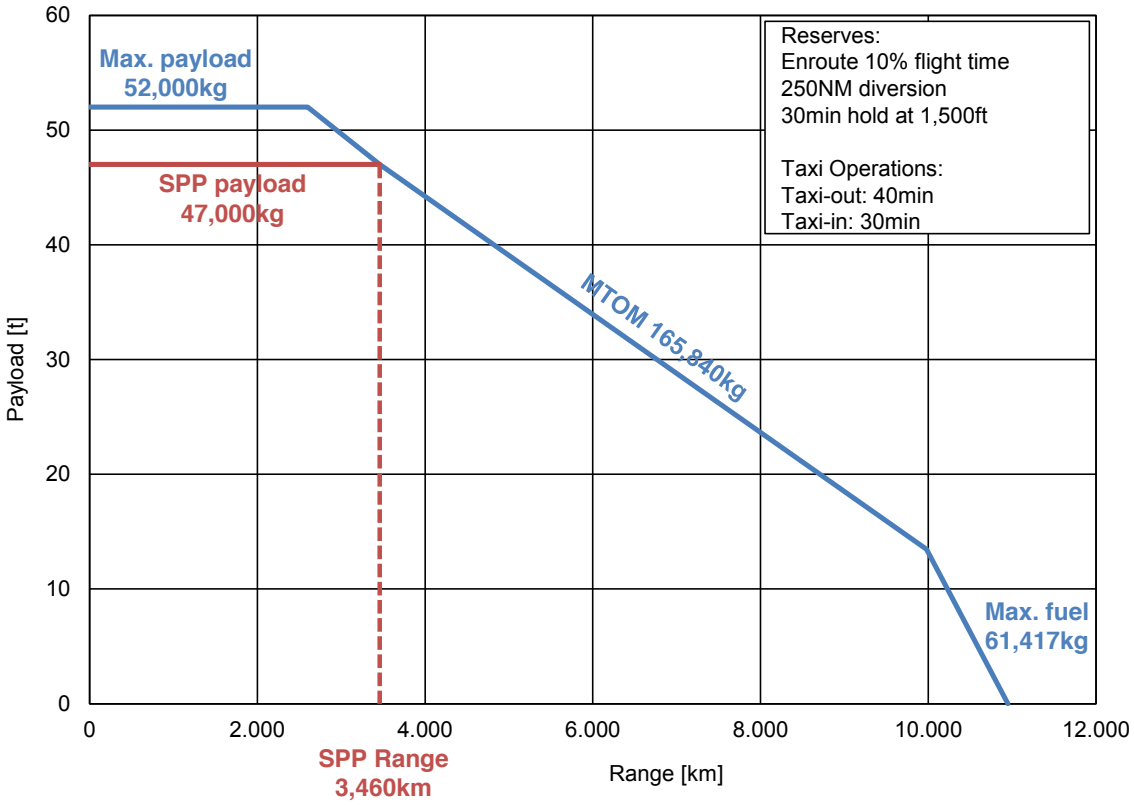

Figure 2.3.: Payload-range diagram of the Propcraft P-420/A. Source: Randt (2014a)

2.2. Development of an integrated design tool and modification of the P-420/A

2.2.1. Introduction of the IDT

In order to reevaluate the calculations and estimations performed in the initial design of the P-420/A, the IDT was developed by Kügler (2014). The tool was designed specifically for the application case of the P-420 high-capacity turboprop concept.

The IDT makes use of a set of essential input parameters and estimates masses, computes the aerodynamic properties and models the propulsion characteristics. In a final step, the overall estimated aircraft performance is calculated and analyzed by performing a full mission as specified in the design mission. The IDT makes use of different methodological approaches to aircraft design described in common aircraft design literature, giving the user an in-depth view of the different results of these methods.

The IDT is implemented in the MATLAB environment (release 2013a). The tool consists of a main file called 'design_tool.m', containing the main code of the IDT and is structured into different sections. Some repeatedly needed algorithms are implemented in separate function files and called by the main script when needed.

The sections of the main file are the following:

- Aircraft concept definition: First, the aircraft concept which is to be investigated is specified with a set of parameters, e.g. geometrical, aerodynamic and mission parameters. After this, the tool automatically computes further parameters like the aspect ratio or the mean aerodynamic chord.
- Mass estimation: In this module, the mass is estimated with the help of four different detailed aircraft mass estimation methods, each written in a sub-function. These four methods were published by Raymer (1992), Torenbeek (1982), Torenbeek (2013) and Howe (2000).
- Aerodynamics: This part computes all relevant parameters of the aerodynamics and estimates lift and drag. Again, methods of various authors, mostly Raymer (1992) and Howe (2000), are used.
- Propulsion: In this module, the performance of the turboprop engine and the propeller are modeled, partly in sub-functions. The methodology used here is based on both published modeling practices as well as the result of the analysis of existing engine data.
- Aircraft performance analysis: This final module makes use of the results of the other modules, modeling and estimating the aircraft performance characteristics. In addition to the simulation of a full design mission, operating limitations are evaluated.

The output of the IDT analysis results is presented in two ways. Many of the important values are displayed directly in the MATLAB Command Window. Additionally, further plots and diagrams are created and opened in separate windows.

Figure 2.4 shows the detailed flowchart of the IDT including all modules and calculation methods.

2.2.2. The P-420/B

The reevaluation of the P-420/A with the IDT showed that while most of the parameters were in a reasonable range as expected and calculated by Iwanizki et al., some parameters showed significant differences and some of the ambitious requirements could not be met.

The requirement of the ICAO ARC could not be met, as the balanced field length and the second segment climb in the case of one engine inoperative (refer to section 3.4) of the P-420/A were too high. Both requirements could not be met with the P-420/A configuration as the drag in this configuration was calculated significantly higher leading to longer field length and smaller climb angles.

Additionally, the projected mission range could not be met due to higher fuel consumption than expected by Iwanizki. Other deviations were a higher OME than expected by Iwanizki, different aerodynamic coefficients, as well as propeller rotating speed and efficiency.

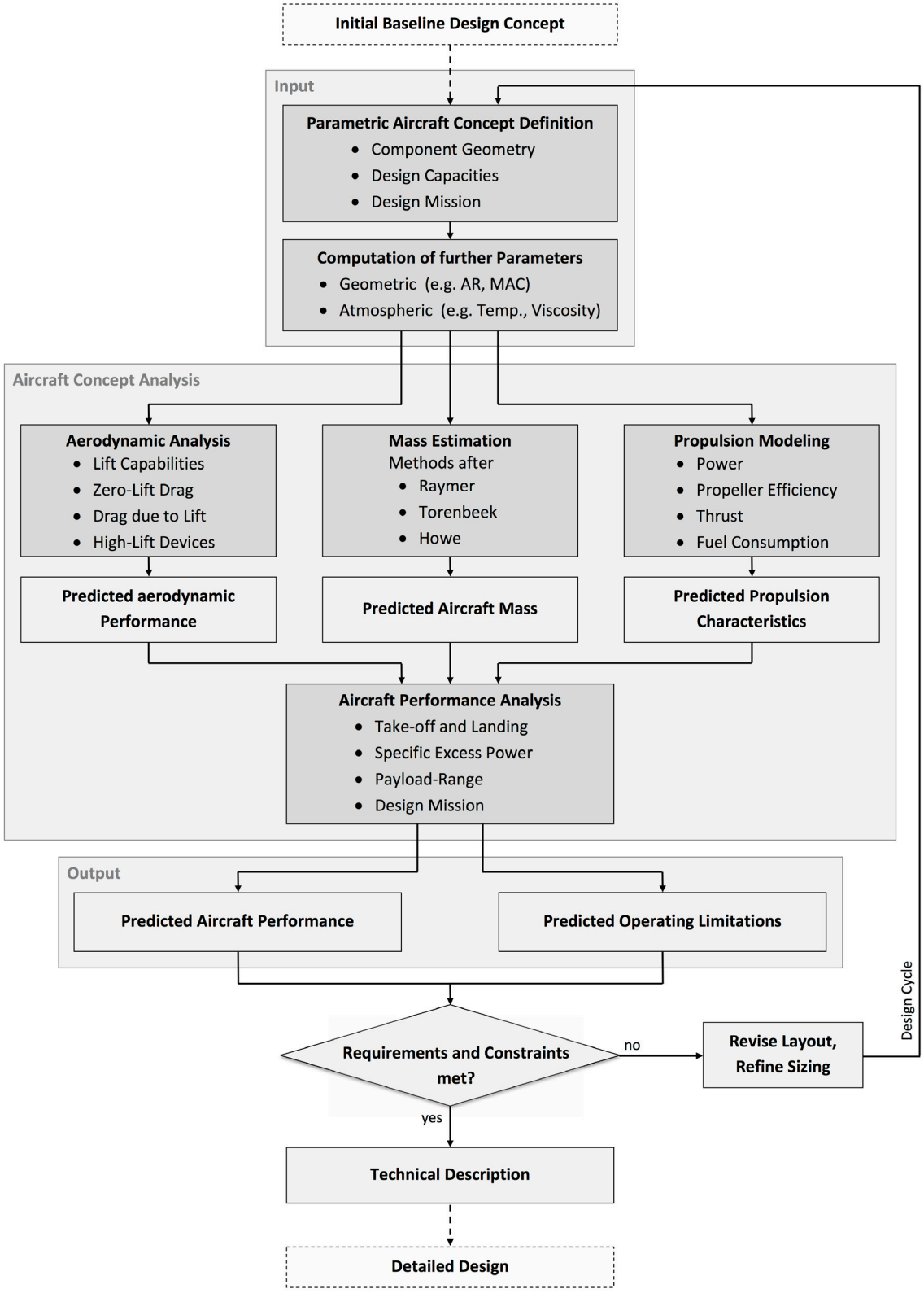

Figure 2.4.: Flowchart of the IDT. Source: Kügler (2014)

As a consequence of these findings, the ICAO ARC requirement of '3D' had to be dropped and was changed to category '4D', allowing for a higher balanced field length as shown in table 2.2.

Passenger capacity	420
Maximum cargo capacity [t]	10
Range of standard mission [km]	3000
ICAO Aerodrome reference code	4D
Field length [m]	>1800
Wing span [m]	<52
ICAO Airport Index	C
Fuselage length [m]	<48.46

Table 2.2.: Summary of the technical features for the P-420/B, derived from the changed requirements of the P-420/A. Source: Kügler (2014)

Additional to these new requirements, Kügler found other parameters to improve the P-420/A, which, in summary, lead to the creation of the P-420/B.

The maximum torque of the engine was raised, which increased the available power during the second segment climb by about 5 %. Additionally, a fudge factor was introduced to improve the efficiency of the propeller during cruise flight to values of about 90 %, which is also claimed by the manufacturers of the baseline propeller, the SV-27 by Aerosila (Aerosila, 2005). Furthermore, the engine fuel consumption was revised with the help of data available of the TP400 turboprop engine of the Airbus A400M military transport aircraft. Finally, the design mission was optimized for lower fuel burn by increasing climb and loiter speeds as well as reducing the diversion distance, which was initially set for long-distance aircraft, but is not necessary for the P-420. The revised design mission is shown in figure 2.5.

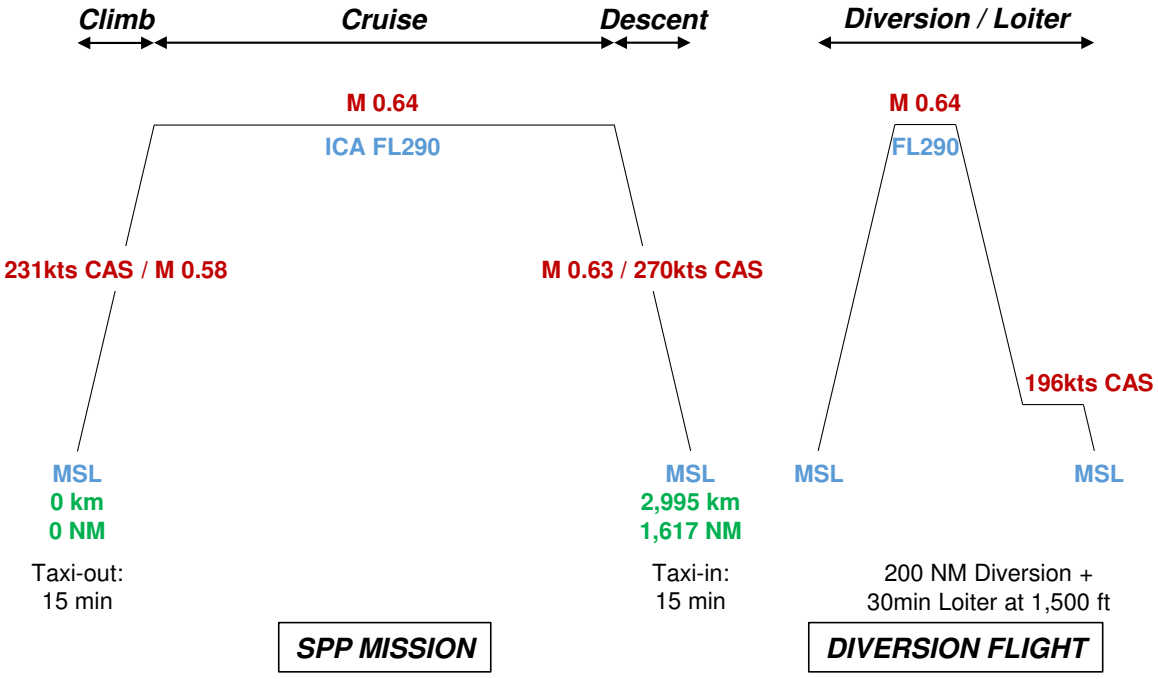

Figure 2.5.: Design mission of the Propcraft P-420/B. Source: Randt (2014b)

2.3. Trade studies

In the beginning of the work on this thesis, the IDT was used to perform trade studies on the P-420/B: This was done to get to know to the tool as well as to understand the impact of small changes in the definition of aircraft parameters to the performance of the aircraft.

The trade studies were carried out with the idea of improving the performance of the P-420/B without altering the entire aircraft concept. One goal was to reduce aircraft mass and drag in order to improve performance especially on the critical balanced field length and the second segment climb.

The impact of changing the number of PAX by $\pm$ 20 was negligible. The MTOW was iterated slightly different, however the impact on the performance was very small. Changing the airspeed of the aircraft in cruise proved to increase drag and thus fuel consumption, both for increasing and decreasing the airspeed. The airspeed was already chosen to be at the point of minimum drag and thus optimal.

When switching the turboprop engines from the D-27 to the TP400 with their respecting propellers, it was found that changing the propeller from a dual-rotating propeller like SV-27 by Aerosila to a single row propeller like the FH386 of the TP400, the MTOW would reduce dramatically, which improves especially the field performance. However, due to the fixed implementation of the propeller efficiency function of the IDT, the change in propeller efficiency, which is expected to decrease, was not further analyzed.

Another study performed was the increasing of the wing span to 60 and 65 m while maintaining the wing area, subsequently increasing the aspect ratio of the wing. The impact of this change was a greatly improved field performance with less engine power required, as the aerodynamic efficiency was increased. However, this change would break the ICAOARC category as defined by the requirements for the P-420/B. It showed however, that improving the aerodynamics of the aircraft, e.g. by introducing winglets or foldable wing tips to the wing is an interesting field of study for the further development of the P-420 aircraft concept. The announced Boeing 777X will be outfitted with 3.5 m long foldable wing tips, increasing the total wing span by 7 m from 64.8 m to 71.8 m while staying in the same ICAO ARC (Steinke, 2015). Torenbeek also suggest winglets as a mean of drag reduction for aircraft with constrained wing span (Torenbeek, 2013, p. 312). However, this is not in the scope of this thesis.

2.4. Analysis and modification of the P-420/B and the IDT

The analysis of the IDT and the P-420/B showed some inaccuracies in the calculation. These are foremost the mass of the propellers and the taxi power setting of the engine, both increasing the aircraft mass. These weaknesses have been overcome with simple adjustments of the IDT and the creation of the P-420/C.

2.4.1. Propeller mass estimation

The first inaccuracy is the mass of the propellers, which is estimated after Torenbeeks calculation method with 12,288 kg total or 3,072 kg per propeller. The datasheet of the SV-27, which is the baseline model for the P-420/B propeller, however states a weight of 1,100 kg per propeller (Aerosila, 2005). In comparison, the FH386, the propeller of the TP400-D6 engine produced by Ratier-Figeac, has a weight of 683 kg (EASA, 2012). As the propeller of the P-420 has a different diameter than the two versions, a factor F_P is introduced to estimate the weight of this propeller. The factor F_P represents the mass per meter of diameter d_P and number of blades N_B of the propeller.

$$F_P = \frac{m_P}{N_B d_P} \tag{2.2}$$

The factors for both the FH386 of 16 and SV-27 of 17.5 are in a similar range, which gives an indication that this simple approach is feasible for propellers of this size. As the propeller of the P-420 is based on the SV-27, the factor 17.5 is chosen to calculate the weight of the propeller. The weight turns out to be 1,225 kg, about 125 kg heavier than the original SV-27 which has a smaller diameter. The total weight of the four propellers now account to 4,900 kg in comparison to the estimated 12,288 kg of Torenbeek - about 60 % or 7,400 kg less.

Parameter	FH386	SV-27	P-420/B	P-420/C
Weight [kg]	683	1,100	3,072	1,225
Diameter [m]	5.334	4.5	5	5
Number of blades	8	14	14	14
Factor	16	17.5	43.9	17.5

Table 2.3.: Propeller mass estimation using a revised propeller mass factor derived from existing large diameter propeller systems. Data sources: Aerosila (2005), EASA (2012), Randt (2014b)

2.4.2. Taxi power settings

The second inaccuracy of the IDT is the taxi power, which Kügler assumed to be at 60% of total power available. This assumption is made with a reference of Bräunling, who assumes that the propeller speed reaches 60 % during idle (Bräunling, 2009, p. 300). After this, the aircraft consumes about 100 kg of fuel per minute of taxi. However, propeller speed does not translate linearly into engine power. The ICAO Landing and Take-Off (LTO) cycle assumes a thrust setting of 7 % for the LTO cycle calculation, which is widely accepted as a standard emissions calculation (International Civil Aviation Organization, 2008). In order to make a reasonable but conservative approach, the taxi power setting is reduced to 10 % for the P-420/C, which reduces the fuel consumption to about 17 kg per minute of taxi.

This and the propeller mass reduction lead to a reduction of the OME, as the lower propeller mass reduces the overall aircraft mass, shown in table 4.9. Additionally, the mission fuel is lower because of the much less necessary taxi fuel. The lower mass initiates a down-scaling spiral in which the fuel consumption drops which again leads to less mission fuel, with final values shown in table 4.10. No other changes to the P-420/B were made. The P-420/C is an additional variant of the P-420 during the course of this thesis.

2.4.3. Limitation of the ROCD

Another flaw that was found in the IDT was the missing limitation of the Rate Of Climb or Descent (ROCD). With the limited power of the P-420/B, the ROCD never reached values that are out of the usual operating limits in actual aircraft operations. However, the power of jet engines during climb led the performance calculation part of the IDT climb at rates that are not reached in the operating limits of passenger transport aircraft. A routine was introduced that limits the ROCD to values defined by the user, which are set to standard values of 3,000 ft/min during climb and 3,500 ft/min during descent.

2.4.4. Usability of the IDT

An additional weakness of the IDT was identified while performing the trade studies and implementing the changes to integrate jet engines regarding the usability of the tool. The original software tool is a collection of MATLAB files and sub-functions that carry out the calculation. Although the IDT is divided in a part where the aircraft input parameters are defined, and parts that calculate initial parameters, mass, aerodynamics, propulsion and the performance analysis, these were kept in a single large MATLAB file. In order to increase clarity and usability of the tool, these sections were put into separate files. Additionally, a starting file was created that first calls the new aircraft definition file containing all input variables describing the aircraft and its design mission and then the separate calculation files. Additionally, it is now possible to activate or deactivate the generation of figures, a new output file, and the BADA file generator.

2.5. Definition of requirements

With the analysis and modification of the IDT, the P-420/B and its alteration into the P-420/C, the foundation for the creation of variants of the P-420 concept with jet engines is laid.

It was found that the requirements identified by Kügler for the P-420/B are a reasonable basis to further develop the P-420 powered with jet engines. The change of the ICAO ARC was considered as the trade studies showed the possibility of greatly improved aerodynamics. However, this would put the P-420 into the same

category with modern long-haul jets. For regional operations, the limitation of the wing span is accepted as a reasonable drawback. In conclusion, the requirements for the integration of jet engines into the P-420 were thus chosen to be the same as identified by Kügler for the P-420/B, presented in table 2.2. Additionally, this enables easy comparison between the different P-420 variants.

In addition to the requirements listed in table 2.2, a general requirement for all aircraft is a minimum climb angle in the second climb segment (see chapter 3.4) of 1.72° for four-engined and 1.38° for two-engined aircraft in the case of one engine inoperable.

CHAPTER 3

Theory

This chapter introduces the basic theoretical concepts needed to interpret the calculations and analysis performed during the course of this thesis. To this end, the principle of the point mass model are explained. Moreover, the mechanics of jet engine thrust and the specific fuel consumption are described.

3.1. Point mass model and total energy method

The point mass model and total energy method is the method used by the software further developed in this thesis and the FCECT which are used to analyze the performance and fuel efficiency of the P-420. The explanations in this section follow those made by Ittel in his work (Ittel, 2014).

The point mass model describes the assumption of the mass of the overall aircraft as a dimensionless point with a finite mass. Applied forces and torques are acting on this point mass. Several reference systems are used to describe the forces and torques, such as the flight-mechanical coordinate system B which is fixed to the body of the aircraft, the aerodynamic reference system A which is aligned with the direction of the True Airspeed (TAS), and the fixed flight path coordinate system K which is aligned with the kinematic velocities and the horizontal line of the earth. To describe the motion of a point mass, the system has to be simplified (Brockhaus et al., 2011):

- Rotatory degrees of freedom are neglected
- The aircraft only performs turns with a low curvature
- No influences of lateral forces, e.g. due to crosswinds
- The Earth E is considered flat and free of rotation
- The bank angle and the aerodynamic sideslip angle can be set to zero

- Pitch and azimuth are also equal to zero
- The engine installation angle is to be neglected
- No influence of wind and moderate angles of attack lead to the unity of the flight-mechanical coordinate system B and the fixed flight path coordinate system K

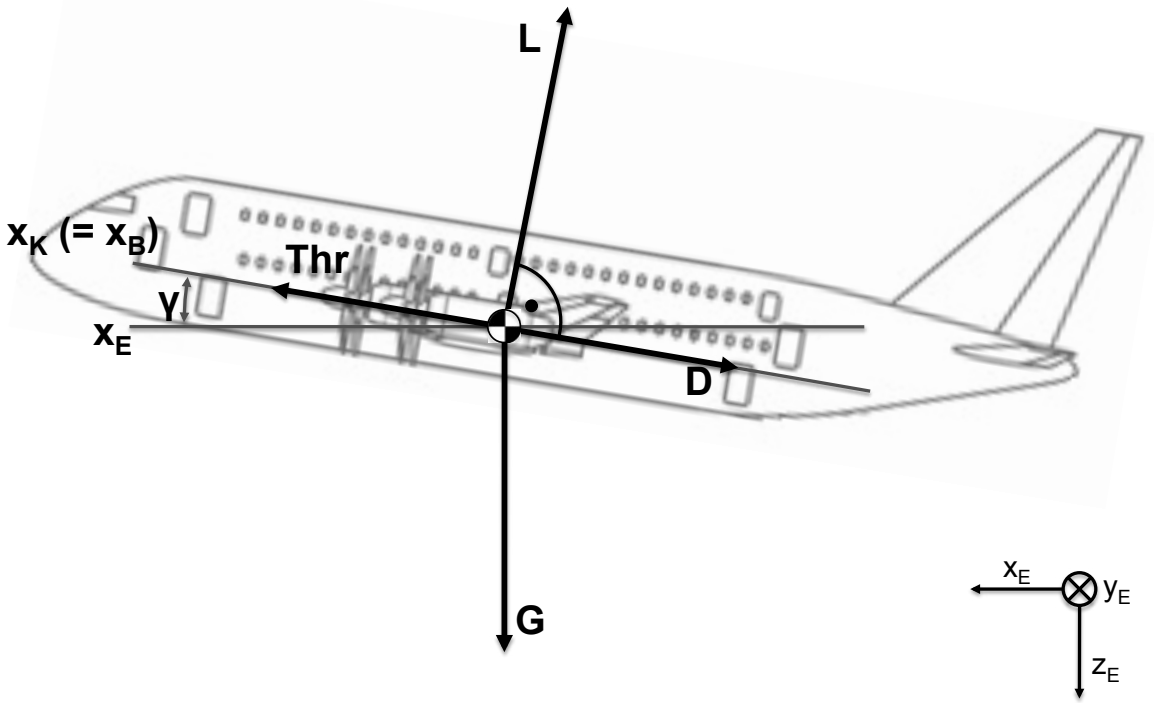

Figure 3.1.: Simplified flight dynamical system of forces. Source: Ittel (2014)

The simplified set of forces consists of the drag, thrust, lift and the gravitational force. These forces are vectors pointing in specific directions. The forces must be balanced in such a way that the aircraft can stay in constant motion or perform the desired maneuvers, e.g. accelerate, decelerate, climb and descent. The following equations describe the forces in the three dimensions:

$$x_K\ direction: \frac{dV_K}{dt} = \frac{Thr - D}{m} - g_0 \cdot sin\gamma \tag{3.1}$$

$$y_K\ direction: \frac{d\chi}{dt} = \frac{L \cdot sin\Phi}{m \cdot V_K} \tag{3.2}$$

$$z_K\ direction: \frac{d\gamma}{dt} = \frac{L}{m \cdot V_K} - \frac{g_0}{V_K} \cdot cos\gamma \tag{3.3}$$

Where Thr is the thrust, D is the drag, L is the lift, V is the velocity, m the aircraft mass and g_0 the gravitational acceleration of the earth.

The total-energy-model evaluates the total energy E_{total} of the aircraft consisting of the kinetic energy E_{kin} and the potential energy E_{pot}. Rotational energy is neglected.

The SEP of the aircraft is determined, which is defined as the time rate of change of specific energy, according to equation 3.4 to 3.7.

$$E_{total} = E_{pot} + E_{kin} = m \cdot g_0 \cdot H + \frac{1}{2} \cdot m \cdot V_{TAS}^2 \tag{3.4}$$

The division by the weight force gives the specific energy H^*

$$H^* = \frac{E_{total}}{m \cdot g_0} = h + \frac{1}{2} \cdot \frac{V_{TAS}^2}{g_0} \tag{3.5}$$

The derivative with respect to time gives the SEP:

$$SEP = \frac{dH^*}{dt} = \frac{dH}{dt} + \frac{V_{TAS}}{g_0} \cdot \frac{dV_{TAS}}{dt} \tag{3.6}$$

After relating the SEP to the forces of the aircraft, the equation looks like this:

$$SEP = \frac{dH}{dt} + \frac{V_{TAS}}{g_0} \cdot \frac{dV_{TAS}}{dt} = \frac{Thr - D}{m \cdot g_0} \cdot V_{TAS} \tag{3.7}$$

Both the IDT and the FCECT work with this equation to calculate the current SEP of the aircraft.

3.2. Jet engine thrust

This section introduces the basics of jet engine thrust generation and shows the differences to that of a turboprop engine. Jet engines can be categorized into turbojets and turbofan engines. As all modern passenger transport aircraft use turbofan engines, this section focuses on the turbofan engine.

The turbofan engine is a gas turbine engine which uses a gas generator as the core. This core consists of a compressor, combustor and a turbine. The gas generator core converts the internal energy of the fuel into kinetic energy of the exhaust gas. Turbofans have a large extra compressor, which is called the fan. The fan is powered by the turbine of the engine. A part of the air flow accelerated by the fan bypasses the gas generator core of the engine as shown in figure 3.2. This bypassed flow has a lower velocities, but a higher mass than the air flow passing through the gas generator core. This makes the thrust produced by the fan more efficient than thrust produced by the core. The ratio of the air flow mass that bypasses the core and the air flow mass that passes through the core is called bypass ratio.

The engine accelerates air which is then faster than the surrounding air. After Newtons third law, this is a force defined as (USAF Test Pilot School, 1991):

$$F = ma = m\left(\frac{dv}{dt}\right) \tag{3.8}$$

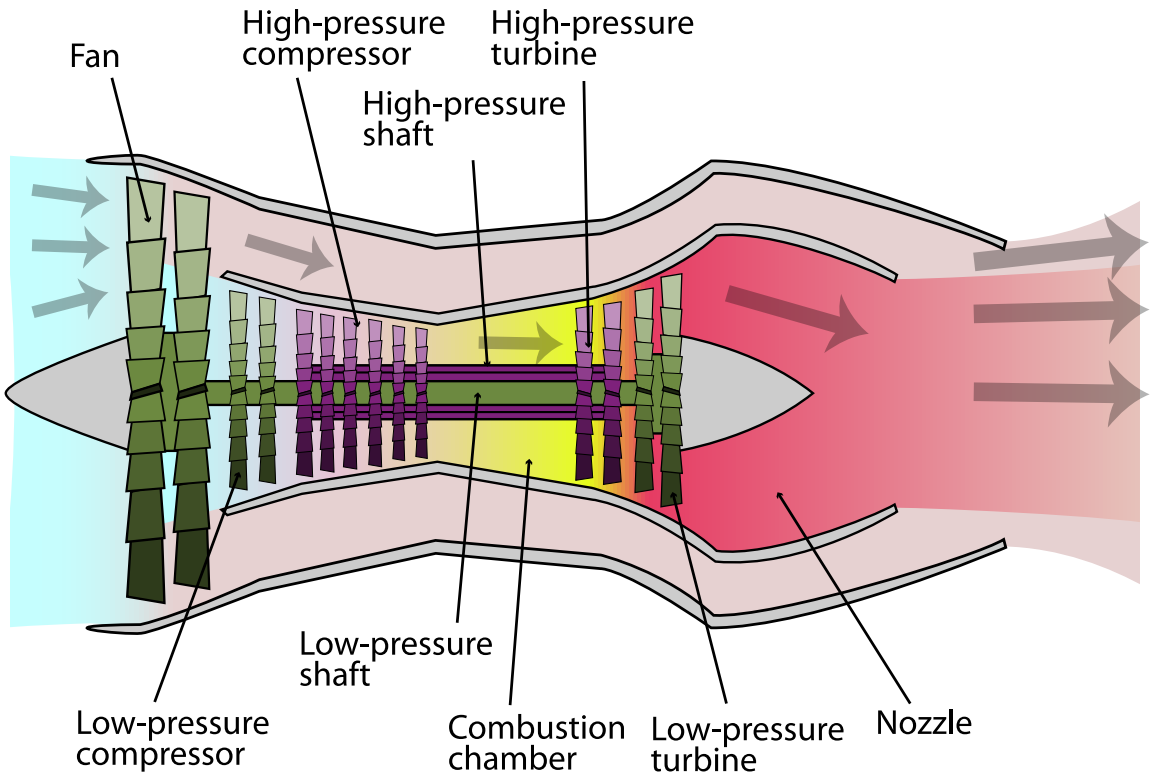

Figure 3.2.: Turbofan Schematic. Source: Wikipedia User 'Aainsquatsi' (2008)

A rearrangement gives the following:

$$F = \frac{d(mv)}{dt} = \frac{dm}{dt}(v_e - v_0) \tag{3.9}$$

Where e is the exit of the core and 0 the free stream entering the engine. With $dm/dt = \dot{m}$ and taking into account that the burned fuel adds to the mass of the air flow at the exit, this results in:

$$F = \dot{m}_e v_e - \dot{m}_0 v_0 \tag{3.10}$$

A turbofan gets some of its thrust from the core and some of its thrust from the fan. The flow through the fan is denoted as f, and the flow entering the core as c, resulting in $\dot{m}_0 = \dot{m}_f + \dot{m}_c$. The above thrust equation is used for each stream to obtain the total thrust:

$$F = \dot{m}_f v_f - \dot{m}_f v_0 + \dot{m}_e v_e - \dot{m}_c v_0 \tag{3.11}$$

As explained above, the ratio of the air flow mass that bypasses the core and the air flow mass that passes through the core is called bypass ratio BPR. Large, modern high-bypass-ratio turbofan engines like the Pratt & Whitney PW1000G engine family have a bypass ratio of up to 12 (Pratt & Whitney, 2014).

$$BPR = \frac{\dot{m}_f}{\dot{m}_c} \tag{3.12}$$

The above terms can be combined by multiplying V_0 and the use of the bypass ratio to obtain the final thrust equation of a turbofan engine:

$$F = \dot{m}_e v_e + BPR(\dot{m}_c v_f) - \dot{m}_0 v_0 \tag{3.13}$$

In turboprop engines, the gas generator core drives the propeller, usually via a gearbox. The largest part of the thrust of a turboprop engine is generated by the propeller, and only a small part by the accelerated core stream. As some of the total air flow entering the area of the engine and propeller flows through the gas generator core, turboprop engines also have a notional bypass ratio which is very high.

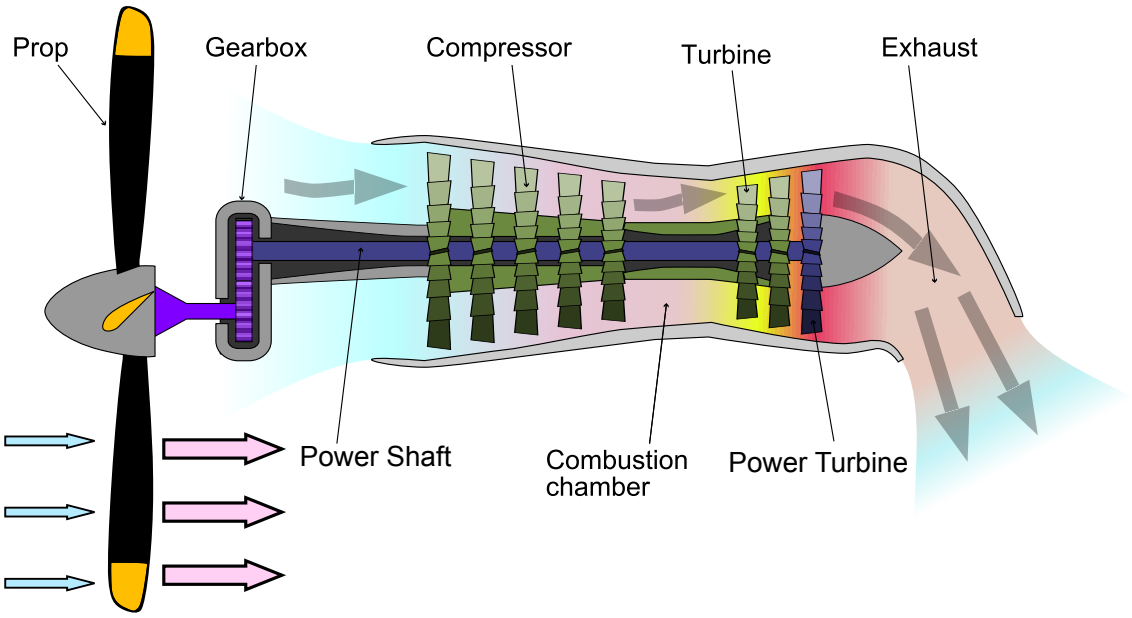

Figure 3.3.: Turboprop Engine Schematic. Figure based on: Wikipedia User 'M0tty' (2009)

The efficiency of a jet engine is defined by many factors. An important factor is the propulsive efficiency, which is defined as the following:

$$\eta_P = \frac{2v_0}{v_e + v_0} \tag{3.14}$$

As explained above and visible in equation 3.13, the fan moves more air mass but accelerates it by a smaller amount than the air flow which exits the core. This is more efficient in terms of propulsive efficiency as shown by equation 3.14.

Other factors are the thermal efficiency of the gas generator core, which converts the internal energy of the fuel into kinetic energy of the air flow. The efficiency of the gas generator core is limited by the maximum turbine entry temperature of the hot

exhaust gases due to the melting point of the used materials. Additionally, internal aerodynamic efficiencies of the rotating blades play a significant role.

Modern high bypass ratio turbofans minimize the gap between turboprops and turbofan engines. They can be almost as efficient as turboprop engines, because the fan is enclosed by the nacelle and is composed of many rigid blades, it can operate more efficiently at higher speeds than a propeller.

3.3. Specific Fuel Consumption (SFC)

This section introduces the concept of the SFC. The SFC is an important value to measure the efficiency of aircraft engines with respect to the thrust output. The fuel efficiency of jet engines is usually expressed as Thrust Specific Fuel Consumption (TSFC), while for turboprop engines, the Power Specific Fuel Consumption (PSFC) is used. Usually, SFC and TSFC are used as synonyms. Per equation 3.15, SFC describes the mass of fuel M_{fuel} per unit of time t needed to generate a unit of thrust T.

$$SFC = \frac{M_{fuel}}{T \cdot t} \tag{3.15}$$

The SFC is dependent on the engine design. More efficient engines have a lower SFC value as they burn less fuel to generate the same thrust. The SFC varies with the working environment of the engine, e.g. speed and altitude. SFC is expressed in $g/(kN \cdot s)$ in SI units or $lb/(lbf \cdot h)$ in imperial units.

Engine	Aircraft	SFC $[g/(kN \cdot s)]$	SFC $[lb/(lbf \cdot h)]$
CFM CFM56-5B4	Airbus A320	15.438	0.545
General Electric GE90-85B	Boeing 777-200	14.729	0.520
Pratt & Whitney JT8D-9	Boeing 737-200	22.661	0.800

Table 3.1.: SFC values in cruise flight of chosen aircraft engines. Data source: Meier (2005)

3.4. Takeoff Climb Gradient Requirements

In this section, the takeoff climb gradient requirements are discussed. These are requirements for any aircraft and are a dominant factor during preliminary aircraft design of civil transport aircraft. The requirements describe the minimum aircraft performance during takeoff and initial climb in the scenario of one engine inoperative. The remaining operative engine(s) must be able to provide enough thrust so that the requirements are met. The requirements are defined in regulatory documents from the FAA (Federal Aviation Administration, 2015).

The climb from the point of lift-off is divided into four segments, the 1st segment, 2nd segment, 3rd segment and final segment. Figure 3.4 visualizes all aircraft settings and conditions during the four segments and additionally the takeoff. Table 3.2 shows the minimum climb gradients necessary during the four climb segments.

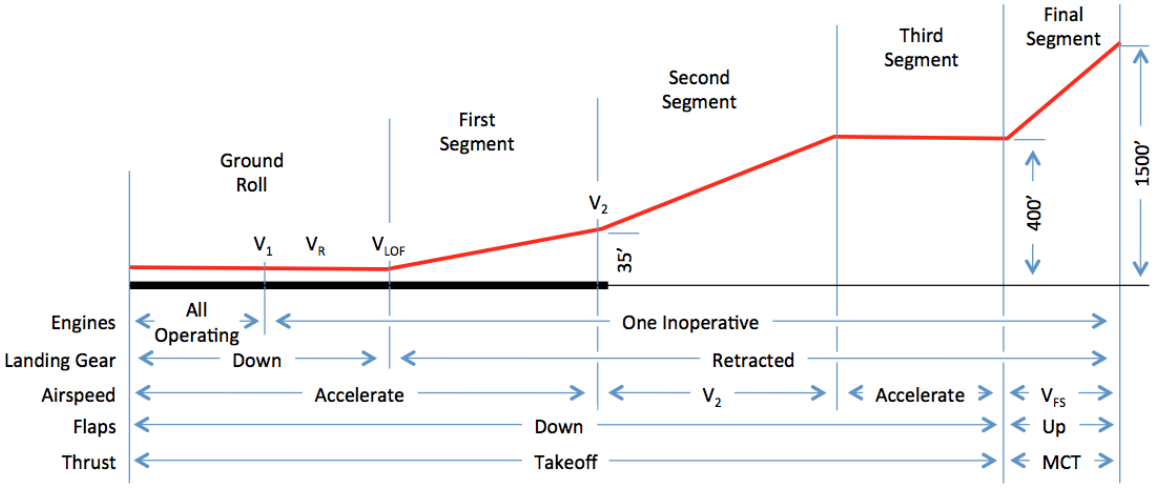

Figure 3.4.: Climb gradient segments and parameters. Source: Albright (2015)

The most interesting segment for this work is the second climb segment. In this segment, the aircraft must climb at a certain angle while maintaining a the takeoff safety speed V2. The value of V2 depends on the aircraft. Kügler found this climb segment to be the most critical, which is why the engine choice is tailored to fulfill this climb requirement.

Engines	1st Segment	2nd Segment	3rd Segment	Final Segment
2	Positive	2.4%	Positive	1.2%
3	3.0%	2.7%	Positive	1.5%
4	5.0%	3.0%	Positive	1.7%

Table 3.2.: Minimum climb performance during the different climb segments. Data source: Federal Aviation Administration (2015)

CHAPTER 4

Integration of turbofan engines into the P-420 aircraft concept

This chapter describes the integration of turbofan engines into the IDT. It explains the motivation too . Also, it discusses the advantages and disadvantages of the jet engine compared with the current turboprop configuration. An overview of the software modifications, namely in the calculation of mass, aerodynamics, engine thrust and SFC, and flight performance is given. Finally, aircraft flight performance is compared to the existing turboprop configurations.

4.1. Motivation

Multiple reasons support the choice integrating turbofan engines into the current turboprop aircraft design. The choice of propulsion type, configuration and model is fundamental for any aircraft. It touches all major aspects of preliminary aircraft design, namely structure, mass, aerodynamics and performance of the aircraft. To find the best possible solution, extensive studies of all possible configurations must be carried out. During the initial idea of designing the P-420, one of the requirements was that the aircraft should meet the ICAO ARC 3D, which implies a balanced field length of only 1,800 m. This category was chosen as the aircraft should also be able to land and take-off from airports with infrastructure limitations. To meet this requirement, a very large amount of static thrust and thrust during take-off is necessary. Additionally, the airspeed is not as important for short distance flights as the time saved by fast aircraft is comparably low to slower ones. These initial requirements led to the decision of very powerful turboprop engines with counter-rotating propellers.

As this requirement is directly linked to the size and capabilities of the propulsion system of the aircraft, the change of the requirements, which were introduced by Kügler, makes room for different approaches in engine choice. As most current generation aircraft use turbofan engines for their propulsion system, a large variety of engine models and types are available on the market today. Different turbofan engine types with similar static thrust as the current turboprop configuration are available and thus it was chosen to study the necessary changes of the aircrafts design as well as its performance.

4.2. Advantages and disadvantages of turbofan engines compared to turboprop engines

In order to understand the major changes in the design of an aircraft when switching from turboprop to jet engines, the respective advantages and disadvantages are discussed in this section.

4.2.1. Mass

The mass of turboprop and jet engines differs due to their different design. To compare the mass of the different installations, the mass of all components, engine, propeller, housing and mounting has to be concerned. To compare the expected differences in installed mass, the thrust-to-weight ratio of different types is analyzed. The thrust-to-weight ratio is calculated at static thrust as the take-off conditions are critical for the choice of engine.

	D-27	TP400-D6	CFM56-5B3	GEnx-1B70
Maximum power [kW]	10,440	8,203	-	-
Static thrust [kN]	200	155	150	320
Dry weight [kg]	1,650	1,890	2,380	5,816
Propeller weight [kg]	1,100	683	-	-
Thrust-to-weight ratio	7.4	6.1	6.4	5.6

Table 4.1.: Different turboprop and turbofan engine thrust-to-weight ratios at static thrust. Data sources: Deagel (2015), Aerosila (2005), EASA (2012), EUROPROP International (2011), CFM International (2015), European Aviation Safety Agency (2013)

As no information is available for the static thrust of the turboprop engines including its propellers, the static thrust was calculated after the methods provided by the IDT. The propeller weight was taken from the datasheets of the engine and propellers as explained in section 2.4.1.

Table 4.1 shows that the thrust-to-weight ratios of turboprops are similar depending on the engine model. Literature states that turboprop engines are generally heavier because of the extra weight required for the mechanisms that alter propeller pitch and

the gearbox that connects the propeller and turbine (Ojha, 1995). However, as the diameter of the nacelle of jet engines is larger and they are mounted on extra pylons under the wing, the additional weight of the installed jet engines is expected to be higher. Additionally, turboprops have less thrust at higher airspeeds and altitude than turbofan engines. In summary, it is expected that the total mass of the installed jet engines is slighty lower than that of the turboprop engines.

4.2.2. Aerodynamics

While the general aerodynamics of the P-420 are not to be changed, the effects of switching from turboprop to jet propulsion are not negligible. The propeller slipstream affects both the lift and drag of the wing as the propellers of the P-420/B are mounted in front of the wing. In the area of the propeller slipstream, the air is turbulent, making laminar flow over parts of the wing impossible. In total, the results from the IDT show that the slipstream effect increases both lift and drag. With turbofan engines mounted in nacelles below the wing, the exhaust air does not influence the air stream around the wing. The jet engine nacelles have a much larger diameter as the nacelle contains the large fan of the engine. This, and the additional pylons to mount the engines to the wing, increase the total wetted area of the aircraft and thus the parasitic drag. In this area, no expectation can be given as the magnitude of the effect can not be estimated. The analysis shows the changes in the aerodynamic values.

4.2.3. Thrust characteristics and flight performance

While the basic concept of thrust generation is the same for both types of engines, the characteristics over airspeed and altitude show significant differences.

According to the explanations in section 3.2, the propeller of the turboprop covers a large area of air stream as it has no housing. It can accelerate a large amount of air by a small difference in speed. At low speeds and low altitudes, the turboprop engine is able to produce large amounts of thrust due to the large mass of air that is accelerated. However at higher speeds and altitudes, as the air density gets lower, the propeller has much less air mass available to accelerate and loses much of its thrust. The turbofan engine creates thrust with two air streams. The first one is the air stream that flows through the core of the engine, being compressed, mixed with fuel, ignited and then expanded. The second stream flows through the fan which is contained by a housing, allowing the fan blade tips to reach higher speeds than a propeller while containing noise. The air stream is accelerated and bypassed the jet turbojet part. Due to the two methods of air acceleration, the turbofan engine loses less thrust in higher speeds and altitudes. However, turbofan engines have less static thrust than a turboprop engine.

As the second segment climb requirement is the critical point of the flight envelope, the engines must be chosen to fulfill this aspect, where both types of engines have about the same total available thrust. As the thrust of the turboprop engine declines

faster, the turbofan engine replacing the current turboprop engine is expected to be a model of lower static thrust. The high thrust at take-off of the turboprop engine is beneficial for field performance, resulting in a shorter take-off distance. As the turbofan still provides more thrust in the flight envelope, higher ROCD, faster airspeeds and higher cruise altitudes are expected.

4.2.4. Fuel consumption

Fuel consumption characteristics also differ for both engine types.

For a turboprop engine, fuel consumption is expressed as PSFC. This is because the propeller and the gas turbine engine are seen as two different parts. The shaft is connecting the two parts, transferring the power. Thus, the fuel consumption is measured by the mechanical power output of the gas turbine engine. The variation of the maximum power output is a function of Mach number and altitude where the power output drops with rising altitude. Additionally, the maximum power output is rising until it reaches a maximum of about $Ma = 0.7$ and starts falling thereafter. The PSFC is a function of Mach number and altitude. The PSFC drops with rising altitude and also drops with higher Mach number.

For Turbofan engines, fuel consumption is expressed as TSFC. The reason for this is because the main output of the engine is thrust, not power. TSFC is falling with higher bypass ratio. The TSFC is a function of Mach number and altitude. TSFC is increasing with higher Mach number and decreasing with higher altitude. The term SFC is sometimes used instead of TSFC.

To compare the fuel consumption of a turboprop and turbofan, the circumstances have to be similar. E.g. measuring the actual fuel flow while producing the same thrust at a certain altitude and Mach number. To get the thrust of the turboprop engine, the propeller efficiency and airspeed has to be incorporated. Generally, turboprops are more fuel efficient than turbofan engines as described in section 3.2.

Generally, turboprop engines should be more fuel efficient than turbofan engines. However, the high-bypass ratio turbofan engines of latest generation are expected to minimize the difference. With better performance, the aircraft could cruise in higher altitudes with lower air density and thus less drag. The fuel consumption is thus expected to be on a similar level compared to the turboprop version.

4.2.5. Noise

The noise of an aircraft, especially on the ground and during take-off and landing, plays an increasingly important role for the air transport industry. Airports are changing the calculation of landing and take-off fees to models where noise is an increasingly important factor. An example is the Frankfurt Airport which increased the noise-based fees in order to encourage airlines to use less noisy aircraft (Hessischer Rundfunk, 2015). Generally, propeller-driven aircraft are much noisier than those with jet engines, as the propellers are not contained. Modern high-bypass turbofan engines have dramatically reduced noise emissions in the past decades, making aircraft

more silent than ever (BDL, 2015). The higher noise levels of turboprop aircraft are a big disadvantage compared to the turbofan aircraft.

4.2.6. Engine availability

As already stated by Iwanizki (Iwanizki et al., 2014), the availability of very powerful turboprop engines is very limited. The engine used in the design of the P-420, the Iwtschenko Progress D-27 is only used in the Antonow An-70, a Ukrainian transport aircraft. The only turboprop engine of this power class available in the western market is the Europrop TP400, used in the Airbus A400M military transport aircraft. However, the TP400 did not meet the requirements of the P-420 design, as it does not provide enough power to propel the aircraft.

However, Turbofan engines in the static thrust region necessary to meet the requirements of the P-420 are available in various markets from several manufacturers with diverse models. Even larger engines for the possibility of a two-engined aircraft are available and operated on civil transport aircraft.

With a prospected EIS in 2025 of the P-420, this is a great advantage from the perspective of the customer and the airframe manufacturer, as the development time for a turbofan engine which fits the P-420 could be much shorter.

4.2.7. Operational aspects

Operational aspects are very important to determine the aircraft and engine choice. This is a major criterion for the right airlines. Maintenance is a high cost factor and plays and important role when selecting a new aircraft. According to (Babikian et al., 2002), turboprop aircraft have comparatively higher maintenance cost over jet aircraft. On the other hand, turboprops are generally more fuel efficient. As this work concentrates on the implementation of the jet engine into the existing aircraft, further discussion of operational aspects is not carried out.

4.3. Modification of the IDT

In this section, the necessary modifications to the IDT are explained. As the IDT was developed only with the turboprop configuration in mind, many of the calculation methods are turboprop-specific. Different methods for calculation of mass, aerodynamics and performance are implemented to accustom to the changes. Additionally, further variables in the aircraft configuration file are introduced.

4.3.1. Mass

The IDT incorporates three different types of mass estimation, which are derived from the methods described in aircraft design literature by Raymer (1992), Torenbeek

(1982), Torenbeek (2013) and Howe (2000). All three methods use the engine dry weight as an input for the mass estimation.

As the engine type and method of installment (pylon under wing) are different than that for the turboprop version, some factors are changed to the corresponding values as described by the respective literature. Additionally, for the possibility of implementing the design as a two-engined aircraft, all factors that concern the number of engines are implemented. This was not consistently implemented in the prior work of Kügler (Kügler, 2014).

These changes enable the user to calculate both turboprop and turbofan configurations as a four- and two-engined aircraft in a single tool. The variables for engine type and number are set in the aircraft definition file.

4.3.2. Aerodynamics

As aerodynamic calculations consider the dimensions and topography of the elements of an aircraft in contact with the air flow around it, changes of the engines have to be accustomed to according to the literature that cover these methods, mainly taken from Raymer (1992) and Howe (2000).

The effects of the propeller on the wing aerodynamics (propwash) are disabled in the case of turbofan engines. However, as these are mounted to pylons under the wing while the turboprop engines are integrated into the wing, the pylons are added to the parasitic drag calculation in case of turbofan engines.

The calculation of additional drag due to engine failure was adopted for turbofan engines to guarantee a correct estimation of the balanced field length.

No further parameters were introduced into the aircraft definition file.

4.3.3. Turbofan engine parameter calculation

In this section, the engine parameter calculation for jet engines is be described.

Requirements and challenges

The requirements for the engine models are rather simple. The model must be able to provide a sufficiently accurate maximum thrust at any given speed and altitude of the flight envelope. These given speeds and altitudes should, as a minimum requirement, incorporate all speeds and altitudes reached during a typical mission of the aircraft. For example, high speeds at low altitudes are not reached during a mission of the P-420. It is not necessary for the model to provide accurate maximum thrust at these conditions. The input data to the model should be publicly available data on existing turbofan engines. As engine manufacturers often provide very limited data, only the actually available data should be used to estimate the engine performance and thrust characteristics.

Methods for thrust calculation

Several different methods are available to model jet engine thrust as a function of Mach number and altitude. These methods are explained in detail in this section. The approach of the methods vary. The methods described by Torenbeek (1982), Howe (2000) as well as Bartel and Young (2007) are based on the analysis of empirical data. However, the method using the GasTurb software is a numerical approach.

Torenbeek Torenbeek (1982) describes a method of maximum thrust calculation which uses the most simple approach of the evaluated methods. It is intended to be used during take-off and initial climb. Thus, it does not incorporate a term depending on the altitude. Additionally, the method is only valid up to $Ma = 0.3$. The thrust is calculated according to equation 4.1.

$$T = T_{TO}\left(1 - \frac{0.45\,(1+\lambda)}{\sqrt{(1+0.75\lambda)\,G}}M + \left(0.6 + \frac{0.11\lambda}{G}\right)M^2\right) \tag{4.1}$$

Where T_{TO} is the static thrust, M is the Mach number, λ is the bypass ratio and G is the gas generator function. The value of the gas generator function ranges from 0.9 to 1.2 and is assumed to be 1.1 for modern high bypass ratio engines.

Figure 4.1 shows the thrust characteristics after Torenbeek. As the calculation of maximum thrust does not include a part for the altitude, only the values for standard thrust are available. The method is thus very limited and only usable for take-off and balanced field length calculation.

Howe Howe (2000) describes a method of maximum thrust calculation which uses a more advanced approach than that of Torenbeek. It can calculate thrust through all altitudes and Mach numbers. The method is valid up to $Ma = 0.9$.

The maximum available thrust is:

$$T = \tau T_0 \tag{4.2}$$

With τ being calculated as follows:

For $0 < M_N \leq 0.9$:

$$\tau = F_\tau\left[K_{1\tau} + K_{2\tau}R + \left(K_{3\tau} + K_{4\tau}R\right)M_N\right]\sigma^S \tag{4.3}$$

For $M_N > 0.9$:

$$\tau = F_\tau\left[K_{1\tau} + K_{2\tau}R + \left(K_{3\tau} + K_{4\tau}R\right)\left(M_N - 0.9\right)\right]\sigma^S \tag{4.4}$$

Where F_τ is unity for engines without afterburner which is the case here. Additionally,

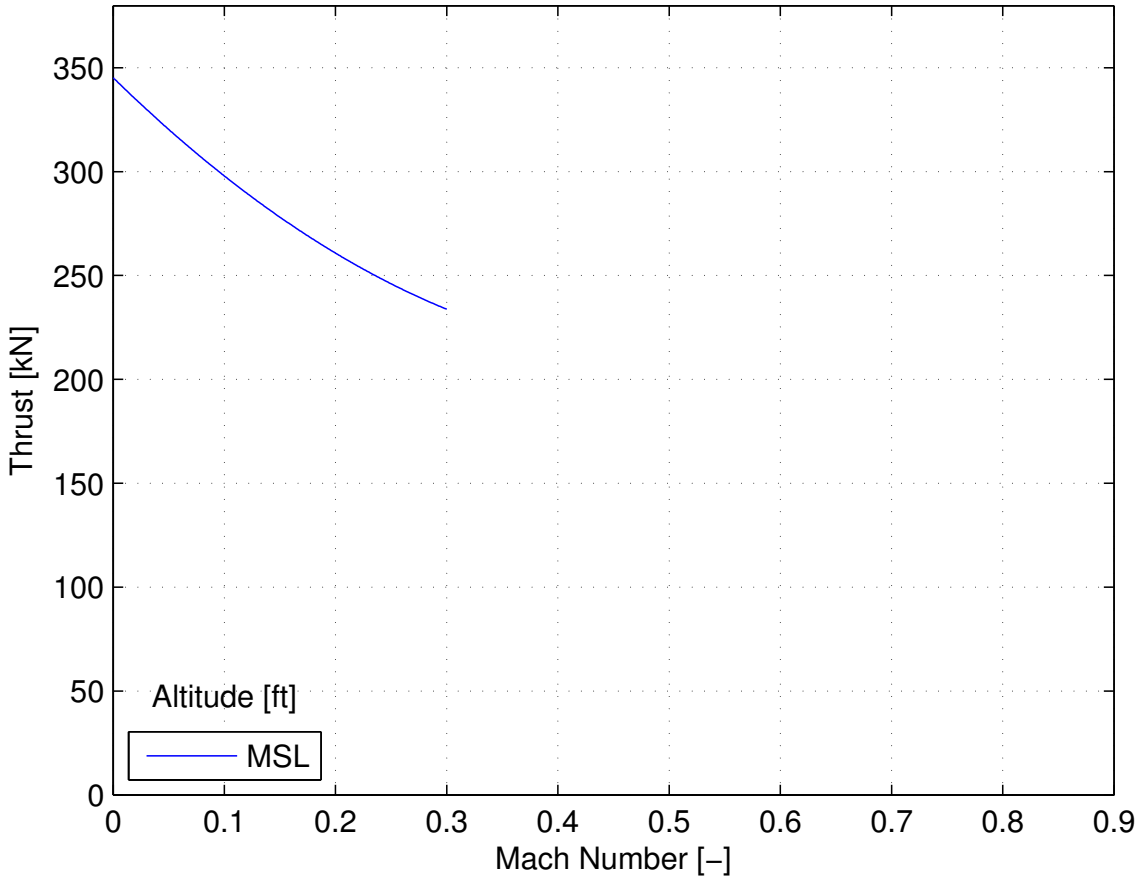

Figure 4.1.: Thrust characteristics after Torenbeek with data of the GEnx-1B76

$S = 1$ for altitudes above 11km. T_0 is the static thrust, M_N is the Mach number, R is the bypass ratio and σ is the relative air density. Further parameters are taken from table 4.2.

Bypass ratio	Mach number range	$K_{1\tau}$	$K_{2\tau}$	$K_{3\tau}$	$K_{4\tau}$	S
0 to 1	0 - 0.4	1.0	0	-0.2	0.07	0.8
	0.4 - 0.9	0.856	0.062	0.16	-0.23	0.8
3 to 6	0 - 0.4	1.0	0	-0.6	-0.04	0.7
	0.4 - 0.9	0.88	-0.016	-0.3	0	0.7
8	0 - 0.4	1.0	0	-0.595	-0.03	0.7
	0.4 - 0.9	0.89	-0.014	-0.3	0.005	0.7

Table 4.2.: Powerplant thrust parameters after Howe. Data source: Howe (2000)

Figure 4.2 shows the plot of the thrust over Mach number and altitude. A characteristic crinkle is visible at $M = 0.4$. This occurs due to the changing parameters in table 4.2. Additionally, the gap in thrust between 35000 and 40000 feet altitude is much larger than at lower altitudes. This is due to the change of S above 11km. All lines are straight. Howe's method of calculating the maximum thrust in any given is

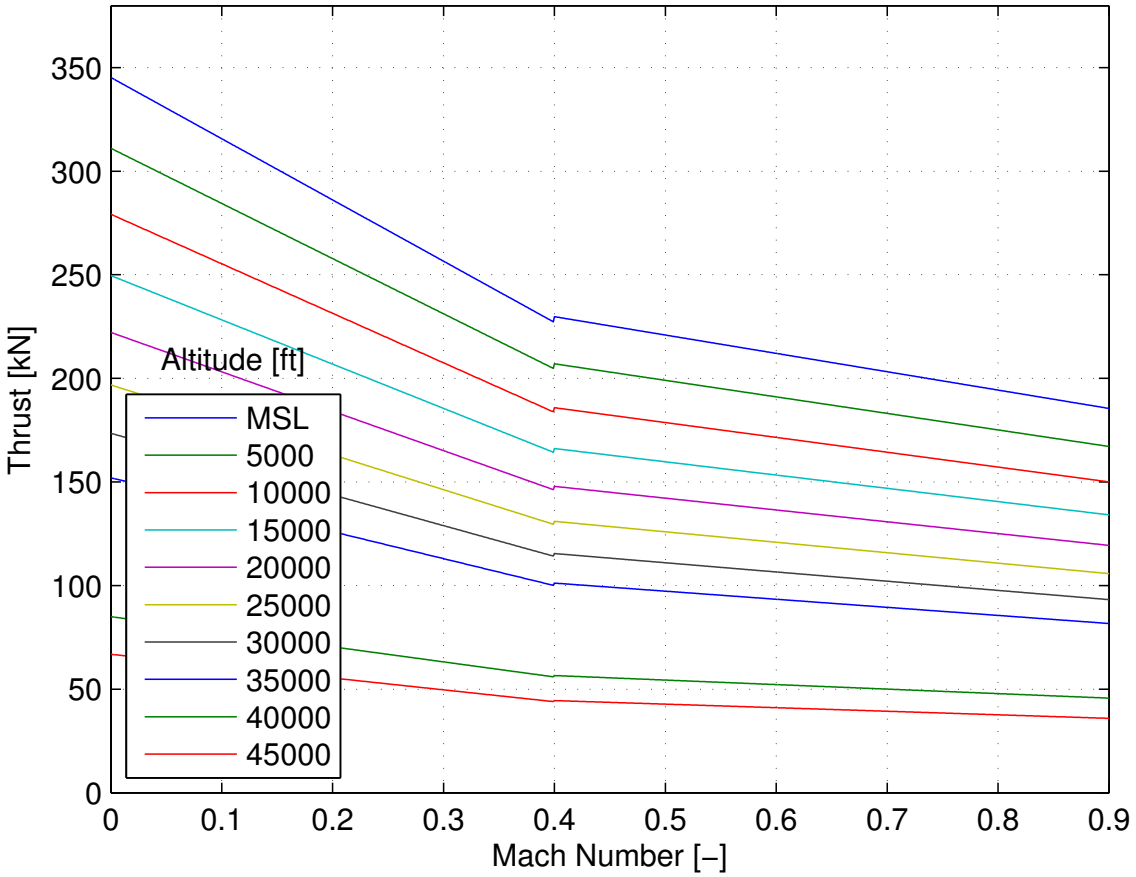

Figure 4.2.: Thrust characteristics after Howe with data of the GEnx-1B76

a solid basis for the preliminary aircraft design, as values for the full flight envelope are calculated.

Bartel and Young Bartel and Young (2007) developed a number of methods of calculating maximum thrust. Different equations for take-off and three climb segments were developed. These equations are introduced here.

The method for Take-Off thrust was created by further developing the work of Torenbeek, whose empirical approach is more than 20 years old and turbofan engine development has seen many changes. Bartel and Young used data of new turbofan engines to create the equation, which is:

$$T = T_0 \left(1 - \frac{0.377\,(1+\lambda)}{\sqrt{(1+0.82\lambda)\,G}} M + \left(0.23 + 0.19\sqrt{\lambda}\right) M^2 \right) \tag{4.5}$$

Where T_0 is the static thrust, M is the Mach number, λ is the bypass ratio and G is the gas generator function. The value of the gas generator function ranges from 0.9 to 1.2 and is assumed to be 1.1 for modern high bypass ration engines.

They further modified this equation to accommodate for different altitudes during take-off:

$$T = T_0 \left(A - \frac{0.377(1+\lambda)}{\sqrt{(1+0.82\lambda)G}} Z + \frac{P_{amb}}{P_{amb0}} M + \left(0.23 + 0.19\sqrt{\lambda}\right) X \frac{P_{amb}}{P_{amb0}} M^2 \right) \tag{4.6}$$

With the parameters A, X and Z being:

$$A = -0.4327 \left(\frac{p_{amb}}{p_{amb0}} \right)^2 + 1.3855 \frac{p_{amb}}{p_{amb0}} + 0.0427 \tag{4.7}$$

$$X = 0.1377 \left(\frac{p_{amb}}{p_{amb0}} \right)^2 - 0.4374 \frac{p_{amb}}{p_{amb0}} + 1.3003 \tag{4.8}$$

$$Z = 0.9106 \left(\frac{p_{amb}}{p_{amb0}} \right)^2 - 1.7736 \frac{p_{amb}}{p_{amb0}} + 1.8697 \tag{4.9}$$

Which allows calculation up to 15000 feet and Ma = 0.4.

The value of the gas generator coefficient is calculated differently. According to Bartel and Young, it is a function of the bypass ratio of the engine.

The climb thrust calculation is divided into three climb segments as presented in table 4.3.

Climb segment	Altitude	Flight speed
1	0 ft - 10 000 ft	VCAS 200 kt - 300 kt
2	10 000 ft - 30 000 ft	VCAS 250 kt - 350 kt
3	30 000 ft - 40 000 ft	M 0.67 - 0.91

Table 4.3.: Climb segments after Bartel and Young. Data source: Bartel and Young (2007)

Climb segment 3 is calculated as follows:

$$T = T_{30} \left(dLn \left[\frac{p_{amb}}{p_{amb30}} \right] + b \right) \tag{4.10}$$

With parameter b being:

$$b = \left(\frac{M}{M_{ref}} \right)^{-0.11} \tag{4.11}$$

Parameter d is defined by table 4.4. For a continuous calculation of the parameter, the data points were interpolated into a polynomial function with the help of MATLAB's curve fitting tool.

M/M_{ref}	d
0.85	0.73
0.92	0.69
1.00	0.66
1.08	0.63
1.15	0.6

Table 4.4.: Correlation between relative Mach number and parameter d after Bartel and Young. Data source: Bartel and Young (2007)

Climb segment 2 is calculated as follows:

$$T = T_{30}\left(a\left[\frac{p_{amb}}{p_{amb30}}\right]^{-0.355\left(\frac{V_{cas}}{V_{casref}}\right)+n}\right) \tag{4.12}$$

Where parameter a is a function of the airspeed.

$$a = \left[\frac{V_{cas}}{V_{casref}}\right]^{-0.1} \tag{4.13}$$

Parameter n takes into account the different climb rates as shown in table 4.5. It was chosen to 0.93 for the moderate climb setting at all times.

	n
Fast climb	0.97
Moderate climb	0.93
Slow climb	0.89

Table 4.5.: Parameter n over climb rate after Bartel and Young. Data source: Bartel and Young (2007)

Finally, climb segment 1 is calculated according to equation 4.14.

$$T = T_{30}\left(m\frac{p_{amb}}{p_{amb30}} + \left(\left[\frac{T_{10}}{T_{30}}\right] - m\left(\frac{p_{amb10}}{p_{amb30}}\right)\right)\right) \tag{4.14}$$

The correction factor m is chosen after table 4.6. Again, the moderate climb setting was chosen and the data points interpolated into a polynomial function for continuous evaluation.

While Bartel and Young's method is created with most recent empirical data, it has the disadvantage of not covering the whole flight envelope. Figure 4.3 shows the gaps in this method. The aircraft has to fly in a very specific altitude and airspeed range in order not to get out of the boundaries. Most civil transport aircraft fly between

	Fast climb	Moderate climb	Slow climb
$Vcas/Vcasref$	m	m	m
0.67	0.4	0.39	0.34
0.75	0.39	0.38	0.33
0.83	0.38	0.37	0.32
0.92	0.37	0.36	0.31
1	0.36	0.35	0.3

Table 4.6.: Correction factor for thrust calculation in the first climb segment after Bartel and Young. Data source: Bartel and Young (2007)

these bounds. However, in the calculations of the IDT, values out of the bounds of this method have to be set to 0 or NaN. This creates issues with many algorithms of the performance analysis in the IDT.

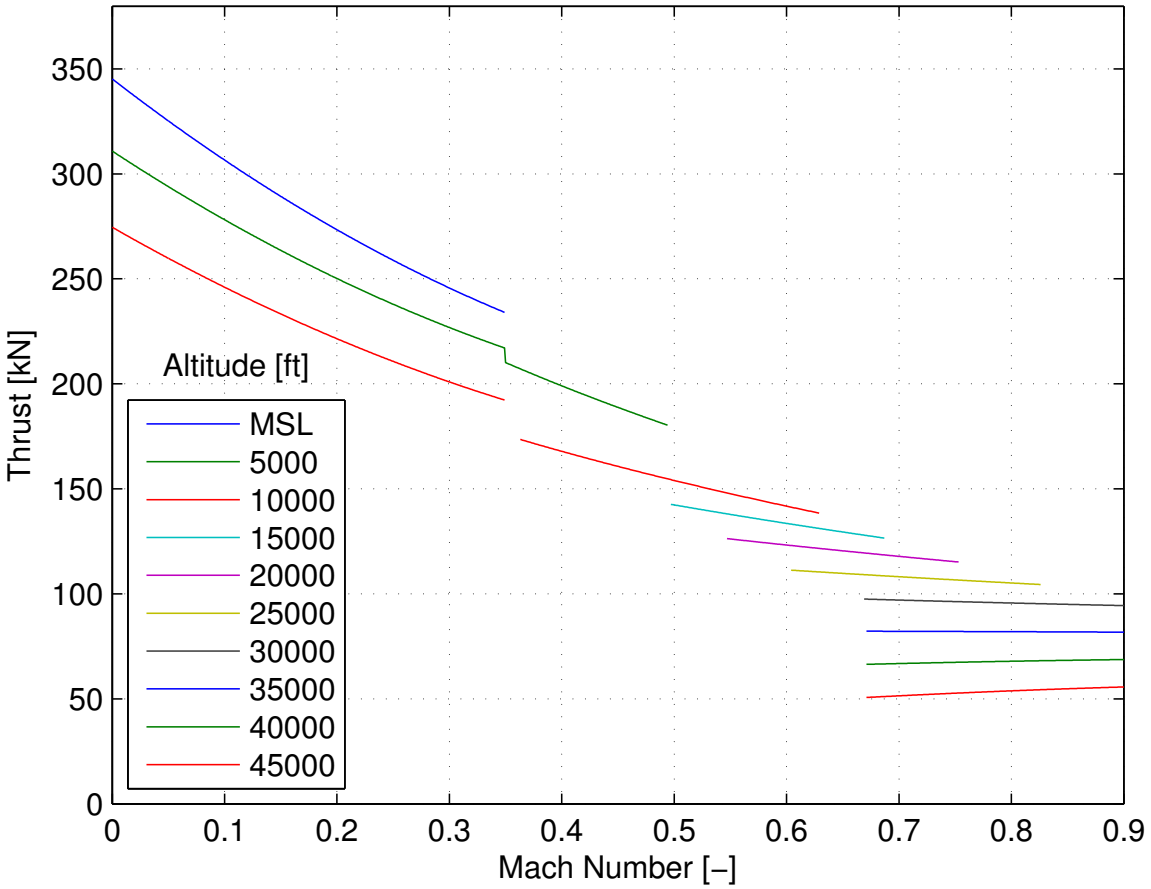

Figure 4.3.: Thrust characteristics after Bartel & Young with data of the GEnx-1B76

GasTurb GasTurb 12 is a software program developed by GasTurb GmbH. It is a well known tool to analyze the performance of various gas turbine engine configurations. An in-depth look into every detail of a gas turbine engine is possible. However,

as this work is in the field of preliminary aircraft design, the required level of detail is rather low. Of interest for the performance calculation of the aircraft is the thrust and SFC at given altitudes and Mach numbers, not the detailed inner workings of the engine.

When using GasTurb, the user has to create a model of the engine that is to be analyzed. A large number of input values may be set to define the model. In this work, the requirement is to recreate the performance model with publicly available information. However, aircraft engine manufacturers do not provide a wide range of information on their products.

It is possible to derive the engine model from standard values in GasTurb. The integrated iteration function then changes specific, user-chosen values in a way that the chosen design point values are met. Valuable data for turbofan engines is usually available for the take-off design point and the cruise design point, which are chosen in this case.

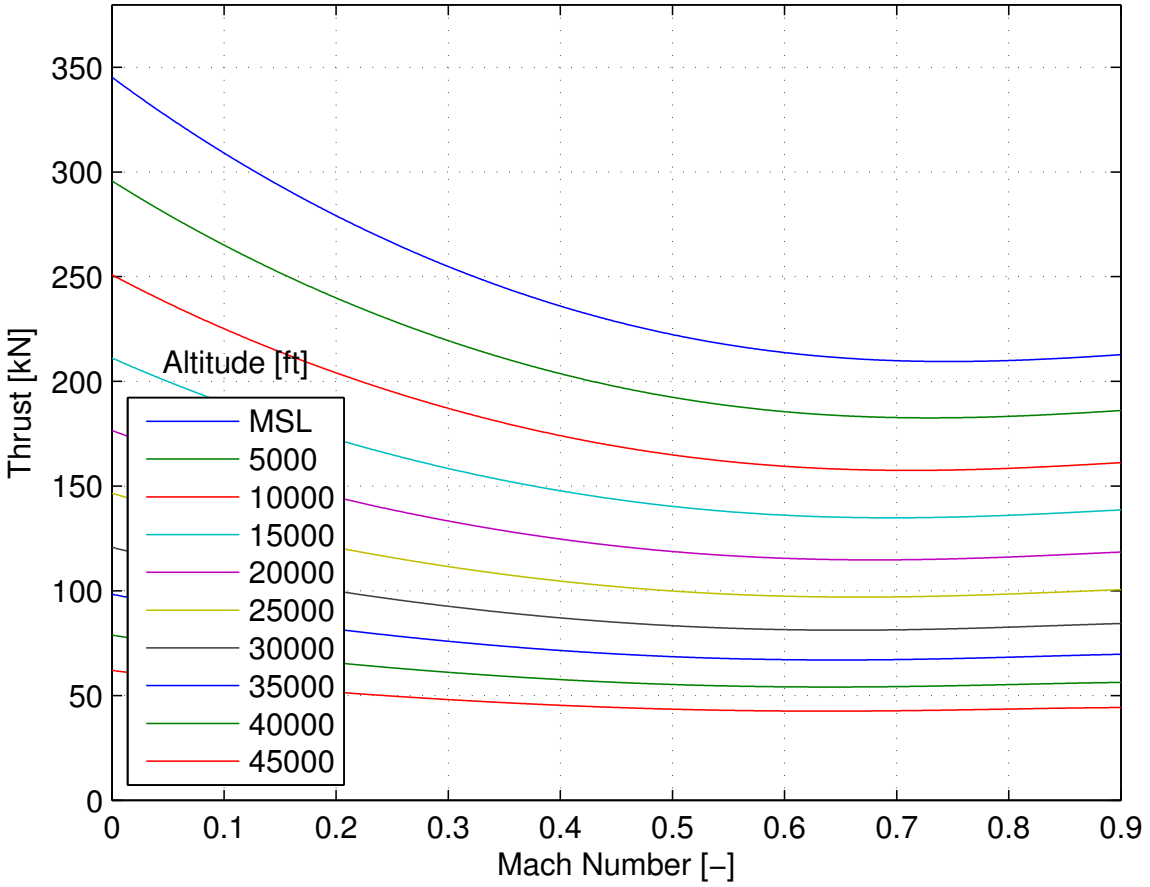

Figure 4.4.: Thrust characteristics from data generated with GasTurb with data of the GEnx-1B76

When the model is created, a parametric off-design study is evaluated to calculate thrust and SFC in the flight envelope from 0 <= Ma <= 0.9 and the altitude 0 <= m <= 14000. These values are imported in MATLAB, and, using its 'Curve Fitting' tool, a polynomial fit is created for thrust and SFC each. This polynomial

functions are integrated into the IDT to calculate the thrust and SFC at any given Mach number and altitude in the specified range.

Figure 4.4 shows the thrust characteristics with the data generated by GasTurb and imported for the use in Matlab and the IDT. The graph shows continuous curves without dents. The thrust slightly increases towards higher Mach numbers which reflects the compression effect at the inlet of the engine at these air speeds.

Comparison of engine model performance

When comparing the four different thrust calculation models, differences become apparent. For the comparison of the methods, the GEnx-1B76 engine was modeled with data given from (Riftin and Hart, 2011), (GE Aviation, 2004) and (European Aviation Safety Agency, 2013). The GasTurb model was based on an existing model of the GE90 engine, which was available at the Institute of Aircraft Design of the Technical University Munich. This is valid as the core of the GEnx is a deviation from that of the GE90.

The requirements for the thrust calculation state that the method must be able to deliver thrust values for the whole flight envelope of the aircraft. While Torenbeeks method shows a curve for take-off and initial climb that is similar to that of Bartel & Young and the GasTurb values, the curve shows a steeper slope and thus the available thrust is falling faster while the aircraft is accelerating. However Bartes & Young and especially Torenbeek can not produce values for the whole flight envelope, which creates problems with the algorithms of the IDT, making them not suitable for this tool. While Howe delivers values for the whole flight envelope, the graph shows dents and incontinuities. The general range of the values lies in a similar area as that of the other values. Additionally, the compression effect at high Mach numbers is not implemented. Additionally to that, the values from the GasTurb software on thrust are less optimistic in almost all cases, resulting in a more conservative approach which is favorable for the preliminary aircraft design. The values from GasTurb are dependent on the quality of the model of the engine that is implemented. As a trustworthy model is available for this work, the GasTurb method is used for further calculation of the engine and aircraft performance.

Methods for SFC calculation

Several different methods are available to model turbofan engine SFC over Mach number and altitude. These methods are explained in detail in this section. The approach of the methods vary. The methods described by Eshelby (2000), Howe (2000) as well as Bartel and Young (2007) are based on empirical data. However, the method using GasTurb is a numerical approach.

Eshelby Eshelby's approach is the most simple one. This method assumes that the SFC is constant both over Mach number and altitude (Eshelby, 2000). For the

calculation in this thesis, the SFC value is assumed to be the cruise SFC value which is defined in the aircraft definition file.

A figure is not shown here as it would only shown a single, horizontal line which represents the whole flight envelope. As in reality, the SFC changes over both Mach number and altitude, this approximation is correct in only a single point - the cruise conditions.

Howe Howe describes a method of SFC calculation which uses a more advanced approach than that of Eshelby. It can calculate thrust through all altitudes and Mach numbers. The method is valid over all airspeeds and altitudes (Howe, 2000).

$$SFC = c_1 \left(1 - 0.15\lambda^{0.65}\right) \left(1 + 0.25 \left(1 + 0.063\lambda^2\right) M\right) \sigma^{0.08} \tag{4.15}$$

Where λ is the bypass ratio of the engine, M is the Mach number and σ is the relative air density. c_1 can be calculated with the above equation, if an SFC is known at a certain altitude and Mach number. Above 11 km, the SFC is assumed to be constant with altitude.

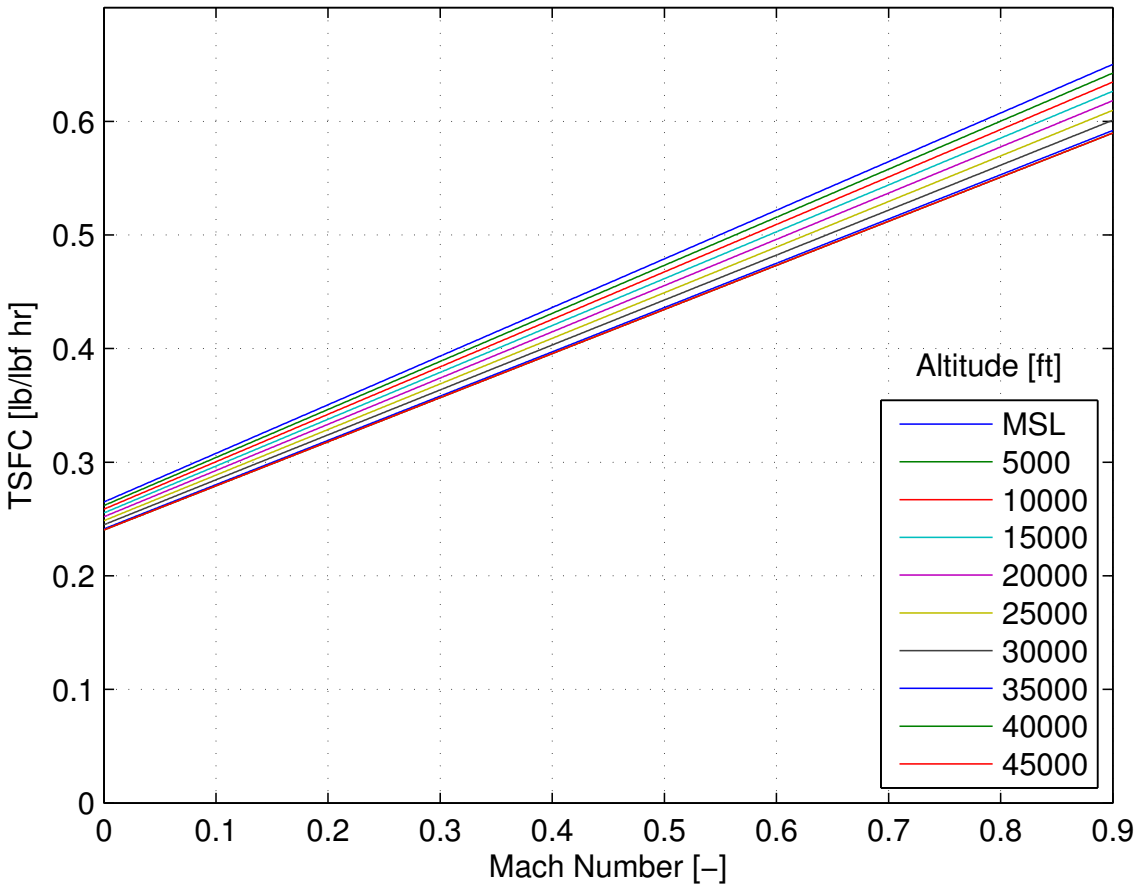

Figure 4.5.: TSFC characteristics after Howe with data of the GEnx-1B76

As shown in figure 4.5, Howe's method shows a variation of the SFC value over both Mach number and altitude. The lines are straight but continuous. Interestingly,

the SFC is decreasing with higher altitude. The thrust plots show that the aircraft is losing maximum thrust output over the altitude. This means that, in order to produce the same thrust at a higher altitude, more fuel would be needed. However, Howe's method suggests that it is the opposite way.

Bartel and Young Bartel and Young developed a method to obtain the SFC for altitudes above 35,000 feet based on data of modern two-shaft high-bypass turbofan engines (Bartel and Young, 2007). The calculation of the SFC is based on a reference SFC that has to be known.

$$SFC = SFC_{ref} \cdot z \left(\frac{M}{M_{ref}} \right)^{n} \tag{4.16}$$

With z in case of $M/M_{ref} > 1$ being

$$z = \left(\frac{F}{F_{ref}} \right)^{-0.1} \tag{4.17}$$

else $z = 1$.

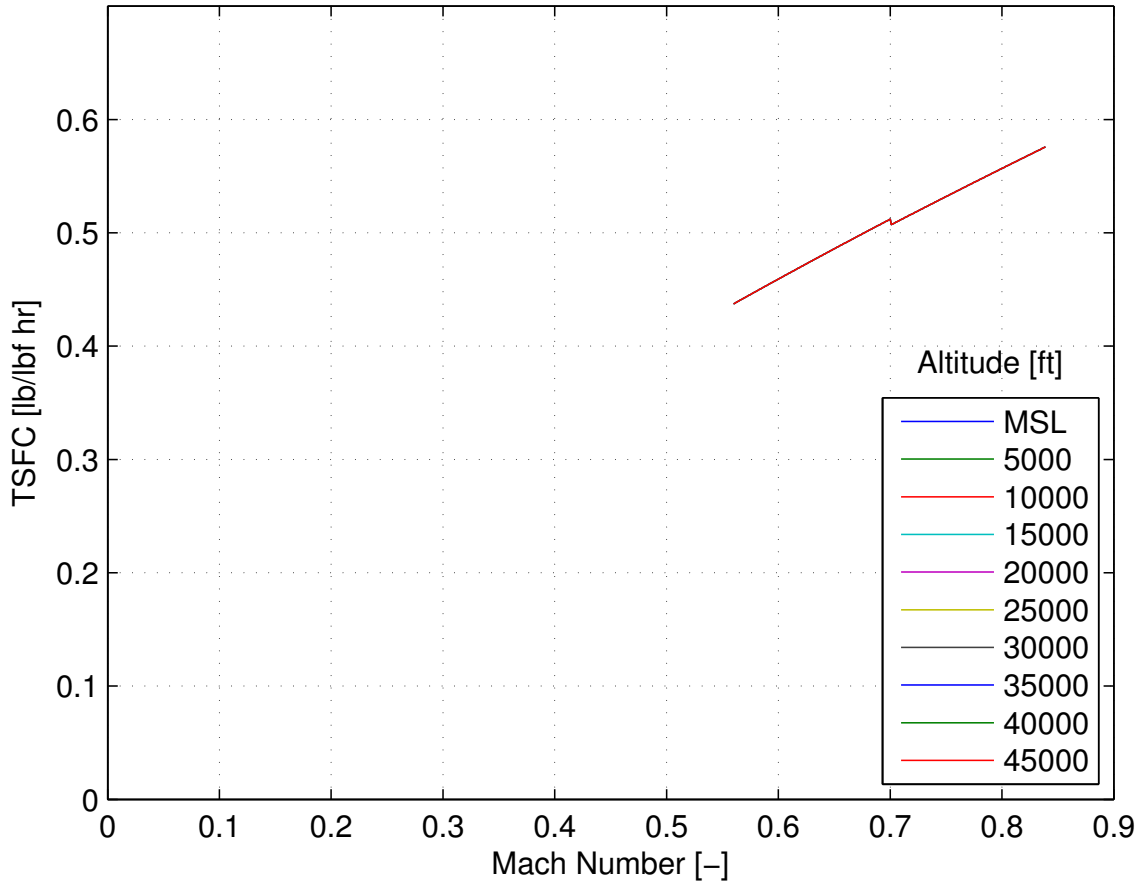

Figure 4.6.: TSFC characteristics after Bartel & Young with data of the GEnx-1B76

Parameter n is taken from the combination of two figures available in Bartel and Young's work (Bartel and Young, 2007). Both graphs were interpolated for the use in the IDT.

The method is only valid for an altitude between 35000 and 47000 ft and a Mach number of $\pm$ 20 % of M_{ref}.

While Bartel and Young's method is the method created with the most recent empirical data, it has the disadvantage of not covering the whole flight envelope, with the available range between 35,000 and 47,000 feet altitude and a Mach number of $\pm$ 20 % of the reference Mach number as shown in figure 4.6. In the calculations of the IDT, values out of the bounds of their method have to be set to 0 or NaN. This creates issues with many algorithms of the performance analysis.

GasTurb The method of SFC integration using GasTurb is the exact same process as for the thrust. Refer to section 4.3.3 for further explanation.

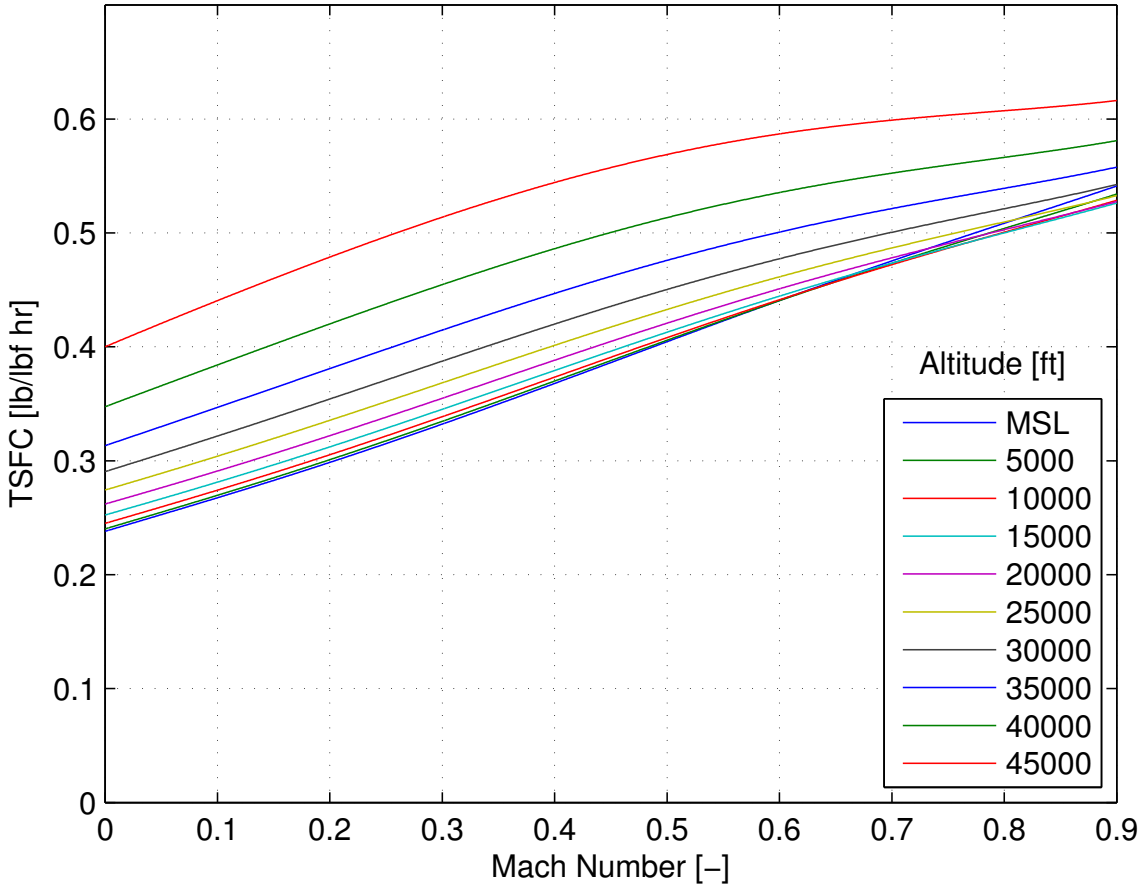

Figure 4.7.: TSFC characteristics from data generated with GasTurb with data of the GEnx-1B76

Figure 4.7 shows the characteristics of the SFC calculated with the values from GasTurb. While the difference in SFC over altitude is very small over low altitude, the deviation increases steadily. The slope of the curves gets flatter towards higher Mach numbers.

Comparison of SFC model performance

When comparing the four different models, some differences become apparent. Bartel & Young's method again is not suitable for the IDT as it can not provide values for the whole flight envelope. Eshelby's approach is too simple and does not reflect that the SFC is changing over airspeed and altitude. Howe's approach shows a similar tendency. However, it can not explain why the SFC is decreasing with increasing altitude. For these reasons, the GasTurb model is again the method of choice for the IDT.

4.4. Turbofan engine choice

As Kügler already determined, a critical performance value of the engine is the available thrust for the second segment climb in the case of one engine inoperative (Kügler, 2014). For this reason, the turbofan engine choice was made with this value in mind.

Several iterations and turbofan engine models were compared to get to the final choice. As the scope of this work is to design an aircraft with existing technology while being fuel efficient, latest generation high bypass ratio turbofan engines were finally chosen. They can fulfill thrust demands while providing promising SFC values.

4.4.1. General Electric GEnx-1B76

The General Electric GEnx-1B76 is a high bypass ratio turbofan from the GEnx series for the Boeing 787-10. It has 2 spools, a bypass ratio of 8.7 and an overall pressure ratio of 47. The core was derived from the GE90 engine which powers the Boeing 777 (Riftin and Hart, 2011). The GE90 is a very efficient engine with a SFC of 0.55 lb/lbf/hr (Cantwell, 2010), (Meier, 2005). Sources say that the GEnx has a 6.9 % better SFC than the GE90 (Tsang, 2011). The GEnx-1B76 was chosen for the twin-engined P-420 variant. This variant is dubbed P-420/T (for Twin jet). The combined thrust of the two engines is higher than that of the four PW1127G's as in the one-engine-inoperative case, just one engine needs to provide all thrust to fulfill the second segment climb angle. Further data on the GEnx-1B76 is shown in table 4.7.

The GasTurb model for the engine was created with the data from table 4.7, based on the available model of a GE90 engine. Figure 4.4 shows the thrust characteristics of the GEnx-1B76 and figure 4.7 shows the SFC characteristics, both modeled with GasTurb.

Parameter	Value
Static thrust [kN]	345.2
Bypass ratio	8.7
Fan diameter [in]	111
Dry weight [kg]	5,816
Cruise SFC [lb/lbf hr]	0.512

Table 4.7.: General Electric GEnx-1B76 data. Data sources: MTU Aero Engines AG (2014), Riftin and Hart (2011), GE Aviation (2004), European Aviation Safety Agency (2013), FAA (2014)

4.4.2. Pratt & Whitney PW1127G

The Pratt & Whitney PW1127G is a high bypass ratio geared turbofan from the PW1000G series for the Airbus A320neo. It has 2 spools, however the fan is connected to the low pressure turbine via a gearbox of the ratio 3:1. This lets the fan rotate slower while the turbine rotates faster, which is beneficial for each part's efficiency. While the gearbox adds weight, a 3rd spool is not necessary to reach similar efficiency. The manufacturer and Airbus claim a 15 % better SFC compared to the A320ceo engine which is the CFM56-5 with a fuel efficiency of 0.545 lb/lbf/hr (Meier, 2005). The PW1127G was chosen as the engine for the four-engined P-420 variant. This variant is dubbed P-420G (for Geared turbofan). Further data on the PW1127G is shown in table 4.8.

A GasTurb model for the engine could not be successfully created during the course of this work with the available data, as the model did not converge at high airspeeds in the internal calculation of GasTurb. However, the converging values showed similar characteristics as the GEnx-1B76 model. Due to this similarity, it was chosen to implement the PW1127G with the same characteristics as the GEnx-1B76. A factor is introduced with respect to the maximum static thrust and cruise SFC respectively in order to apply the characteristics to the PW1127G. This is feasible as the two engines are from the same generation. This characteristic, as shown in figures 4.13 and 4.8, is still more conservative than the modeling after Howe. Additionally, using two different methods to compare the same aircraft would be inconsistent and lead to faulty results. Thus, this approach was chosen.

Parameter	Value
Static thrust [kN]	120
Bypass ratio	12
Fan diameter [in]	81
Dry weight [kg]	2,600
Cruise SFC [lb/lbf hr]	0.463

Table 4.8.: Pratt & Whitney PW1127G data. Data sources: MTU Aero Engines (2014), Finkenstein (2013), Sabnis and Winkler (2010), Pratt & Whitney (2014)

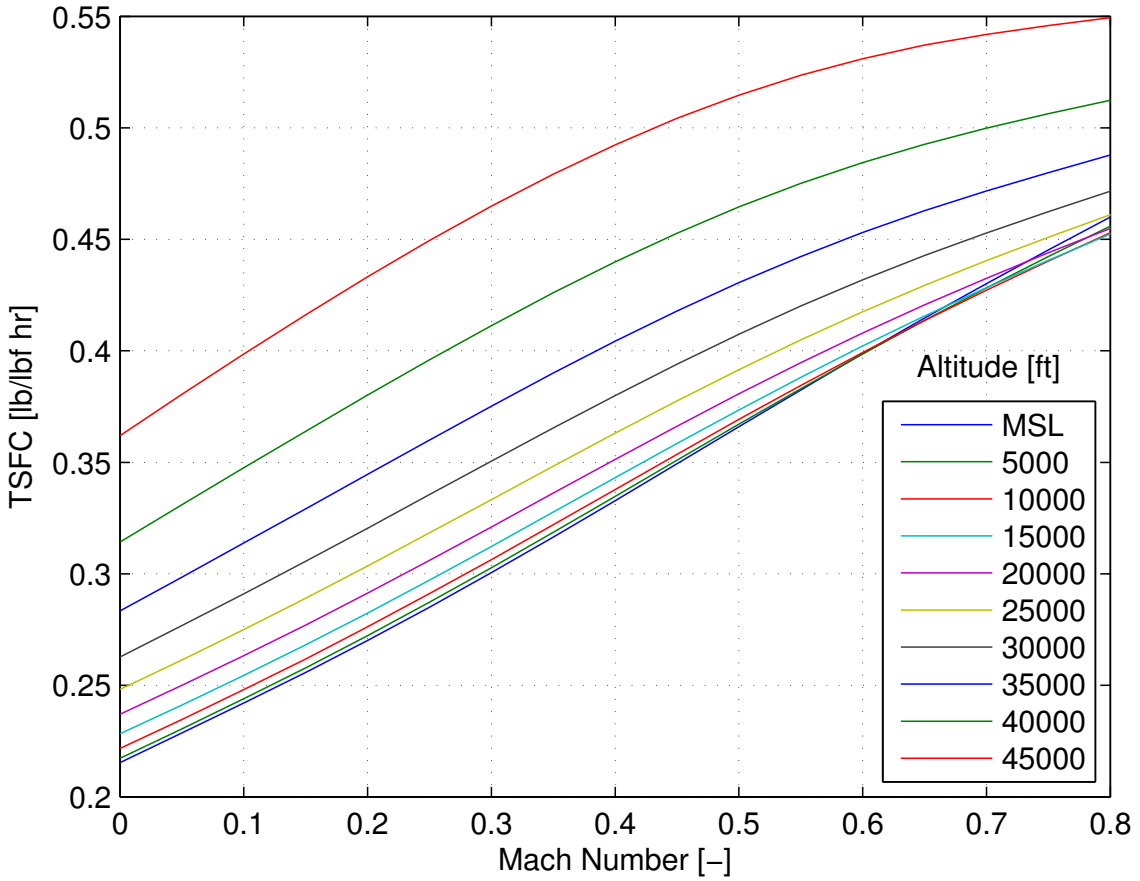

Figure 4.8.: TSFC characteristics of the PW1127G from data generated with GasTurb

4.5. Analysis of aircraft performance

In this section, the performance of the two newly created P-420 variants, the P-420/G and the P-420/T, is analyzed. They are compared to the performance of the P-420/B which was created by Kügler (2014) and the P-420/C, which was created in this work as explained in section 2.4.

The two new turbofan versions of the P-420 were created by the above explained adaptations to the IDT. The aircraft definition file was changed to allow the integration of these two types. In an iterative process, the aircraft mass and design mission fuel were adjusted while analyzing the output of the IDT to make sure that the requirements and expectations are met. After the successful iterative process, the four aircraft are compared against each other to analyze and understand the effects on the aircraft and its performance that come with the change to turbofan engines. An isometric view of the two new P-420 variants is shown in 4.9. Three-view drawings of the two aircraft are available in figure 4.21 and 4.22.

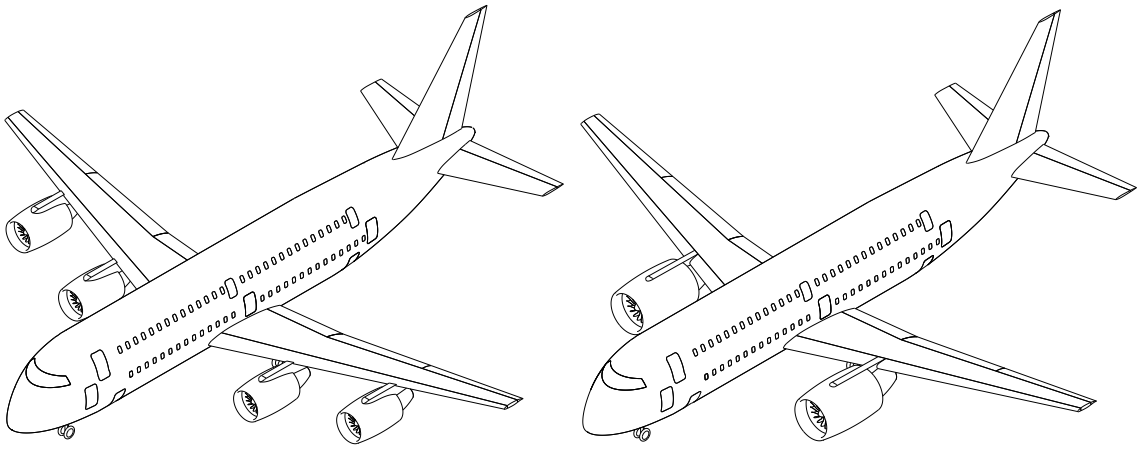

Figure 4.9.: Isometric view of the P-420/G (left) and the P-420/T (right). Based on the 3D-model of the P-420/A provided by Iwanizki (2014)

4.5.1. Mass

The change to turbofan engines comes with changes in the mass of the aircraft. Table 4.9 shows the changes in the OME. The P-420/G has a OME that is 13,400 kg or 13.5% lower, and the P-420/T saves 9,230 kg (9.5%). The biggest factor for the decrease of the mass is the propeller installation which is more than 12 t alone and not present on the turbofan aircraft, compared to the P-420/C. However, turbofans engines are heavier than turboprop engines without gearbox and propellers. Additionally, the nacelles of the engines are lighter. Other factors have a minor impact on the OME.

Parameter [kg]	P-420/B	P-420/C	P-420/G	P-420/T
Structure	44,167	42,970	40,900	43,193
- Nacelle group (all engines)	4,144	4,144	2,422	3,484
Propulsion group	22,373	14,985	13,056	14,501
- Engines	7,600	7,600	10,400	11,632
- Gear boxes, controls, starter	1,416	1,416	143	195
- Oil system and cooler	532	532	104	116
- Fuel system	537	537	537	464
- Propeller installation	12,288	4,900	0	0
Systems	24,291	23,995	23,868	24,000
Miscellaneous	963	874	832	871
Operational items	5,531	5,531	5,531	5,531
Operating mass empty	97,326	88,355	84,186	88,096

Table 4.9.: OME comparison of the four P-420 variants. Data taken from the IDT.

When comparing the mass of the aircraft on its design mission, the lower OME reflects into the design mission mass as well. While the P-420/T has a similar fuel

burn compared to the P-420/B and thus has to carry a similar amount of fuel, the P-420/G's fuel burn is substantially lower, leading to a lower MTOW. The total mass difference on the design mission is 17,838 kg (11.5 %) for the P-420/G and 10,720 kg (6.6 %) for the P-420/T. This can be explained with the weight spiral, where a lower OME leads to lower MZFW and thus lower fuel consumption which then enables the aircraft to take-off with less fuel mass. In total, the lower MTOW is a big advantage of the turbofan-powered P-420 variants over the turboprop version, as less thrust is required for similar performance and overall less fuel needs to be burned.

Parameter [kg]	P-420/B	P-420/C	P-420/G	P-420/T
Maximum ramp mass	180,000	180,000	180,000	180,000
Maximum take-off mass	172,552	157,636	154,714	161,832
Mission fuel	22,335	17,546	19,782	22,105
Reserves	5,891	4,735	3,747	4,631
SPP zero-fuel mass	144,326	135,355	131,185	135,096
SPP cargo loading	5,000	5,000	5,000	5,000
SPP passenger loading	42,000	42,000	42,000	42,000
Operating mass empty	97,326	88,355	84,186	88,096

Table 4.10.: Design mission mass comparison of the four P-420 variants. Data taken from the IDT.

4.5.2. Aerodynamics

As described in section 4.2.2, the aerodynamics are also affected by the changes done to the aircraft and the most important parameters are summarized in table 4.11. The lift-to-drag ratio at cruise conditions (L/D) is lower for both turbofan versions. The zero-lift drag C_{D0} is about 20 % lower for both turbofan versions. This is due to the installment of the turbofan engines under the wing and the smaller area that is affected by the engines compared to the 4 large propellers. However, the propeller effect on lift is non-existent for the turbofans which lowers the lift. Also, the additional zero-lift drag in the case of one engine inoperative is different. The four-engined P-420/G has a slightly lower additional drag as the diameter of the inoperative engine is smaller compared to that of the propeller. The two-engined P-420/T has a much higher additional drag due to the rather large turbofan now being inoperative. This is a disadvantage for the P-420/T, as even more thrust is required from the remaining single engine to overcome the drag and fulfill the minimum climb requirements in the case of one engine inoperative. The lift-drag characteristics of the P-420/T and P-420/G are shown in figure 4.11 and 4.10.

The maximum lift coefficient C_{Lmax} is largely dependent on the wing. As the wing was not changed for the turbofan version, it is the same. Also, additional zero-lift drag like the extension of the landing gear stays the same, as no changes were made in this regard. The P-420/B and /C have identical aerodynamic characteristics as the changes do not effect the aerodynamics.

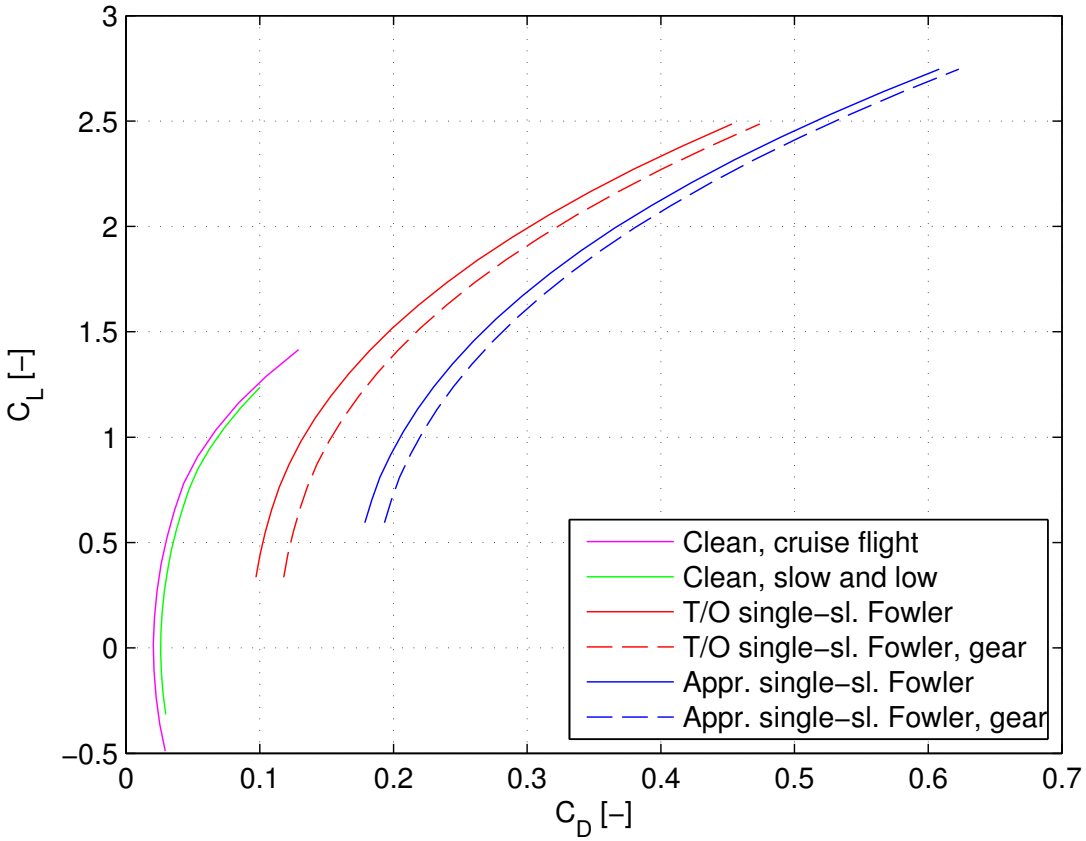

Figure 4.10.: Lift-drag characteristic of the P-420/G

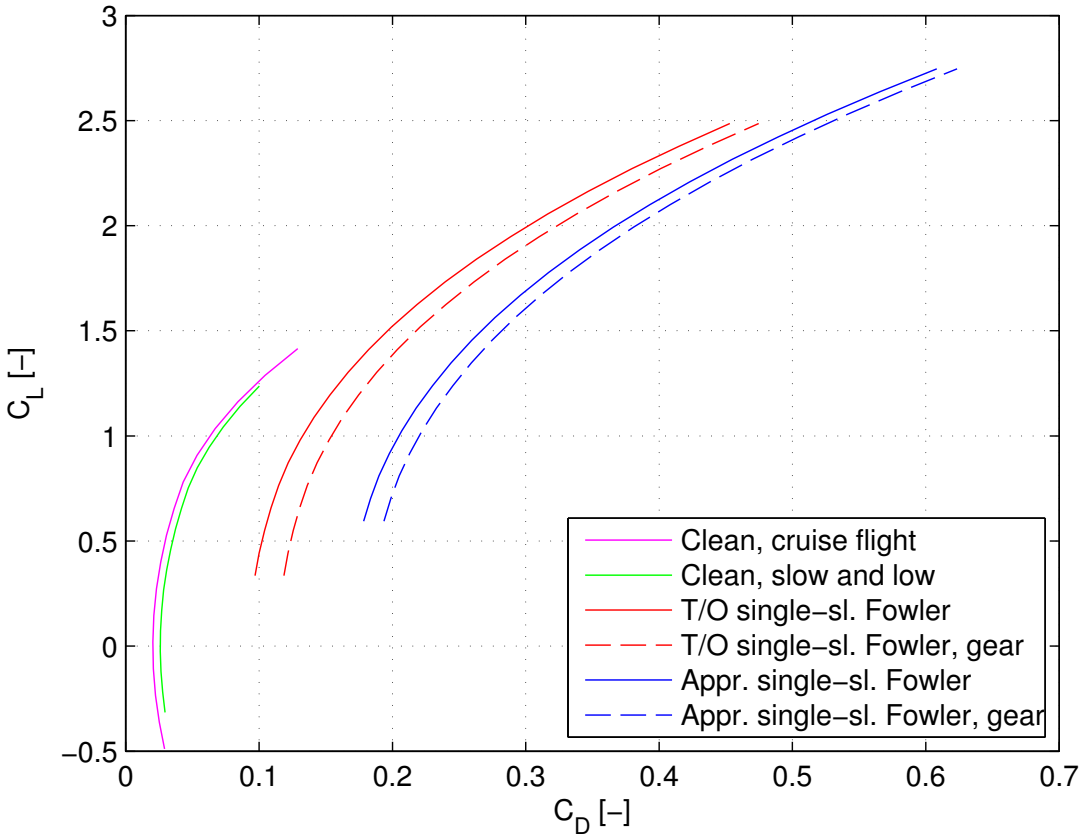

Figure 4.11.: Lift-drag characteristic of the P-420/T

Parameter	P-420/B	P-420/C	P-420/G	P-420/T
L/D (cruise, design lift coefficient)	18.48	18.48	18.129	18.167
C_{D0}	0.0218	0.0218	0.0183	0.0182
C_{Lmax} (clean, $\alpha_{max} = 10°$)	1.527	1.527	1.527	1.527
ΔC_{D0} (one engine inoperative)	0.0044	0.0044	0.0040	0.0075
ΔC_{D0} (extended landing gear)	0.0273	0.0273	0.0273	0.0273
C_{D0} (slow and low)	0.0237	0.0237	0.0190	0.0189

Table 4.11.: Aerodynamic characteristics of the four P-420 variants. Data taken from the IDT.

4.5.3. Engine Characteristics

Turboprop and turbofan engines have very different thrust characteristics due to their design (see section 3.2). This is visualized by figure 4.12, which shows the propeller thrust characteristics of a P-420/B engine and figure 4.13 which shows the thrust characteristics of a PW1127G engine of the P-420/G (Note the different scaling of the Mach number on the horizontal axis). It becomes visible, that while the single P-420/B engine can provide large amounts of thrust at slow speed, the thrust output drops quickly with increasing speed. The turbofan engine loses much less thrust when speed increases and has more thrust available at higher speeds. During take-off and initial climb at Mean Sea Level (MSL), the thrust of the turboprop and the PW1127G are similar at around Ma = 0.3 which is the approximate take-off speed. The engine was chosen to fulfill the one engine inoperative minimum climb requirements, which is at this point.

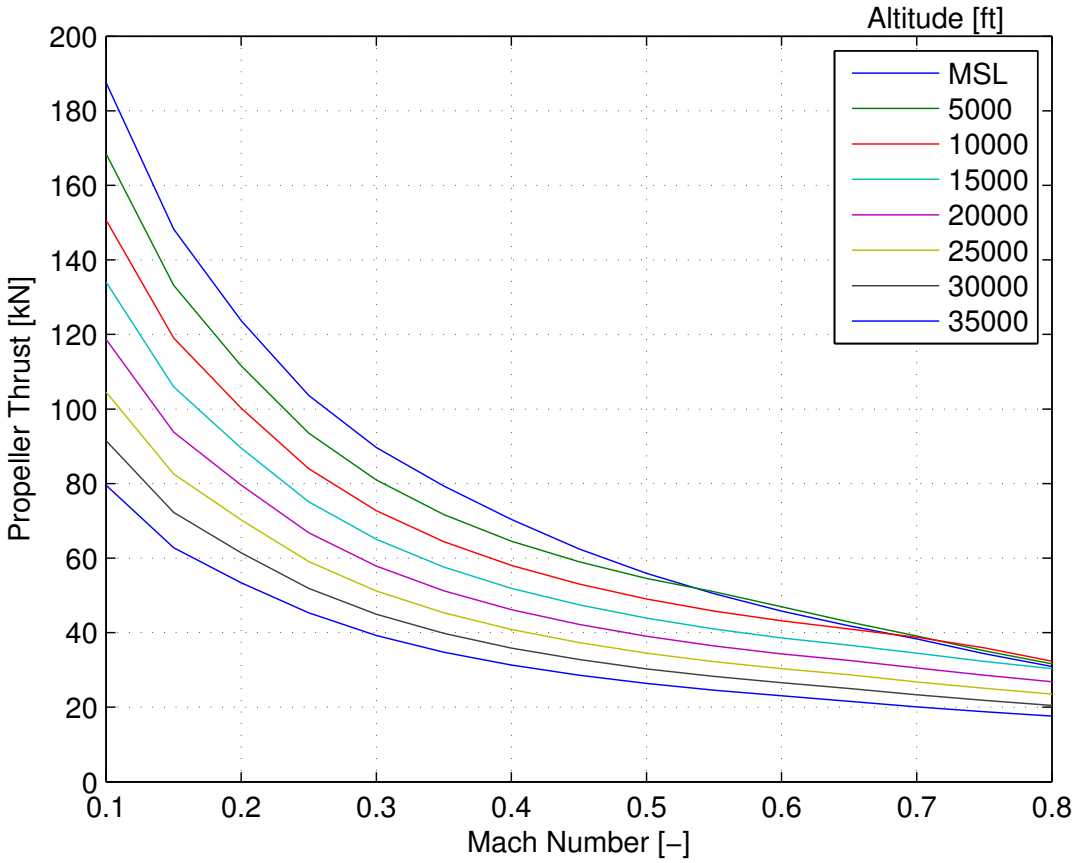

Figure 4.12.: P-420/B propeller thrust characteristics

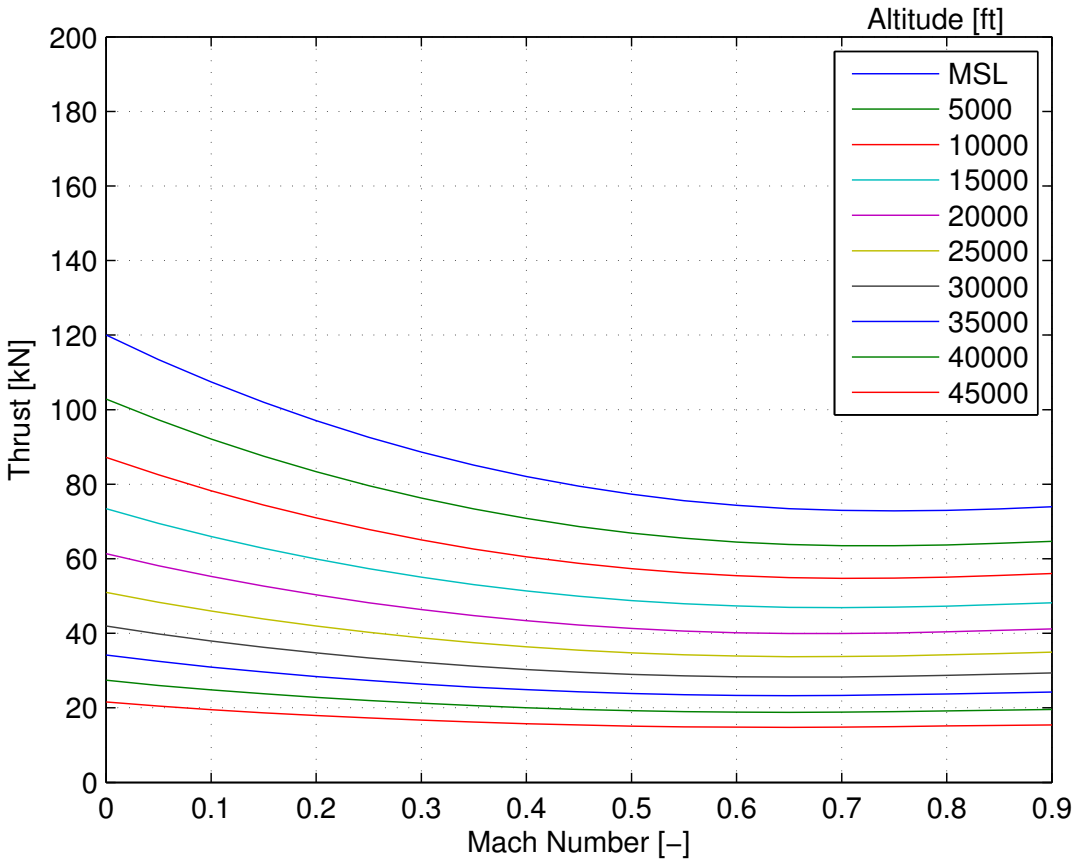

Figure 4.13.: P-420/G engine thrust characteristics

4.5.4. Performance

The changes in mass, aerodynamics and engine characteristics are directly connected to the performance of the aircraft. Table 4.12 summarizes the key parameters of the performance of the P-420 variants. Due to the much lower mass, lower zero-lift drag and thrust characteristics, the P-420/G has a better field performance than the P-420/B. The P-420/T suffers from the higher mass compared to the P-420/G and has a much worse balanced field length and lower second segment climb angle in one engine inoperative conditions. This is supported by the higher additional drag and only one engine remaining to power the aircraft. With all engines operative, the P-420/T has more thrust available at all times, enabling it to cruise at higher altitudes than the other versions. However, the fuselage of all P-420 variants was built for altitudes of up to 32,000 ft which limits the operating altitude of both turbofan versions. In summary, both turbofan versions meet the requirements of the design set in section 2.5.

Parameter	P-420/B	P-420/C	P-420/G	P-420/T
FAR25 landing distance [m]	2,332	2,157	2,120	2,204
Balanced field length [m]	3,466	2,756	3,395	3,946
Second segment climb angle [°]	2.133	3.354	2.885	1.781
Maximum operating Mach number	0.75	0.77	0.90	0.90
Service ceiling (100 fpm ROC) [ft]	32,200	34,800	37,700	45,300
Maximum operating altitude [ft]	33,100	35,600	38,700	45,900

Table 4.12.: Performance characteristics of all four P-420 variants. Data taken from the IDT.

The plots of the SEP in figure 4.16 and figure 4.15 show that the P-420/T, is, like many twin-jets an 'overpowered' aircraft due to the minimum climb requirements. In fact, it could fly in Mach number ranges and altitudes which are not supported by the structure of the aircraft, making the extra thrust unnecessary. On the other hand, it enables the P-420/T to climb quickly to its altitude or operate at high-altitude airports. The P-420/G has not as much additional thrust at high Mach numbers and altitudes as the P-420/T due to the sizing of the engine from the second segment climb requirement. This reflects in the SEP, which has less SEP remaining. However, this is still enough for sufficient altitudes and Mach numbers.

According to the performance analysis, the design mission was adjusted. Being able to fly at higher altitudes and faster airspeeds, this was incorporated in the design mission profile. Both aircraft now cruise at 32,000 ft and have higher climbing and descent airspeeds. Additionally the Mach number was raised to 0.7 as this proved feasible. The design mission is shown in figure 4.14.

The constraint diagrams in figure 4.17 and 4.18 show the constraints of the two turbofan-powered aircraft. It is visible, that the second segment climb constraint has a higher requirement for the P-420/T, due to the higher drag for the this configuration, which requires a higher static thrust to take-off weight ratio at the design point.

Other values are very similar due to the similar aerodynamic characteristics. Due to the design point necessary at this point, the P-420/T can almost fulfill the take-off with All Engines Operative (AEO) at field length 1 (1,800 m).

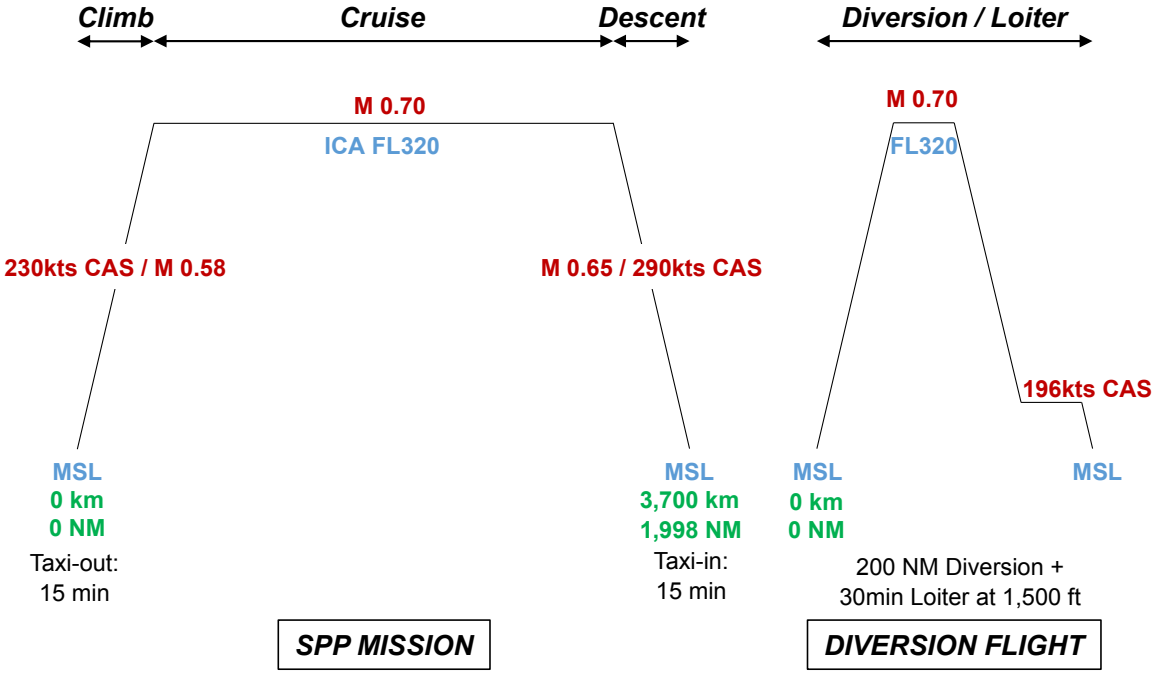

Figure 4.14.: Design mission of the Propcraft P-420/G and /T. Figure based on Randt (2014b).

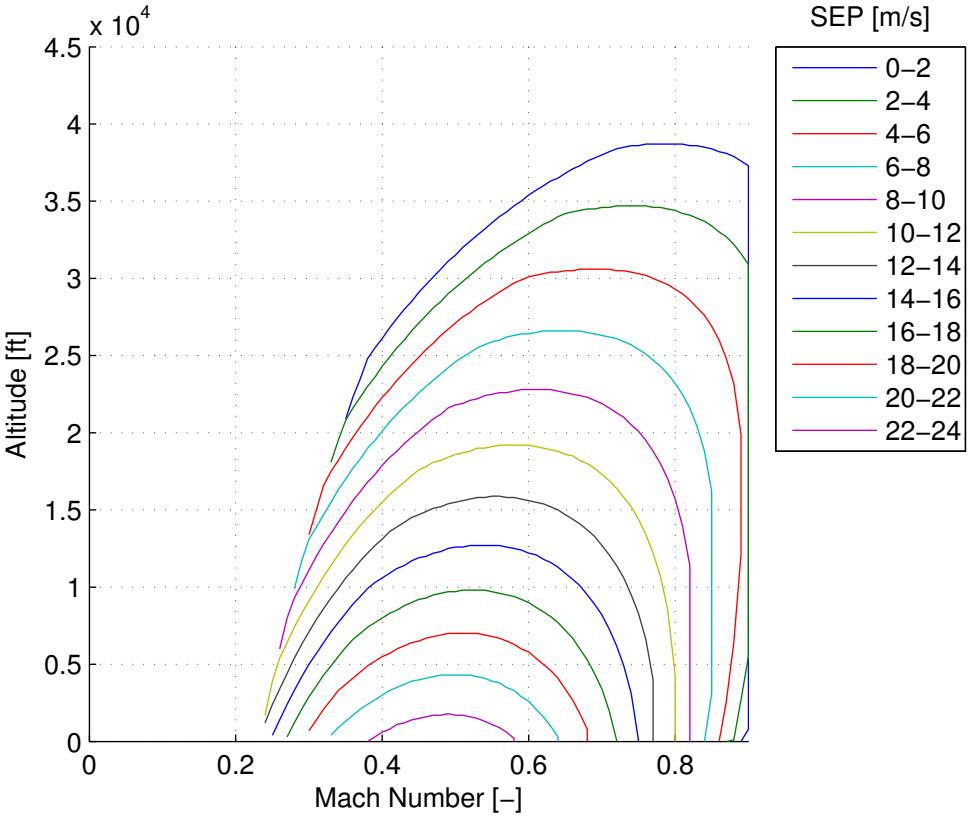

Figure 4.15.: P-420/G SEP diagram

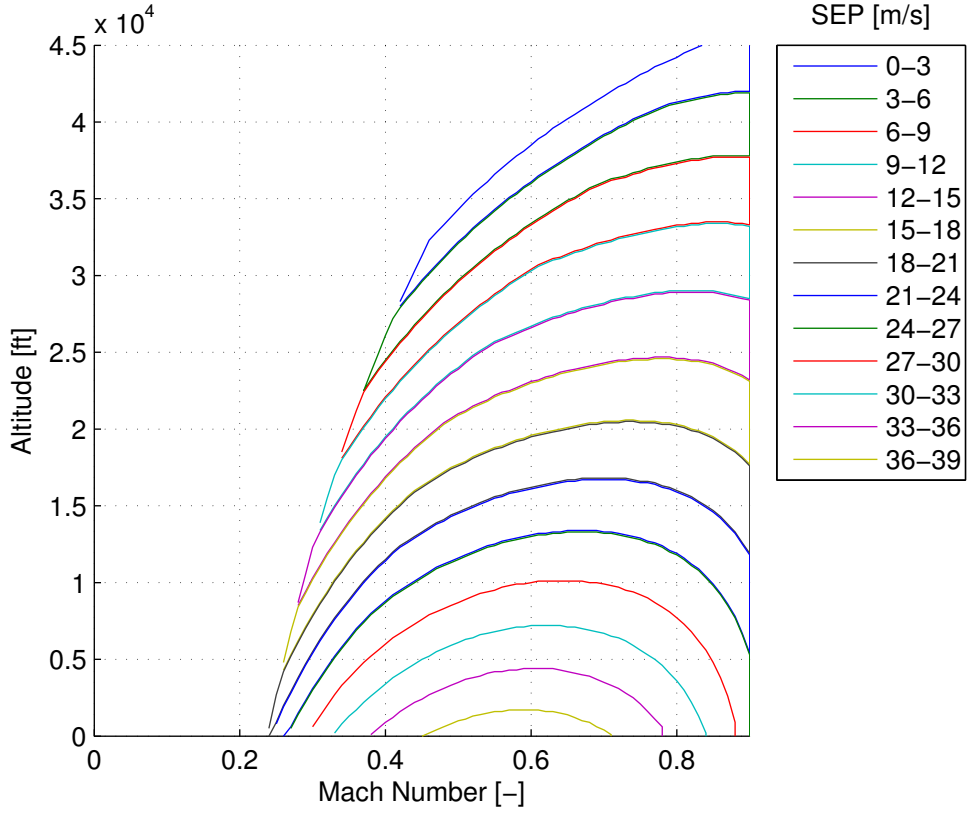

Figure 4.16.: P-420/T SEP diagram

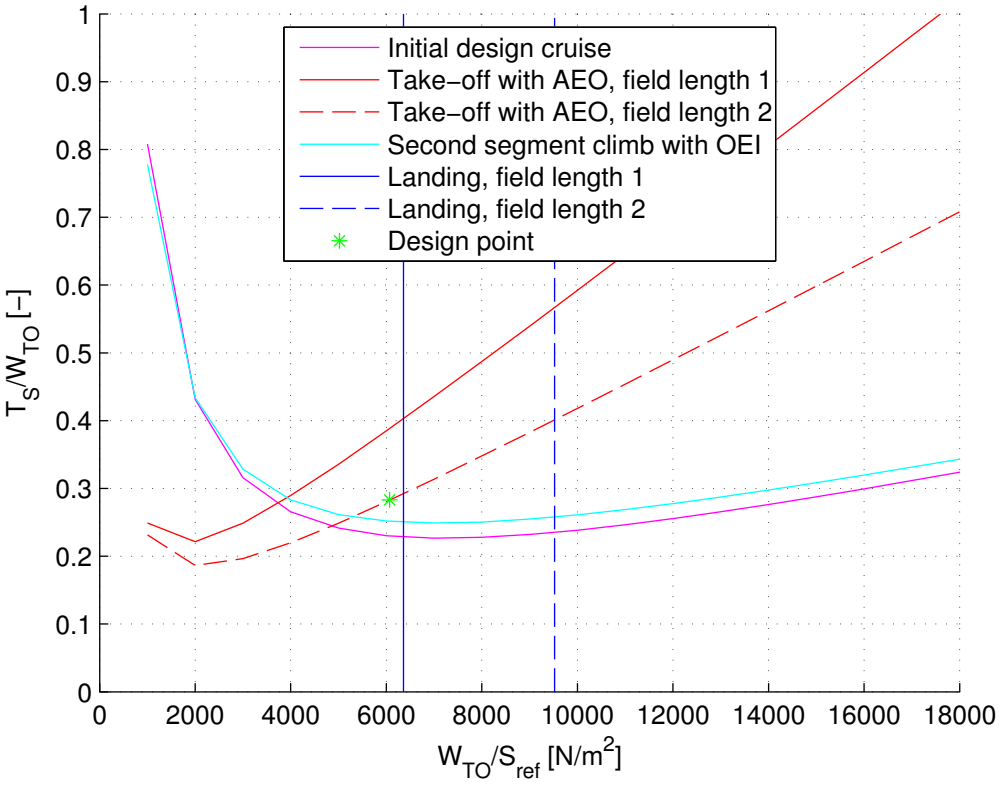

Figure 4.17.: P-420/G constraint diagram

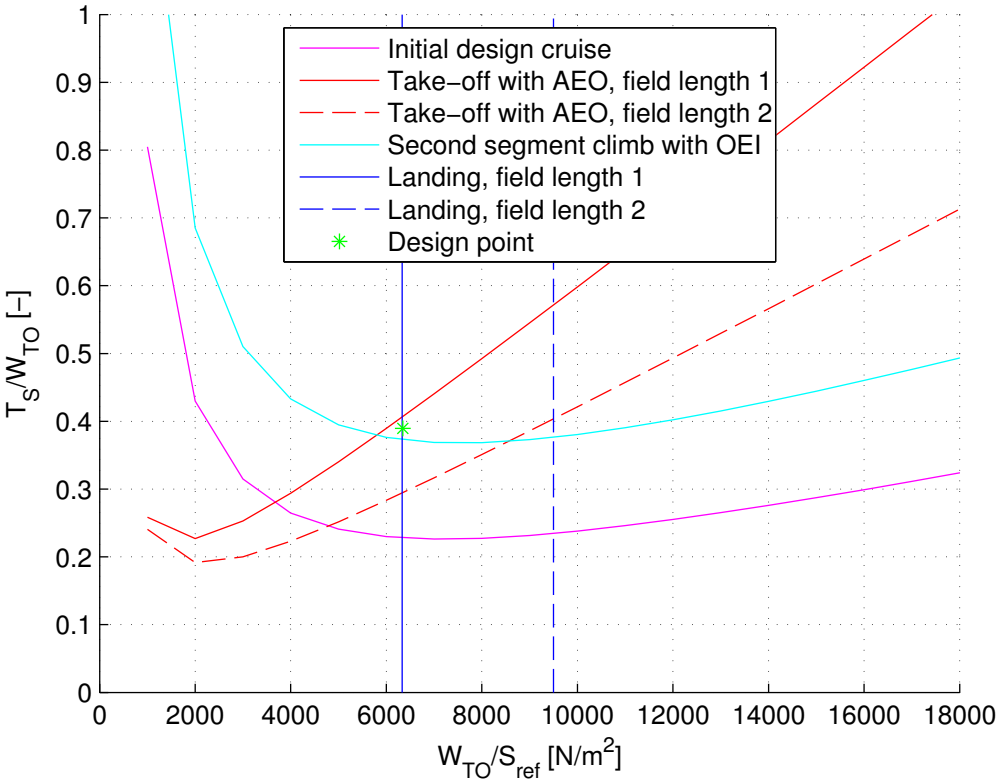

Figure 4.18.: P-420/T constraint diagram

4.5.5. Fuel consumption and payload-range characteristics

The payload-range and fuel consumption characteristics are of particular interest due to the application case of the aircraft. This analysis is carried out with the internal fuel calculation of the IDT. For a thorough analysis using BADA, refer to chapter 5.

Table 4.13 shows the detailed analysis of fuel consumption during the different phases of the flight on the design mission. Large differences are visible in the taxi-out/in and take-off consumption. This is due to the approach of taxi power setting of 60% in Küglers work (Kügler, 2014) for the P-420/B. The P-420/C shows more reasonable values. The P-420/T uses more fuel especially during cruise due to the higher mass of the aircraft and SFC of the engine. The P-420/C is the most fuel efficient aircraft in this comparison, with 12.7 % advantage over the P-420/G.

The payload-range diagrams in figure 4.19 and 4.20 reflect the trend shown in the design mission fuel consumption analysis. The P-420/G has a considerably higher range at all points.

Fuel mass [kg]	P-420/B	P-420/C	P-420/G	P-420/T
Taxi-Out & Take-Off	1,728	431	456	621
Climb	2,634	1,975	2,087	2,159
Cruise	14,773	14,058	14,078	17,564
Descent/Approach/Landing	1,642	788	1,102	1,222
Taxi-In	1,558	260	218	297
Total mission fuel	22,335	17,546	19,782	22,105
Total reserve fuel	5,891	4,735	3,747	4,631
Total fuel to board	28,226	22,281	23,529	26,736

Table 4.13.: Design mission fuel consumption of the four P-420 variants. Data taken from the IDT.

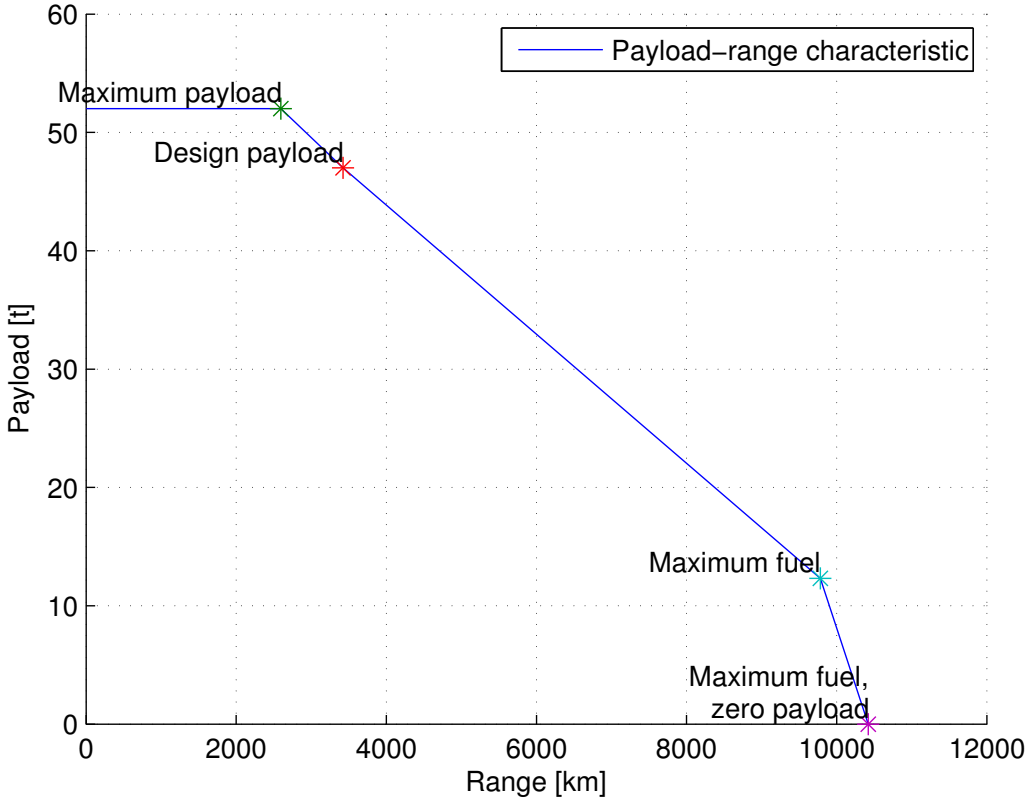

Figure 4.19.: P420/T payload-range diagram

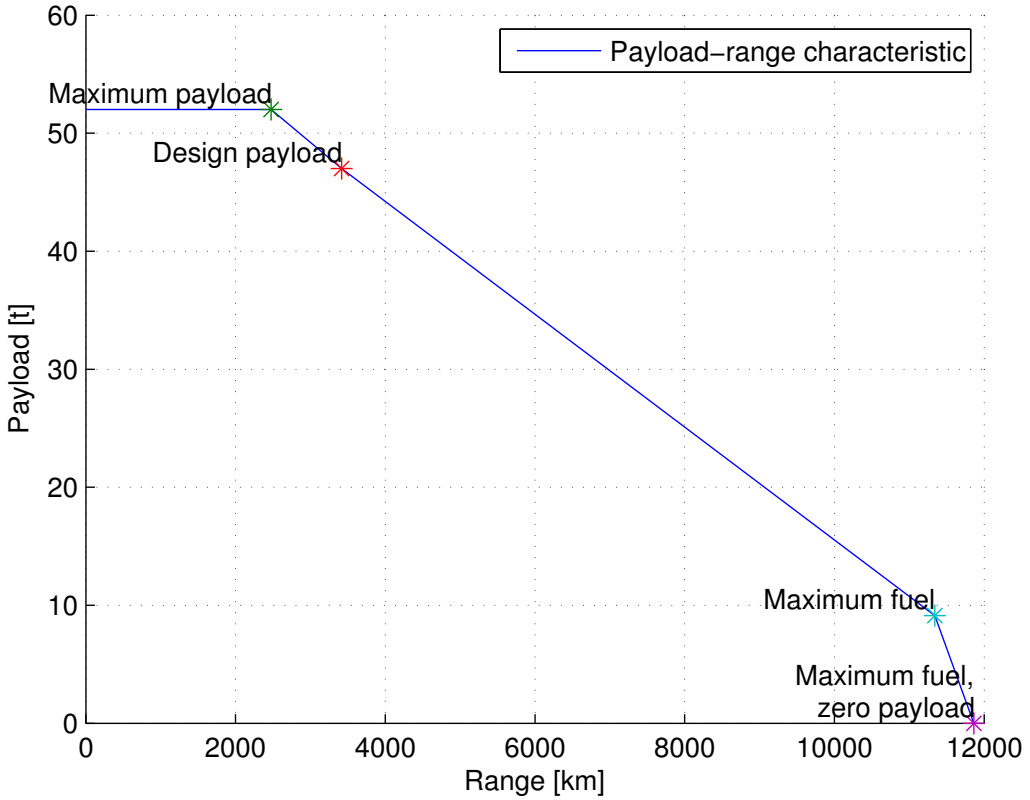

Figure 4.20.: P-420/G payload-range diagram

4.5.6. Discussion of engine number

In this thesis, the option of a two- as wells as a four-engined P-420 is analyzed. This choice was made as the requirement for the P-420 with turbofan engines was to keep changes from the P-420/B to a minimum while making the aircraft as fuel efficient as possible. A first look at the necessary thrust to fulfill all requirements deemed the possibility of creating a two-engined version next to the obvious four-engined version. The changes, advantages and disadvantages are discussed in this section.

Fuel consumption

The analysis in section 4.5.5 shows that the fuel consumption of the two versions of the aircraft differ. Generally, due to the efficiency law of gas turbines (refer to section 3.2), larger engines with higher bypass ratio are more efficient. However, the actual efficiency depends on the design of the engine. In this case, the gearbox of the PW1127G creates an advantage for the efficiency of the fan and low-pressure turbine, as they operate on optimal speeds and enable a higher bypass ratio. Overall, the P-420/G shows a better fuel efficiency.

Maintenance

Maintenance costs are a large factor for the operating costs of an aircraft. The maintenance costs of a four-engined aircraft are higher than those of a two-engined, as each engine has to be thoroughly and regularly checked. Thus, checking more engines is more cost intensive (Markou et al., 2011). These days, many airlines are retiring four-engined aircraft, like the Airbus A340 or the Boeing 747 and replacing them with new twin-engined aircraft like the Airbus A330/A350 or the Boeing 777/787 due to high maintenance and fuel cost (Kaminski-Morrow, 2013), (Haria, 2014), (CAPA, 2013), (Riva, 2013). This supports that twin-engined aircraft have an advantage in maintenance cost.

Extended-range Twin-engine Operational Performance Standards (ETOPS)

A major reason for some airlines to choose aircraft with more than two engines was to avoid the need to take long detours. To fly routes over large stretches of water or desert with no diversion airport immediately available, twin-jets need to be certified for ETOPS. This rating stipulates the maximum flight time (in minutes) which the aircraft can be distant to any airport with a runway long enough for the aircraft to land on. The manufacturer of the aircraft and engine have to prove the reliability of their products, which results in the rating. The ETOPS rating has to be incorporated during flight planning. Four-engined aircraft do not have these limitations. However, recent aircraft like the Boeing 787 have received an ETOPS rating of 330 minutes (5 hours 30 min) which is higher than the design mission flight time of the turbofan variants of the P-420 (Boeing, 2014b). The ETOPS rating is not a necessary require-

ment of this aircraft so that it is not a disadvantage for the two-engined version of the P-420.

Structural rework

When re-engining the P-420/B with four jet engines, structural changes have to be made on the wing to accommodate to the different mounting position of the engines. Jet engines are mounted on pylons under the wing, while the P-420/Bs inner engines are mounted into the leading edge of the wing. Changes for pylon-mounted engines need to be made. The general wing design for the four-engined turbofan variant is already set up to support four engines at distinct positions which is an advantage. However, changing the structural design of the wing to a twin-engined variant with heavier engines is a much bigger task and would require major structural changes to the wing and center wing box. The necessary effort for the twin-engined variant would be greater and thus the cost to do so. This is a major disadvantage of the P-420/T. Additionally, the GEnx engines of the P-420/T have a large diameter, making ground clearance an issue. The engine ground clearing of the P-420/T is only 0.5 m as shown in the three-view drawing in figure 4.21. A three-view drawing of the P-420/G is available in figure 4.22.

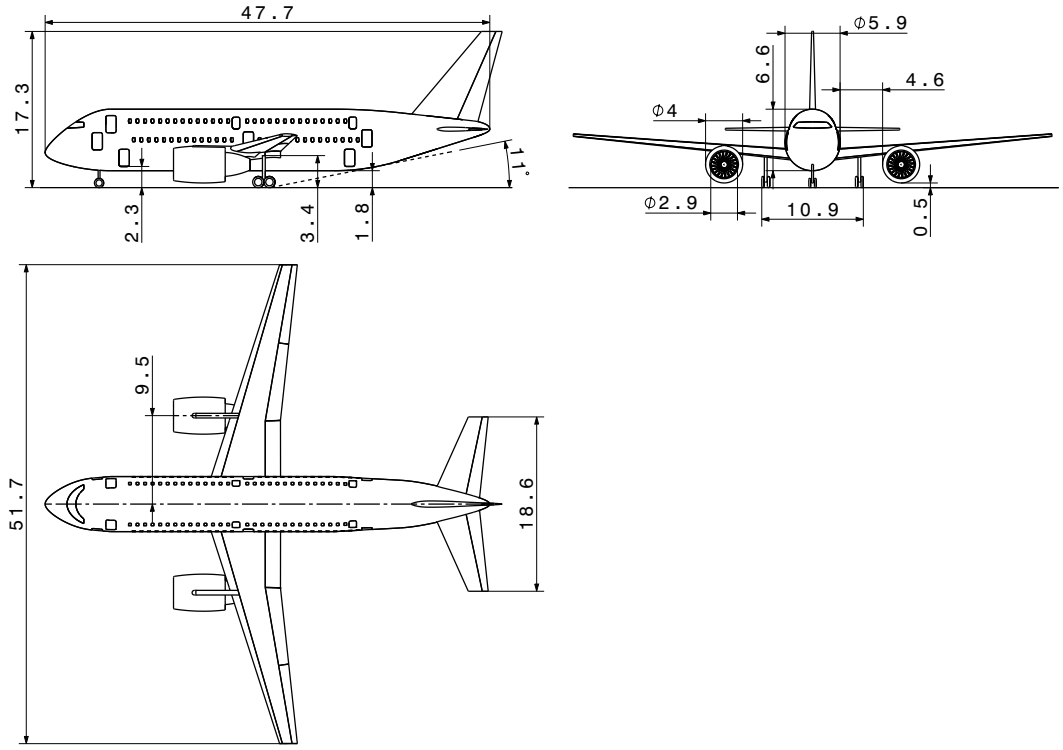

Figure 4.21.: P-420/T three-view drawing. Based on the 3D model of the P-420/A provided by Iwanizki (2014)

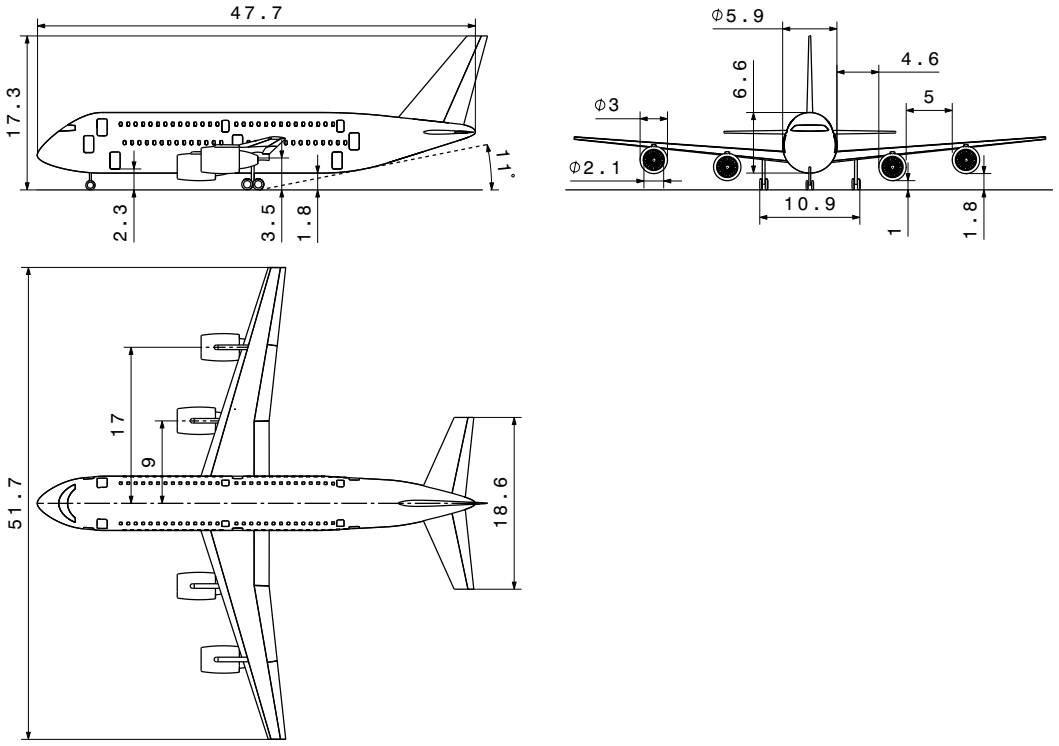

Figure 4.22.: P-420/G three-view drawing. Based on the 3D model of the P-420/A provided by Iwanizki (2014)

Performance

As explained in section 4.5.4, the balanced field length is a major criterion for engine choice. As the twin-engined variant needs more power in case of an engine failure during take-off, the twin-engined P-420/T would be, like other twin-engined aircraft, overpowered compared to the four-engined variant. This results in better climb performance, SEP and thus a higher operating altitude. The additional thrust is not necessary in any other flight condition except for the balanced field length.

Summary

Table 4.14 shows the overview of advantages and disadvantages for two- and four-engined aircraft. While the two-engined P-420/T has a slight overall advantage according to these categories, this short analysis does not provide information detailed enough for a clear choice of one of the concepts.

	Two engines	Four engines
Fuel consumption	0	+
Maintenance	+	-
ETOPS	0	0
Structural rework	-	0
Performance	+	0

Table 4.14.: Overview of engine number advantages and disadvantages

CHAPTER 5

Fuel efficiency analysis

In this chapter, the fuel efficiency of the P-420 variants is thoroughly analyzed. In order to carry out the analysis, the FCECT is used. This tool uses BADA, an aircraft performance database provided by the European Organisation for the Safety of Air Navigation (EUROCONTROL). It consists of a database of many existing aircraft. The chapter will explain the integration of the P-420 with this database and the inner workings of the FCECT. Finally, competitors are chosen and different analyzes are carried out.

5.1. Problem statement

To carry out a meaningful analysis of the fuel efficiency of different aircraft, many factors have to be taken into account. The method which is used to carry out the analysis must be valid and deliver good results. Any method relies on valid data as an input to get these results. This data must be available and of good quality to serve the method. Additionally, the parameters of the analysis must be chosen carefully to receive good results. In this context, these parameters are those of the mission profile, e.g. the payload, flight levels and altitudes as well as desired flight distance. The aircraft has to be evaluated against possible competitors in favorable and unfavorable conditions.

However, valid data is an issue as aircraft manufacturers do not publish detailed information about the performance of their aircraft. They claim that the fuel economy of their new aircraft improves upon it's predecessor or their competitor aircraft, however they do not name the exact conditions of this comparison. Nor do they give fundamental data to prove this claim.

5.2. Base of Aircraft Data (BADA)

BADA is a database of aircraft data which is built on an aircraft performance model. This model and the database are developed by EUROCONTROL BADAs. The model was developed as a tool to simulate aircraft trajectories for Air Traffic Management applications with a focus on fuel consumption (Ittel, 2014). BADA is available in two versions: BADA 3(.11) and BADA 4. The main difference in these versions is the concept and storage of the performance parameters. Fundamental to both versions is the same Total-Energy Model (see section 3.1), which is used to calculate the aircraft performance. A documentation of BADA 3.11 is to be found in EUROCONTROL (2014) and a documentation of BADA 4 can be found in EUROCONTROL (2012).

The concept of BADA is to reduce the aircraft to a point mass with forces resulting in motion of the aircraft. The key principle of this Total-Energy Model is that it is based on the SEP.

As explained by Ittel (Ittel, 2014), only BADA 3.11 is currently a suitable option for the integration of a new aircraft model, as all necessary variables which are saved in the aircraft-specific BADA files and used for the calculation by the FCECT are derivable with functions explained in the respective BADA documentation. Thus, BADA 3.11 will be used in this analysis.

5.2.1. Limitations of BADA

The BADA database and the calculation have some limitations that must be considered when used. As Ittel (Ittel, 2014) states, the BADA database does not include a parameter for the maximum fuel capacity of an aircraft. Without this parameter, it is not possible to calculate the 'maximum fuel' point of the payload-range-diagram. BADA assumes that the aircraft has no fuel capacity limit until MTOW. This limitation is not important in this thesis, as the fuel efficiency analysis will not include the payloads and ranges of the third segment of the payload-range diagram.

Another limitation is that not all existing aircraft and its versions are available in BADA. Some aircraft have different versions available, e.g. the Boeing 777-200 and 777-200ER. BADA only supports the 777-200ER. Also, some aircraft are available with different engine option, e.g. the Airbus A320 family with CFM56 or V2500 engines. Only the A320 with V2500 engines is available in BADA. In addition to this, newer aircraft like the Boeing 787-9 or Airbus A350-900 are not available at the time of writing, although both aircraft are already in commercial service.

5.3. Fuel Consumption and Emissions Calculation Tool (FCECT)

The FCECT, developed by Ittel (2014) and Engelke (2015) is a MATLAB-based software tool which transfers the methods of aircraft performance analysis described

by EUROCONTROL into a user-friendly calculation tool. The FCECT imports all available BADA aircraft files and lets the user define the type of mission the chosen aircraft should perform with the help of an input dialog. The tool then calculates the performance of the aircraft on the specified mission. Finally, it generates output-files that help the user to read and store the results of the calculation. The FCECT contains two major tools, the Global Fleet Calculator as a tool to analyze the fuel consumptions of a fleet of aircraft on a number of routes, and the Single Mission Calculator, which is of interest in this case to compare different aircraft on single, similar missions.

5.3.1. Single Mission Calculator

The Single Mission Calculator is the key element of the FCECT. It simulates single flights of aircraft with regard to fuel consumption. The full mission movements, from departure from the gate to the arrival at the gate of the destination, is calculated. The atmospheric conditions during the mission are always assumed to be ISA condition in which the geopotential altitude is always equal to the geopotential pressure altitude.

Figure 5.1 shows a flow chart of the Single Mission Calculator. First, the user enters the relevant input data. The corresponding BADA data is loaded from the database and global constants are set. In the next step, the aircraft masses are calculated. After this, the simulation begins. An iterative process to determine the optimal Initial Mission Mass, as well as the fuel consumption, characterizes this computation cycle. The Initial Mission Mass is optimized such that the mission fuel mass is still sufficient to perform the mission. In addition to the actual mission distance, the necessary fuel mass for reserves, finding an alternate airport and holding procedures is calculated. Finally, the simulation data is stored in a text file for subsequent evaluation.

Parameter	Unit
Aircraft Type	[-]
Payload Factor Seats	%
No. of Seats	[-]
Payload Factor Freight	%
Tons of Freight	t
Flight Mission Distance	km
Initial Cruise Altitude	ft
Step Climb	On/Off
Flight distance inefficiency factor	On/Off
Taxi-out time	min
Taxi-in time	min

Table 5.1.: FCECT Single mission calculator input variables. Source: Ittel (2014) and Engelke (2015)

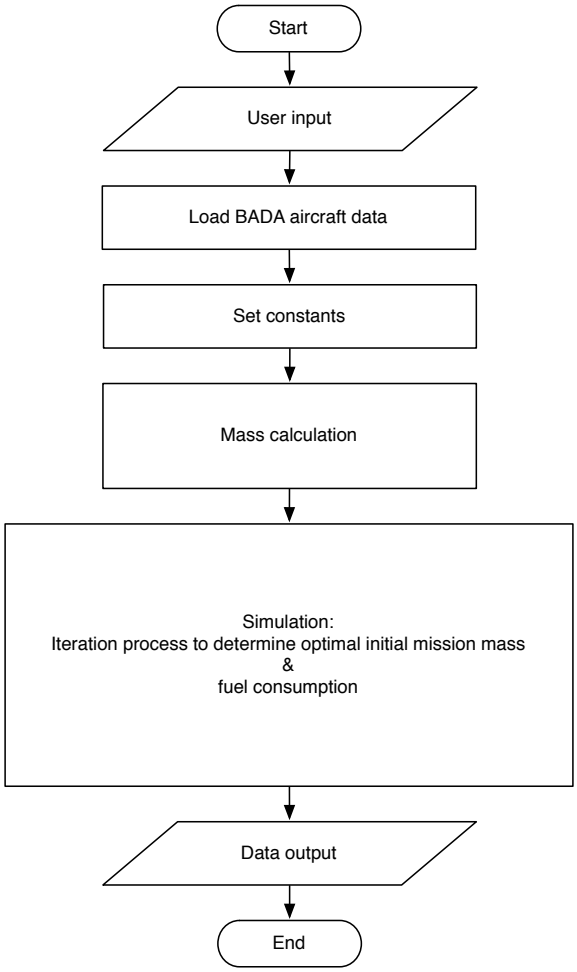

Figure 5.1.: FCECT Single Mission Calculator flowchart. Source: Ittel (2014)

5.3.2. Modifications to the FCECT

In order to deeply analyze the performance of the P-420 variants and compare them with existing aircraft, many single missions with different input parameters have to be performed. To do this in an efficient manner, some modifications were made to the FCECT.

In a new input file, the aircraft to be analyzed, the mission distance, PAX and cargo as well as the taxi-times and other input variables can be defined. The tool will automatically calculated all missions for every aircraft that is defined in this file.

Section 5.5.2 explains why the initial cruise altitude of the mission needs to be chosen as the optimum altitude for minimum fuel consumption. To find this optimal altitude, an algorithm was implemented which starts from the maximum operating altitude and lowers the altitude in 1,000 ft steps, comparing the fuel consumption to the previous altitude. Once the minimum fuel consumption is found, the algorithm stops.

Additionally, to compare the results of all performed flight missions, the most important parameters of every mission are saved into a spreadsheet. All variables are listed in appendix A.1. This can be used to plot figures, visualizing the results of the analysis.

5.4. Derivation of BADA coefficients

To implement the P-420 versions into the FCECT, aircraft-specific filesets have to be generated. Two files have to be generated, the Operations Performance File (OPF) and the Airline Procedure File (APF). A third file, the SYNONYM_ALL.LST file which contains a list of all available aircraft, has to be modified.

To generate the BADA 3.11 dataset, several parameters can be used directly from the IDT. A new MATLAB file was created, in which all essential parameters are gathered or calculated. The routine then outputs the necessary files in the exact format as specified in BADA. These files can be used like any other original aircraft files in the FCECT.

The integration and derivation of the coefficients is based on the approach by Ittel (Ittel, 2014) who integrated an early version of the P-420/A aircraft into BADA. The derivation of BADA coefficients is provided by EUROCONTROL (2009) Some parameters that were not available during the initial approach were estimated by Ittel. However, most of these parameters are now available through the IDT and can be included to create a comprehensive and accurate set of BADA files for the various P-420 versions. Additionally, as the process is now automated, it is easy to quickly calculate various missions with changed configurations of the P-420.

5.4.1. OPF

The OPF contains most of the aircraft performance data. It is divided into eight blocks, which are explained below. The OPF files of the four P-420 variants are displayed in appendix A.2.

File identification block

The file identification block contains the file name, the date of creation and the date of modification of the file. As all files are newly generated and never updated, the current time is used to fill in both the date of creation and the date of modification. The file name is in the same format as the other BADA files, derived from the ICAO code for an aircraft, e.g. 'A321__.OPF' for the Airbus A321 or 'B738__.OPF" for the Boeing 737-800. According to this scheme, the name for the P-420, e.g. P42G is specified in the aircraft definition file and this variable is used.

Aircraft type block

The aircraft type block contains the full name of the aircraft as well as the name of the engine type. Additionally, once again, the ICAO-code style short aircraft name is displayed. Furthermore the number of engines and the type of propulsion, 'Jet', 'Turboprop' or 'Piston' is set. All these parameters are available from the aircraft definition file of the IDT and are written into the BADA file accordingly.

Mass block

In the mass block, four parameters are necessary. These are the 'reference' mass, the 'maximum' mass, the 'minimum' mass and the maximum payload mass. The reference mass is set at 5,000 kg below MTOW as a typical take-off weight. The maximum mass equals the MTOW, which is calculated in the IDT after Torenbeeks method. The minimum mass equals the OME, which is also calculated in the IDT after Torenbeeks method. The maximum payload mass is the maximum number of PAX multiplied with the weight per PAX plus the maximum cargo mass. These are defined in the IDT aircraft definition file.

Flight envelope block

The flight envelope block contains parameters about the flight envelope of the aircraft. These are the maximum operating Calibrated Airspeed (CAS), Mach and altitude as well as the service ceiling. Values for maximum operating Mach and altitude are available through the IDT in the algorithm of SEP calculation. The parameter of service ceiling is set to an altitude with 100 fpm remaining SEP, however BADA expects the parameter for 300 fpm remaining SEP. The calculation is changed accordingly to calculate the correct service ceiling for BADA. The parameter of maximum operating CAS is not implemented in the IDT. However, the FCECT does not make use of this parameter, which is why it is not necessary.

Aerodynamics block

The aerodynamics block contains parameters describing the aerodynamic characteristics of the aircraft. It contains the surface area of the wing as well as different drag parameters for different configurations of the aircraft during flight. The surface wing area is defined in the aircraft definition file. The drag parameters consist of a table of each the stall speed, the parasitic drag CD0 and the lift-induced drag CD2 for the five configurations during (1) take-off, (2) initial climb, (3) cruise, (4) approach and (5) landing. Furthermore, the additional drag due to the extended landing gear in landing configuration needs to be specified. The IDT provides all drag values in the aerodynamics calculation as they are also necessary for the included performance analysis. However, the IDT automatically incorporates the additional parasitic drag of the landing gear which has to be subtracted and put into the corresponding BADA term. The stall speed for take-off and initial climb configuration are set as the same

value, as further values are not calculated in the IDT. This is the same for approach and landing configuration. This assumption is acceptable, as the FCECT does not rely on this data. Ittel set these values to zero in his work.

Engine thrust block

The engine thrust block contains parameters describing the engine thrust characteristics of the aircraft. These are three maximum climb coefficients, five descent thrust coefficients as well as descent CAS and Mach number. The maximum thrust during climb in BADA is calculated according to equation 5.1 for jet aircraft and equation 5.2 for turboprop aircraft, which use three coefficients C_{Tc}. The engine model in the software program provides thrust as a function of Mach number and altitude. The three coefficients can be found with generating a solvable system of three equations and three unknown variables. Thus, the equations are evaluated using three data points. Here, Ittel's approach of setting the altitude H_p to 1,000 m, 4,000 m and 7,000 m is followed. The corresponding maximum thrust values are calculated. The set of equations is then solved by MATLABs 'fsolve' function to acquire the three values for the maximum climb thrust coefficients C_{Tc}. As the coefficients and equations differ for turboprop and jet aircraft, both sets of equations are implemented.

$$Thr_{max,CL,Jet} = C_{Tc,1} \cdot \left(1 - \frac{H_p}{C_{Tc,2}} + C_{Tc,3} \cdot H_p^2\right) \tag{5.1}$$

$$Thr_{max,CL,Turboprop} = \frac{C_{Tc,1}}{V_{TAS}} \cdot \left(1 - \frac{H_p}{C_{Tc,2}}\right) + C_{Tc,3} \tag{5.2}$$

The five descent thrust coefficients are the fraction of the available maximum thrust used during descent in four configurations (high altitude descent, low altitude descent, approach and landing). The fifth value is the transition altitude during descent. These values are directly available from the performance analysis part of the IDT.

Parameter	Altitude [ft]
High altitude descent	300 below cruise altitude
Low altitude descent	3000
Approach	1000
Landing	0
Transition altitude	Evaluated in IDT mission

Table 5.2.: Descent thrust coefficient altitudes

Descent CAS and Mach number are directly available from the aircraft definition file and are adopted to the OPF file.

Fuel consumption block

The fuel consumption block describes the fuel consumption characteristics of the aircraft. It consists of two thrust specific fuel consumption coefficients, two descent fuel flow coefficients and the cruise correction coefficient.

Similarly to the maximum climb thrust coefficient, BADA calculates the SFC with an equation consisting of two parameters C_{f1} and C_{f2}, equation 5.3 for jet aircraft and equation 5.4 for turboprop aircraft. Another set of two equations is created with SFC at two points: at loiter altitude and the corresponding Mach number as well as cruise altitude and corresponding Mach number. The set of equations is solved with the 'fsolve' function provided by MATLAB and the two SFC coefficients C_f are found.

$$\eta_{Jet} = C_{f1} \cdot \left(1 + \frac{V_{TAS}}{C_{f2}}\right) \tag{5.3}$$

$$\eta_{Turboprop} = C_{f1} \cdot \left(1 - \frac{V_{TAS}}{C_{f2}}\right) \cdot \left(\frac{V_{TAS}}{1000}\right) \tag{5.4}$$

The cruise fuel flow correction coefficient is set to unity as the SFC coefficients were evaluated at cruise condition.

The fuel flow during descent is directly available from the performance calculation of the IDT. Again, BADA calculates the descent fuel flow with equation 5.5 which consists of two coefficients C_{f3} and C_{f3}. Similarly to the SFC coefficients, a set of two equations is created and evaluated at two specific descent altitudes (3,000 ft and 25,000 ft) to calculate the two descent fuel flow coefficients. In this case, the equation for both turboprop and jet aircraft is the same.

$$FF_{min} = C_{f3} \cdot \left(1 - \frac{H_p}{C_{f4}}\right) \tag{5.5}$$

Ground movements block

The last block of the OPF is the ground movements block. It contains the values for take-off length, landing length, wingspan and overall length of the aircraft. Wingspan and overall length of the aircraft are directly available from the aircraft definition file. take-off and landing length are calculated in the performance section of the IDT and thus directly available as well.

5.4.2. APF

The APF contains the speed schedule of the aircraft. The APF files of the four P-420 variants are displayed in appendix A.1.

The speed schedule of the P-420 is defined in the APF. For the three flight phases 'climb', 'cruise' and 'descent', the speed can be defined via three values each, a low

altitude CAS, a high altitude CAS and a Mach number (above transition altitude). Each flight phase can be defined for different aircraft masses. The FCECT only works with the 'average' aircraft mass which is why the other values are set equal to that of the average aircraft mass. Additionally, in this case, no distinction is made between the two CAS below transition altitude. Thus, these two parameters are always the same. The speeds are defined in the aircraft definition file of the IDT and are taken from there. Similar to the OPF, filename, creation date and modification date are written into the header of the file.

5.4.3. SYNONYM_ALL.LST file

In order for the FCECT to include the newly generated BADA files of the P-420, the SYNONYM_ALL.LST file has to be extended with a line containing the following information. The file is a list of all available aircraft that can be chosen for analysis with the FCECT.

- ICAO code of aircraft
- Full aircraft name and manufacturer
- Filename of the corresponding OPF and APF

An example for line the P-420/G looks like this:

```
CD - P42G   P-420G        LLS-TUM            P42G__
```

5.5. Analysis

In this section, the detailed analysis of the performance of the different P-420 versions compared to existing competitor aircraft will be discussed.

5.5.1. Competitor aircraft

In this section, possible competitors of the P-420 are introduced and chosen for comparison in the fuel efficiency analysis.

Single-aisle aircraft

Single-aisle aircraft like the Airbus A320 family and Boeing 737 family are the most commonly used aircraft on short to medium haul routes. These aircraft are used on many routes which the P-420 was designed for. However, they do not have the same passenger capacity as the P-420. On the other hand, some versions of these aircraft are able to fly much longer routes than the P-420 was designed for.

Airbus A320 family As the P-420 can transport 420 PAX, a worthy competitor would be an aircraft which can deliver the same transport capacity with the least number of flights. For that reason, out of the A320 family, the A321 with a maximum capacity of 220 seats is the best competitor, as it can provide the same transport capacity with two flights. Airbus announced the A321NEO (New Engine Option) with new engines and a number of other improvements to make the aircraft more efficient. Additionally, through optimized seating layout, the maximum capacity is increased to 240 seats. In order to match the transport capacity of the P-420, the aircraft needs to fly the same route twice. The smaller A320 has a maximum seat capacity of 180 (189 for the NEO version), which does not match the capacity of the P-420 on two flights. As the A321NEO is not in service yet, BADA data is not yet available. However, through careful modification of the BADA files, the performance can be estimated. To do this, the original A321 file was changed in a way to adjust the OME, MTOW, wing span and length. Additionally, the fuel consumption parameters were lowered by 15% to imitate the better fuel efficiency. The new BADA-fileset was tested to validate the lower fuel consumption. Further technical data for both aircraft is available in table 5.3 with data from the BADA-fileset, AIRBUS (2014a), and AIRBUS (2015a).

Boeing 737 family The variant of the Boeing 737 family which can best match the P-420s seat capacity is the 737-900, and the successor 737 MAX 9, which are direct competitors of the A321/A321NEO. Both aircraft have a maximum seating capacity of 220 PAX. The 737 MAX 9 BADA fileset was created in line with that of the A321NEO, having 15 % less fuel consumption. Further technical data for both aircraft is available in table 5.3.

Parameter	A321ceo	A321neo	737-900	737 MAX 9
MTOW [kg]	93,500	93,500	85,130	88,314
Fuselage length [m]	44.51	44.51	42.1	42.2
Wing span [m]	35.80	35.80	35.7	35.9
Max. PAX	240	240	220	220
Cruising speed [Mach]	0.78	0.78	0.79	0.79
Range [km]	5,950	6,760	5,665	6,658
Engines (2x)	V2500-A5 CFM56-5B	PW1100G CFM LEAP	CFM 56-7B27	CFM LEAP

Table 5.3.: Single aisle competitor aircraft data. Data sources: BADA-filesets, Boeing (2013b), Boeing (2014c), Trimble (2012), Dwyer-Lindgren (2014)

Long haul aircraft

Long haul aircraft are designed for intercontinental routes while carrying more passengers than single-aisle aircraft. Both leading aircraft manufacturers Airbus and Boeing offer aircraft in this market and almost exclusively share it.

Airbus A330 family Airbus offers the two-engined A330 in various versions, the shorter A330-200 with up to 404 PAX and the A330-300 with up to 440 seats. Just as with the A320 family, Airbus announced a 'NEO' of both A330 versions. With new engines as well as additional improvements, the manufacturer claims an improved fuel burn by 11 % (Kaminski-Morrow, 2014). Additionally, the 'A330 regional' was announced, an optimized version for short and medium routes with large passenger capacity (Airbus, 2013), (Airbus, 2014a). Few characteristic numbers are available, however some sources claim that the A330 regional will have a lower OME due to less fuel tank systems as well as smaller, less powerful engines (Hamilton, 2013), (AIRBUS, 2013), (Bhaskara, 2014). Although originally intended for longer routes, this aircraft might be a competitor of the P-420 in the short to medium haul market where large capacity is needed. Technical data of the A330 versions is available from table 5.4. The BADA-filesets for the A330-800neo, -900neo and regional were created with the information available from the mentioned sources.

Parameter	A330-200	-300	-800neo	-900neo	regional
MTOW [kg]	242,000	242,000	242,000	242,000	205,000
Fuselage length [m]	58.82	63.69	58.82	63.69	63.69
Wing span [m]	60.3	60.3	64	64	64
Max. PAX	404	440	404	440	440
Cruising speed [Ma]	0.82	0.82	0.82	0.82	0.82
Range [km]	13,400	11,300	13,797	11,482	5556
Engines (2x)	CF6-80E1 PW4000 Trent 700	CF6-80E1 PW4000 Trent 700	Trent 7000	Trent 7000	Trent 7000

Table 5.4.: Airbus A330 aircraft data. Data sources: BADA-filesets, Airbus (2015a), Airbus (2015b), Airbus (2014), Leahy (2014), Kaminski-Morrow (2014), Airbus (2013), Airbus (2014a), Hamilton (2013), AIRBUS (2013), Bhaskara (2014)

Boeing 767 and 787 In the same market segment of the A330 are Boeing's products, the 767 and 787. As the 767-400 features an almost identical wingspan and similar MTOW, a comparison with the P-420 is expected to be valuable. However, it was designed for long-haul routes, especially the transatlantic flights and has a maximum passenger capacity of only 375. Some airlines are starting to retire their 767 in favor of more fuel efficient aircraft. The successor of the 767 is the 787, with many parts made of Carbon Fibre Reinforced Plastic (CFRP) to decrease mass as well as latest generation engine technology. The 787-9 with a maximum certified passenger capacity of 420 (FAA, 2014) matches that of the P-420 and is analyzed as the best competitor. Technical data of the 767-400 and 787-9 is available from table 5.5 with data from the sources above, the BADA-fileset, as well as Boeing (2005), Boeing (2011) and Boeing (2013c). The BADA-filesets for the 787-9 was created on basis of the existing fileset of the 787-8 with the information available from the mentioned sources.

Boeing 777 Boeing also offers the 777 family, a series of wide-body long range aircraft. The 777 is larger than the 787 and can carry more passengers with the 777-200 of up to 440 and the 777-300 of up to 550 passengers. Boeing announced plans for improved and re-engined variants of the 777, dubbed 777-8X and 777-9X which supposedly burn 16 % less fuel than their respective predecessors (Tsang, 2011). It was chosen to analyze the performance of the 777-200 and the 777-8X for this analysis, as they match the P-420s seating capacity with lower structural weights, promising less fuel burn. This has been validated with a quick analysis using the single mission calculator of the FCECT. Technical data of the 777-200 and 777-8X is available from table 5.5. The BADA-filesets for the 777-8X was created with the information available from the mentioned sources on the basis of the available fileset of the 777-200.

Parameter	767-400	787-9	777-200	777-8X	A350-900
MTOW [kg]	204,120	253,000	247,200	351,500	268,000
Fuselage length [m]	61.4	62.8	63.7	69.5	66.89
Wing span [m]	51.9	60.1	60.9	71.8	64.8
Max. PAX	375	420	440	440	440
Cruising speed [Ma]	0.80	0.85	0.84	0.84	0.85
Range [km]	10,418	15,400	9,700	17,224	14,350
Engines (2x)	PW4062 CF6-80C2	GEnx-1B Trent 1000	PW4077 RR877 GE90-77B	GE9X	Trent XWB

Table 5.5.: Long haul aircraft data. Data sources: FAA (2014), BADA-filesets, Boeing (2005), Boeing (2011), Boeing (2013c), Boeing (1998), Boeing (2009) and Boeing (2013a), Tsang (2011)

Airbus A350 Airbus' answer to the success of the 777 is the A350, a large twin-engined jet. The A350-900 with a maximum passenger capacity of 440 is the right competitor for the P-420. Similar to the Boeing 787, it features modern materials and engines to reduce weight and fuel consumption. Although already in service, no official BADA datasheet is available for the analysis. The BADA-filesets for the A350-900 was created with the information available from the mentioned sources. Technical data of the 767-400 and 787-9 is available from table 5.5.

Airbus A380 and Boeing 747 The largest variants of the long haul aircraft market are the Airbus A380-800 as well as the Boeing 747-400 and the newer, overhauled 747-8I. With a maximum passenger capacity of 853 (A380), 660 (747-400) and 605 (747-8I), all three aircraft can carry more passengers than the P-420. However the A380-800 as well as the 747-400 are currently operated on short and medium routes (see section 5.5.2), which is why these aircraft will be compared to the P-420 as well. Technical data of the 747-400, 747-8I and A380-800 is available from table 5.6.

Parameter	747-400	747-8I	A380-800
MTOW [kg]	396,890	448,000	575,000
Fuselage length [m]	70.6	76.3	72.73
Wing span [m]	64.4	68.5	79.75
Max. PAX	660	605	853
Cruising speed [Ma]	0.85	0.855	0.85
Range [km]	13,450	14,800	15,700
Engines (4x)	PW 4056 CF6-80C2B1F RB211-524H	GEnx-2B67	GP7270 Trent 970/B Trent 972/B

Table 5.6.: Very large aircraft data. Data sources: BADA-filesets, AIRBUS (2015b), Airbus (2014b), Kingsley-Jones (2006), Boeing (2002), Boeing (2012), AIRBUS (2014b)

Turboprop aircraft

As the P-420/B and /C are a turboprop aircraft for short routes, it should be compared to other available turboprop aircraft. The largest modern currently operated turboprop aircraft are the Bombardier Dash 8 and the ATR 72.

Bombardier Dash 8 The Bombardier Dash 8 Series 400 is the largest modern passenger turboprop aircraft. With a high wing configuration this small aircraft is comparably lightweight. However, with a maximum capacity of 86 passengers, it has to fly 5 times to transport the 420 PAX the P-420 can transport in a single flight. The range of the Dash 8 is only 2500 km with a typical payload. Technical data is available from table 5.7.

Parameter	Dash 8	ATR 72
MTOW [kg]	29,260	22,800
Fuselage length [m]	32.81	27.17
Wing span [m]	28.4	27.05
Max. PAX	86	74
Cruising speed [kn]	360	275
Range [km]	2,522	1,528
Engines (2x)	PW150A	PW127F

Table 5.7.: Turboprop aircraft data. Data sources: BADA-filesets, Bombardier (2014a), Bombardier (2014b), ATR (2014a), ATR (2014b)

ATR 72 The ATR 72-600 is turboprop short-haul airliner and a direct competitor of the Dash 8. However, with a maximum passenger capacity of 74 and a maximum range of about 1500 km it is even more limited than the Dash 8 and has to fly the

same route six times to match the transport capacity of the P-420. Technical data is available from table 5.7.

5.5.2. Mission parameters and boundary conditions

Carefully chosen boundary conditions are a prerequisite for valid results of an analysis. The mission parameters can be set in the input dialog of the FCECT tool. These will be explained in the following sections.

Payload

The payload is the carrying capacity of the aircraft measured in terms of weight. The payload is divided into PAX and cargo with a payload factor each.

In order for a fair comparison of the fuel efficiency of the different aircraft models, all aircraft must transport the same payload over a certain distance. Smaller aircraft may need to perform more than one flight to achieve this.

Two payload configurations were chosen to carry out the analysis. The first one is the design payload of the P-420 with 420 PAX and 5 tons of cargo. The other aircraft are configured accordingly in order to transport the same total amount of payload. As explained in section 5.5.1, smaller aircraft that cannot transport the payload in one flight have to perform multiple flights. In this case, the PAX and cargo are split evenly between all flights. This payload configuration is the most advantageous for the P-420 as it was specifically designed for this transport capacity.

A second configuration puts the P-420 into a less advantageous position. For this the payload factors are both set to 75%. This means that 315 PAX and 3.75 tons of cargo must be transported by each aircraft type. Again, the other aircraft are configured accordingly and smaller aircraft have to perform multiple flights to accomplish the goal.

Flight mission distance

The flight mission distance, measured in km, is an important factor to analyze the fuel efficiency of an aircraft type. Different aircraft types are designed for specific flight mission distances. Each aircraft has a "design mission point" at which it reaches its best performance and efficiency. However, deviations from the design mission may result in a different fuel efficiency. An example is a long-haul aircraft which was designed for flight mission distances of around 10,000 km and very efficient at this distance. However on short routes of e.g. 1,500 km the efficiency may be lower, as the aircraft now carries the weight of empty fuel tank that it does not need for this mission.

For the analysis, a wide range of flight mission distances from 500 km to 3,500 km in steps of 500 km was chosen. This spectrum covers all possible routes of the P-420.

Basis for the determination of the design range of the P-420 was the analysis of database of flight movements (Iwanizki, 2014), OAG (2014). The result of this

analysis carried out by Iwanizki was that 90% of flight movements had a distance of less than 3,000 km.

Examples for actual routes are shown in the following. The world's busiest route in terms of passengers per year is the route from Seoul-Gimpo (Republic of Korea) to Jeju-do (Republic of Korea) with a direct distance of only 450 km but more than 10 million passengers per year (Amadeus, 2013). Local carriers Asiana Airlines and Korean Air use large aircraft like Boeing B747-400 (365 seats) or Airbus A330-300 (290 seats) on this route (Korean Air, 2015b), (Korean Air, 2015a), (Asiana Airlines, 2015b), (Asiana Airlines, 2015a). Further examples of routes are available in 5.8, e.g. Tokyo to Okinawa in Japan (1,500 km and 4.5 million PAX p.a.), which is served by Japan Airlines with Boeing B777-300 aircraft in 500 seats domestic configuration (Japan Airlines, 2015a), Japan Airlines (2015b). An example for a longer route is Singapore to Hong Kong (2,600 km) which is served by Singapore Airlines with Airbus A380-800 (471 seats) and other widebody jets from other airlines multiple times daily (Singapore Airlines, 2015a), (Singapore Airlines, 2015b).

Route	PAX 2012 (Thoursands)	Growth 2011-2012
Jeju-Seoul	10,156	2 %
Sapporo-Tokyo	8,211	8 %
Rio de Janeiro-Sao Paulo	7,716	-1 %
Beijing-Shanghai	7,246	7 %
Melbourne-Sydney	6,943	-2 %
Osaka-Tokyo	6,744	-11 %
Fukuoka-Tokyo	6,640	-3 %
Hong Kong- Taipei	5,513	2 %
Okinawa-Tokyo	4,584	12 %
Cape Town-Johannesburg	4,407	-1 %

Table 5.8.: Top 10 global air travel busiest routes by passenger volume. Data source: Amadeus (2013)

Initial cruise altitude

The initial cruise altitude is the altitude to which the aircraft climbs until it enters the horizontal cruise flight. The optimal initial cruise altitude for highest efficiency is dependent on aircraft type, payload, mission distance and airspeed. However, cruise altitude is given by the Air Traffic Control (ATC) and depends on weather, traffic situation and other variables. A pilot may request a different cruise altitude for higher efficiency. However, this is mostly practiced on long intercontinental routes only.

For the analysis, it is assumed that the initial cruise altitude is the optimal altitude for each aircraft type. As a fixed initial cruise altitude might be an advantage or disadvantage for any aircraft type, it would be unfair to compare those. Additionally, typical cruise flight altitudes are different between jet and turboprop aircraft. Due to their propulsion type, the thrust of turboprop aircraft decreases in higher altitudes

and speeds which respectively limits the cruise altitude. The optimal initial cruise altitude with lowest fuel consumption is iterated, as explained in section 5.3.2.

Additionally, a sensitivity analysis will be performed to assess the magnitude of differences in fuel consumption a different initial cruise altitude would create, see section 6.

Step climb

The step climb describes the change of altitude of an aircraft over the course of a mission. It results from the balance of forces of the aircraft. While burning fuel, the aircraft loses mass, lowering the gravitational force. Less lift is necessary to keep the airplane at the same altitude. Thus, the forces are changing (refer to section 3.1). To compensate this change, there are three possibilities:

- lower the airspeed, which is not desirable
- lower C_L which, if the flight is performed at maximum aerodynamic efficiency, is not desirable
- lower ρ, which results in a higher altitude

As two airplanes flying into the same direction must have a minimum vertical distance of 1,000 ft up to FL290 or up to FL410 if aircraft and airspace are operated under 'Reduced Vertical Separation Minimum'. Else, the minimum vertical distance is 2,000 ft (United States Department of Transportation, 2008).

Ittel analyzed the actual step climbs of aircraft, which shows that the average distance between step climbs of an Airbus A340-300 aircraft is 3,189 km. This is almost the maximum flight mission distance for this analysis, and the impact of a single step climb shortly before descent is negligible. Additionally, as the analyzed routes show heavy traffic, it is less likely that ATC would allow changes of cruise altitude of the aircraft.

Accordingly, the step climb is deactivated for this analysis.

Flight distance inefficiency factor

The flight distance inefficiency factor multiplies with the flight mission distance. In real flight operations, aircraft can never fly a perfect straight line between the origin and destination airports. Already the approach on specific airways add some distance to the actual flight distance. Additionally, restricted areas or fixed airways increase the actual flight distance. As this analysis compares the aircraft types in the BADA files but not with actual airport distances or real flight data, the factor does not impact the results as all types would fly a longer mission. However, the readability of the results would be impacted negatively. For an easier understanding of the results, this factor is deactivated.

Taxi times

Taxi times play an important role for overall mission fuel consumption, especially for short-haul flights. The time an aircraft spends during taxi depends on the airport layout, traffic congestion, weather and delay situation. Average taxi times are thus hard to estimate. The ICAO LTO suggests a total taxi time of 26 minutes (International Civil Aviation Organization, 2008). This is used to calculate local airport emissions. For this analysis, this total taxi time is split into a taxi-out time of 16 min and a taxi-in time of 10 min, as usually the time from touch-down to the parking position is shorter than that to the runway and waiting for departure. The impact of the taxi times however will be analyzed in the sensitivity analysis, as very long or short taxi times can influence the total mission fuel consumption.

Airspeed

The airspeed of the aircraft is another important factor of the efficiency analysis. With different airspeed, the aircraft has other fuel efficiency as the drag increases. Flying slower creates less drag, but also less lift. Due to this, the aircraft might need to lower the cruise altitude, where drag subsequently increases. While the purpose of aircraft is to transport payload relatively fast, the time lost by flying slower is not substantial for the overall mission time on short missions. During the analysis, all aircraft will fly at their design airspeed. In a sensitivity analysis, the impact of changing airspeed will be analyzed.

Summary

The missions to be analyzed with the chosen aircraft are listed below. Table 5.9 summarizes the necessary FCECT parameters and missions that were defined for the analysis.

List of aircraft compared in the fuel efficiency analysis:

- Propcraft P-420: /B, /C, /G, /T
- Single-aisle: A321ceo, A321neo, 737-900, 737 MAX 9
- Turboprop: ATR 72-600, Dash 8-400
- Two-engined wide-body: A330-200, A330-300, A330-800neo, A330-900neo, A330 regional, 787-9, 767-400, 777-200ER, 777-8X
- Four-engined wide-body: 747-400, 747-8I, A380-800

5.6. Results

In this section, the results of the analysis are described, analyzed and discussed. The section gives an overview of the results of the analysis divided by the payload definition. In addition, the design mission of the P-420 is analyzed in depth. Furthermore,

Parameter	Mission 1	Mission 2
Flight mission distance (FMD) [km]	500 - 3500	
FMD step [km]	500	
Flight distance inefficiency factor	off	
PAX	420	315
Cargo [t]	5	3.75
Initial cruise altitude	optimal	
Step climb	off	
Taxi-out [min]	16	
Taxi-in [min]	10	

Table 5.9.: Mission definition summary

a comparison only between the different P-420 versions is carried out. Finally, the results are summarized and discussed.

The output of the FCECT calculation is a textfile with information about the input and output parameters for a single mission each. It also includes a detailed course of the aircraft during the single mission. All parameters are listed in table A.2. The most interesting parameter for the fuel efficiency analysis is the mission fuel consumption. This parameter describes the burned fuel during the mission. The value is converted into a cargo- and PAX-specific fuel consumption for easier comparison.

Additionally to the textfiles of the FCECT, a spreadsheet containing all information from table A.1 is generated for each flight mission.

5.6.1. 420 PAX and 5 t cargo

This section shows the analysis results for the mission with 420 PAX and 5 t cargo for all mission distances and aircraft.

Figure 5.2 visualizes the total fuel consumption to deliver the payload of 420 PAX and 5t of cargo over all specified mission distances. All aircraft consume more fuel with larger mission distances, with a seemingly linear trend. It is clearly visible that the larger aircraft consume the most fuel. Especially the Airbus A380-800 and the two Boeing 747 versions stick out in this plot. The two turboprop aircraft ATR 72-600 and Dash 8-400 are only seen in the bar graph for 500 km mission distance. Due to the high payload factor, both aircraft cannot perform longer mission distances than 500 km. The P-420s have the lowest fuel consumption of all aircraft at 500 km, however other aircraft like the 737 MAX 9 and the A330neos have a similar fuel consumption at 3,500 km.

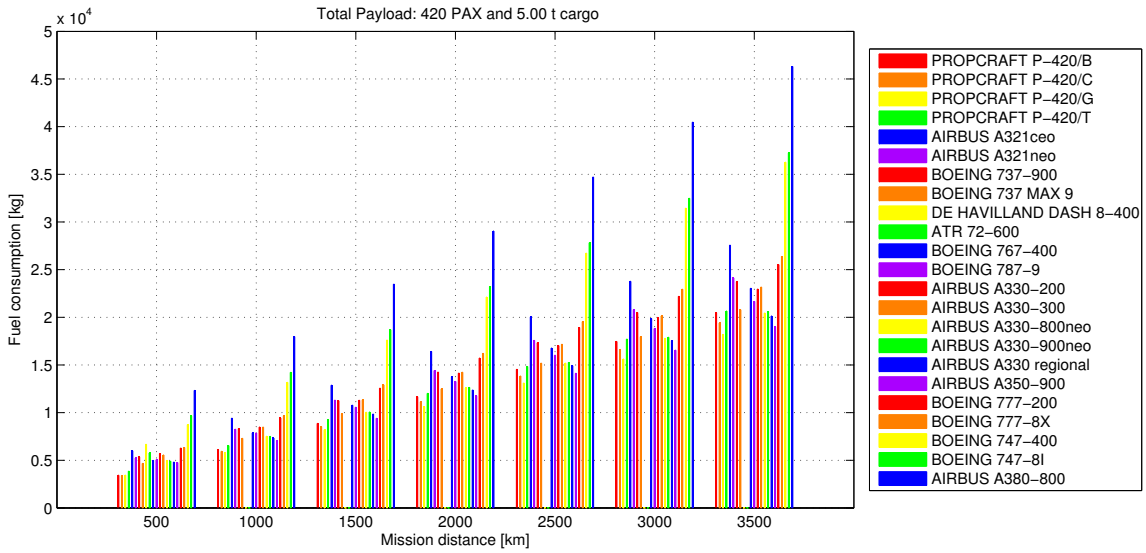

Figure 5.2.: Overview of total fuel consumption for all mission distances and aircraft with a payload of 420 PAX and 5 t cargo

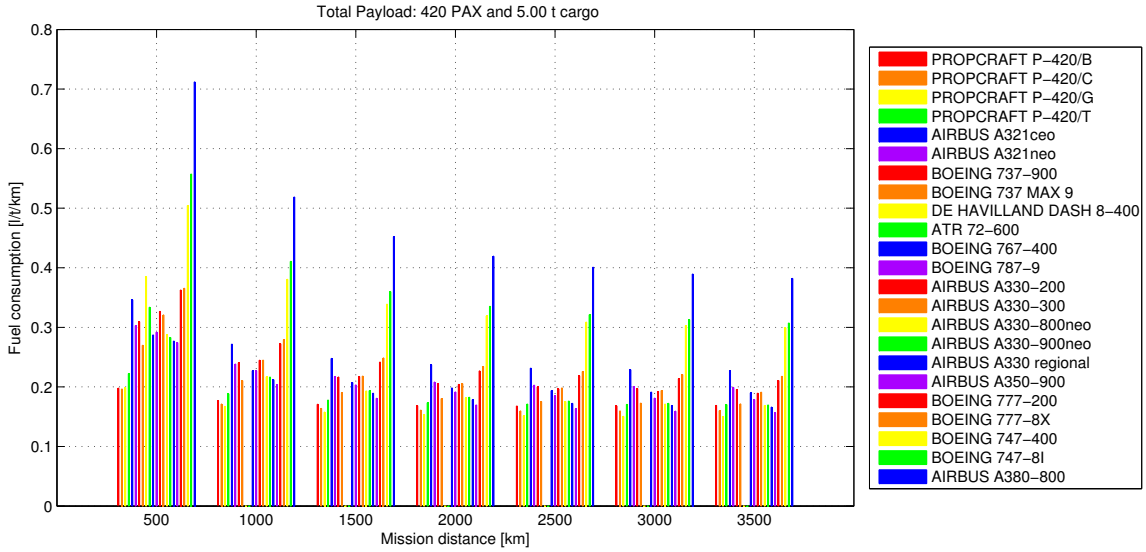

Figure 5.3.: Fuel consumption [l/t/km] for all mission distances and aircraft with a payload of 420 PAX and 5 t cargo

Figure 5.3 shows the fuel consumption in liters per ton of payload and km. The general trend of the fuel consumption over the mission distance is hyperbolic, where the gradient of the curve is higher at the beginning and tends towards zero with higher mission distance. This trend is much stronger for large aircraft like the Airbus A380 and Boeing 747. This trend is due to the relatively high fuel consumption during take-off and climb. With longer mission distance, the importance of take-off and climb becomes less significant and the overall fuel consumption shows little deviation. Additional to that, the larger aircraft were designed for high passenger capacities and long mission distances and are not as efficient with this comparatively

low payload. Again, the P-420s are leading the fuel consumption at short mission distances with other aircraft catching up as the distances are getting longer. The most competitive aircraft are the A321neo, the Boeing 737 MAX 9, the 787-9 and the A330neos as well as the A350.

A common and popular unit to compare fuel efficiency of different aircraft is the fuel consumption in liters per PAX and 100 km which is shown in figure 5.4. For the calculation it is assumed that the additional cargo is distributed evenly to all PAX.

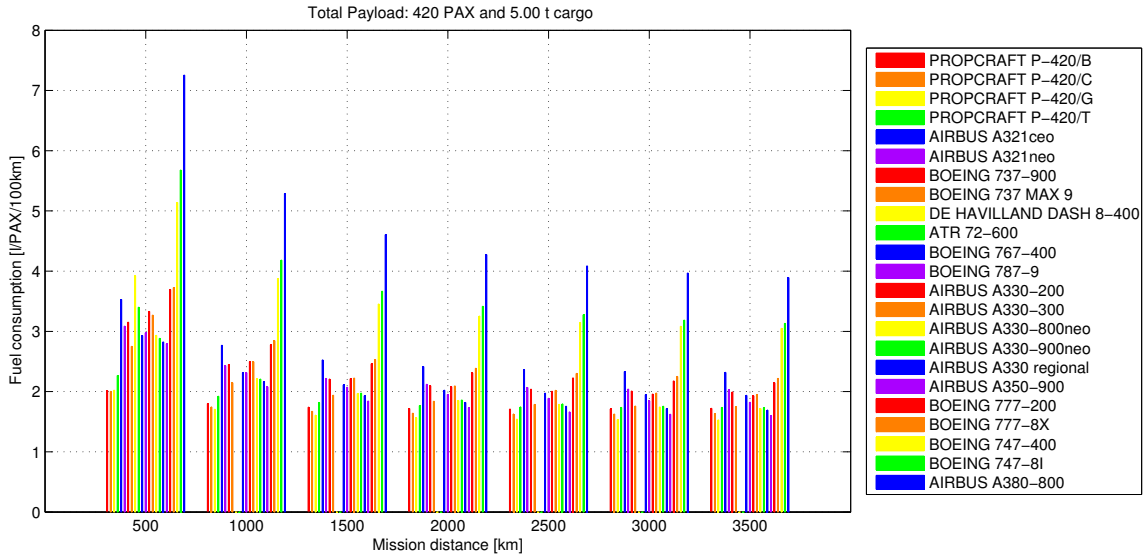

Figure 5.4.: Fuel consumption [l/PAX/100km] for all mission distances and aircraft with a payload of 420 PAX and 5 t cargo

The general trend of the graph is almost identical to that of figure 5.3, however the actual numbers are of interest here. It is visible that the P-420s have a fuel consumption of less than 2 liters per PAX and 100 km at 500 km mission distance, where other aircraft show 3 or more liters. The large aircraft consume more than 2 to 3 times the amount on this distance. With increasing mission distance, the average fuel consumption drops. Many of the competitive aircraft can drop the fuel consumption well below 2 liters per PAX and 100 km.

A more in-depth look is given by figure 5.5 which shows the fuel savings in [l/PAX/100 km] compared to the consumption of the P-420/B in l/PAX/100 km on all mission distances. The P-420/B is chosen as the reference aircraft, as it is the baseline for all changes made in this work. Some values are cut off to improve the readability of the figure.

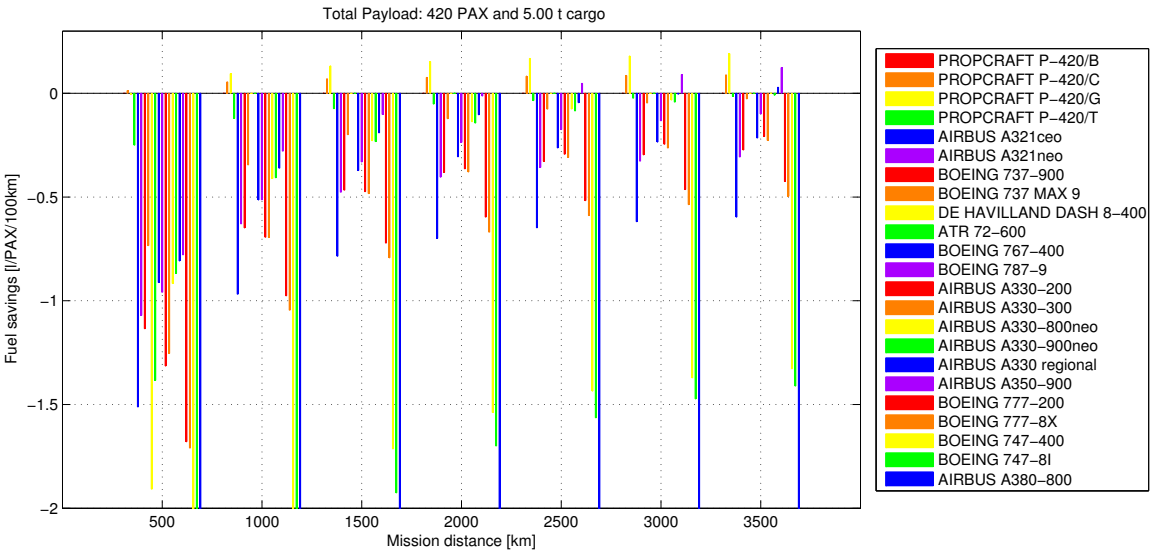

Figure 5.5.: Fuel savings [l/PAX/100 km] compared to the P-420/B (in l/PAX/100 km) for all mission distances and aircraft with a payload of 420 PAX and 5 t cargo

Finally, figure 5.6 shows the fuel savings in percent of each aircraft compared to the fuel consumption of the P-420/B on all mission distances. Some values are cut off to improve the readability of the figure. The P-420/C, /G and /T can save from 0% up to 12% compared to the P-420/B. The P-420s dominate especially the shorter mission distances of up to 2,000 km, where the other aircraft use between 10% up to more than 80% more fuel. On the longer distances, they are still leading the efficiency values, however especially the A350-900 as well as the A330neos and the Boeing 737 MAX 9 can almost match the P420s efficiency. Overall, the P-420/G is the most efficient aircraft in this analysis.

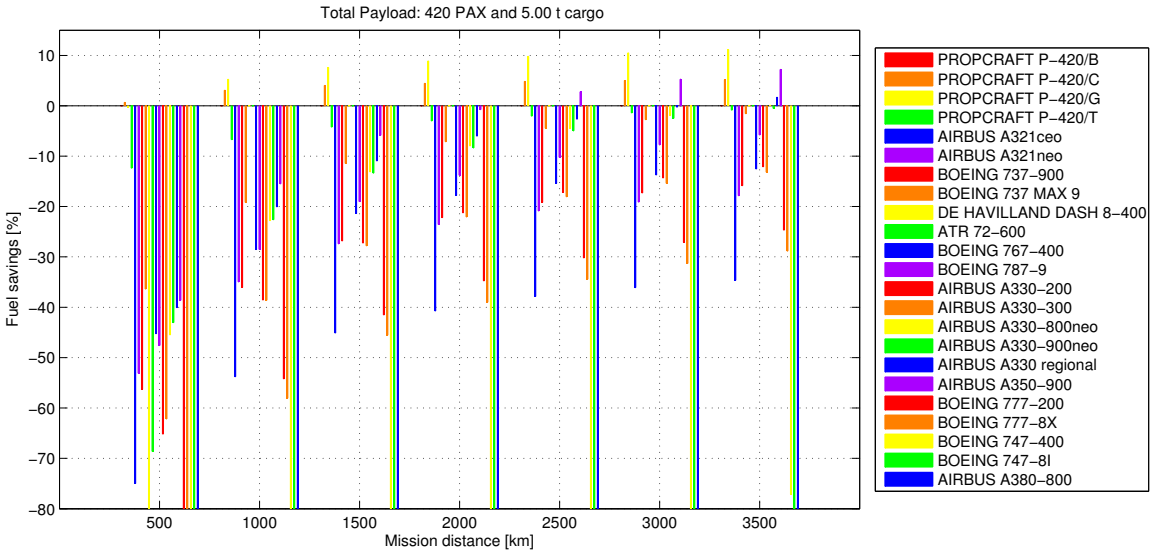

Figure 5.6.: Fuel savings [%] compared to the P-420/B for all mission distances and aircraft with a payload of 420 PAX and 5 t cargo

5.6.2. 315 PAX and 3.75 t cargo

The second mission was defined with a payload of 315 PAX and 3.75 t of cargo with mission distances ranging from 500 to 3,500 km with all aircraft as shown in table 5.9.

Figure 5.7 shows the fuel consumption in liters per PAX and 100 km for this mission. Compared to figure 5.4, the fuel consumption is higher, as the total fuel consumption is now divided by less PAX. The general trend however remains hyperbolic. In this case, the P-420s have a fuel consumption of about 2.5 to 3 liters per PAX and 100 km at a range of 500 km. This drops to slightly above 2 liters at the range of 3,500 km. Competitor aircraft can again catch up with the P-420s over longer mission distance.

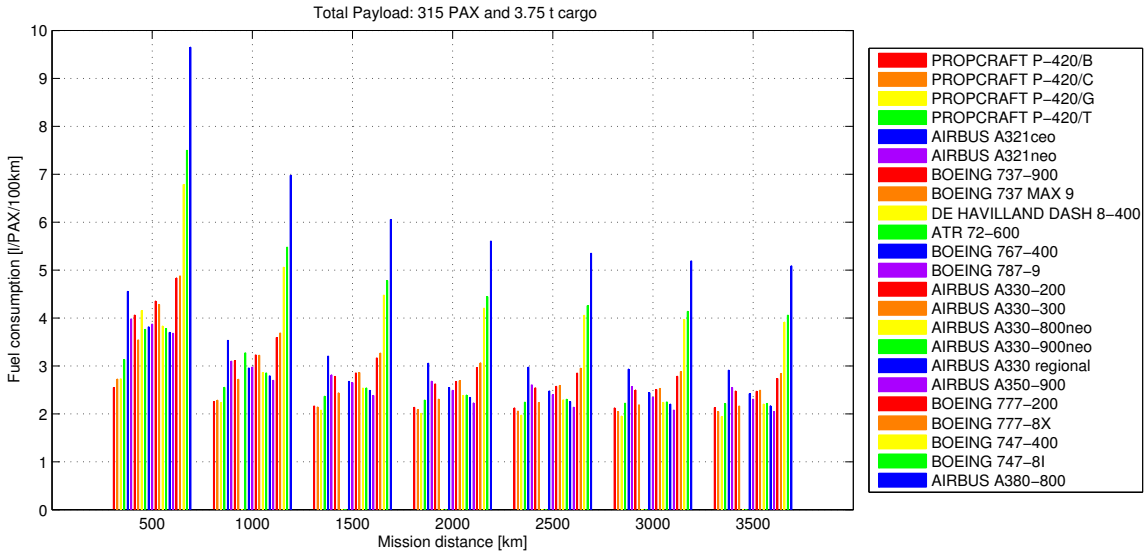

Figure 5.7.: Fuel consumption [l/PAX/100 km] for all mission distances and aircraft with a payload of 315 PAX and 3.75 t cargo

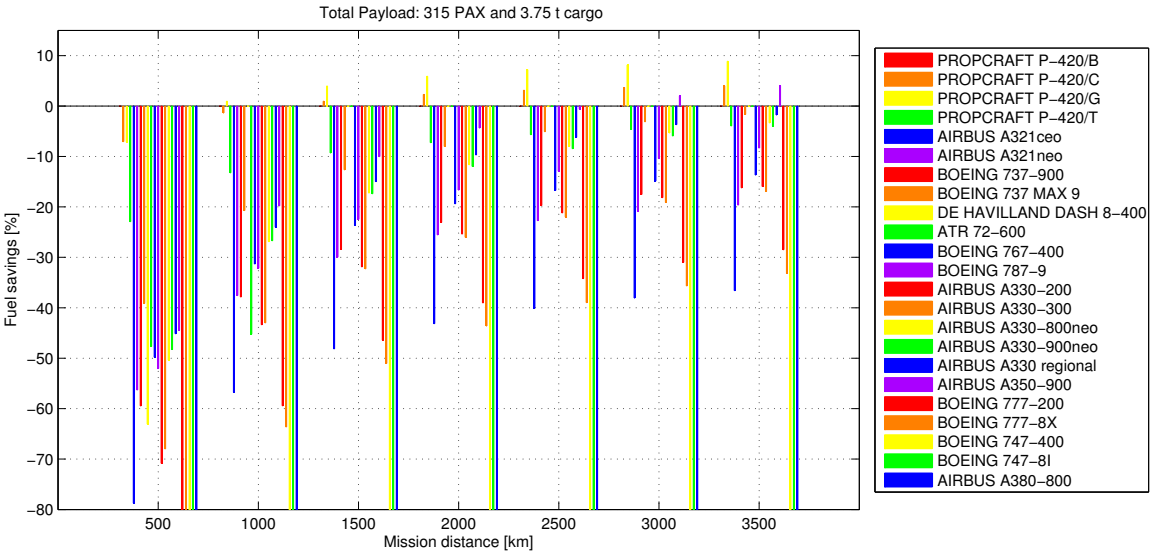

Figure 5.8.: Fuel savings [%] compared to the P-420/B for all mission distances and aircraft with a payload of 315 PAX and 3.75 t cargo

Figure 5.8 shows the fuel savings in percent of each aircraft compared to the P-420/B on all mission distances. Here, the savings are less than when compared to figure 5.6, as explained above. When comparing the two figures, it is visible that the competitor aircraft to the P-420 cannot get as close to the P-420s as before, where the A350-900 was using less fuel than the P-420/B. Here, the other aircraft are about 10 % behind. The P-420/G is overall still the most efficient aircraft in this analysis.

5.6.3. P-420 design mission

The design mission of the P-420 was defined by Iwanizki et al. (2014) with a mission distance of 3,000 km and a payload of 420 PAX and 5 t cargo. In this section, this mission is analyzed in detail.

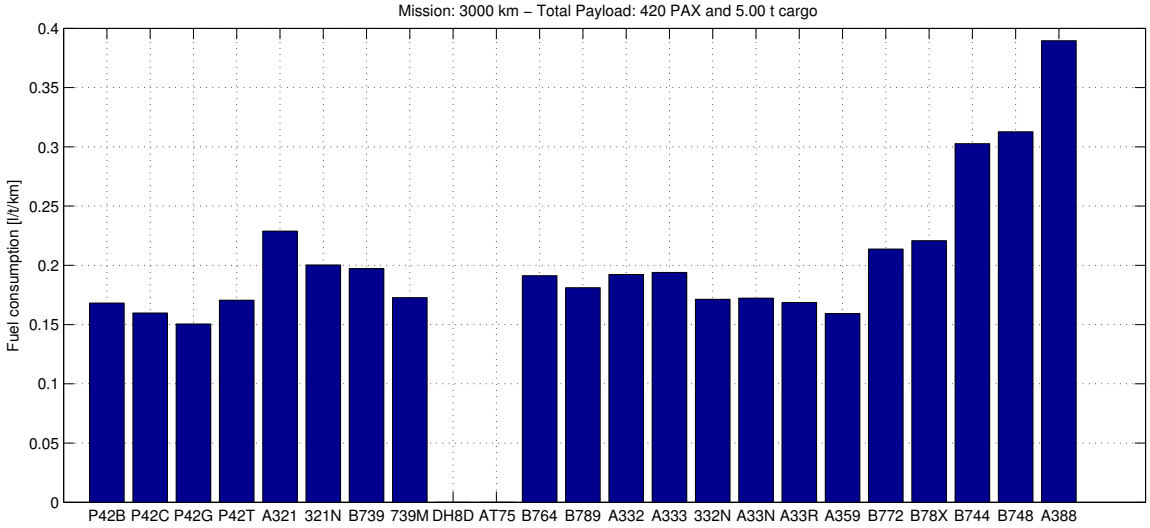

Figure 5.9.: Total fuel consumption [l/t/km] for the design mission distance of 3,000 km and all aircraft with a payload of 420 PAX and 5 t cargo

Figure 5.9 shows the fuel consumption in liter per ton cargo and km of the different aircraft on the design mission. As the ATR 72-600 and the Dash-8 400 cannot perform this mission, their value is zero. The P-420/G has the lowest fuel consumption of about 0.15 [l/t/km]. However, the A330neos and the A350-900 are almost on par with the P-420/G.

Figure 5.10 shows the fuel savings in percent compared to the fuel consumption of the P-420/B. It is visible, that the P-420/G is over 10% better than the P-420/B in this comparison. The A350-900 places second with about 5%. The P-420/C follows up with about 4% less, followed by the P-420/B and the A330 regional. The 737 MAX 9 is the only single-aisle aircraft that can keep up to the leading aircraft.

The P-420 aircraft prove a great fuel economy on their design mission and beats most competitors. However, at this mission, the newer versions of the A330 can almost match the performance. The A350-900 is even more efficient than the P-420/C turboprop version.

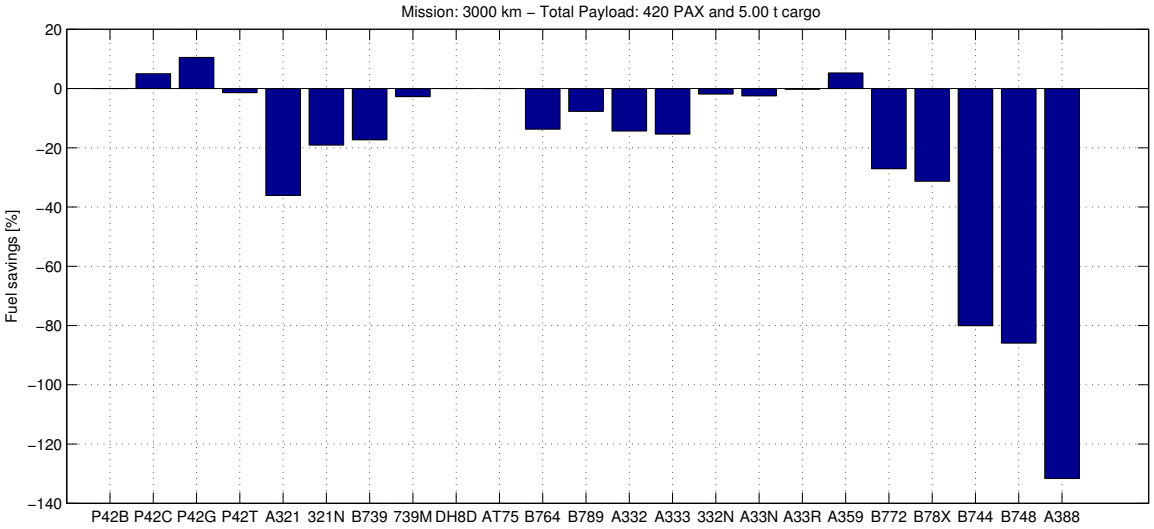

Figure 5.10.: Fuel savings [%] compared to the P-420/B for the design mission distance of 3,000 km and all aircraft with a payload of 420 PAX and 5 t cargo

5.6.4. P-420 versions

This section will provide a closer look at the fuel consumption of the four different P-420 versions on all mission distances and both payloads.

The four versions of the P-420 show different characteristics in fuel consumption due to their different engine types and OMEs. Figure 5.11 shows the fuel consumption in liter per PAX and 100 km for all mission distances at a payload of 420 PAX and 5 tons of cargo. The curves behave differently over the mission distance. While at 500 km the P-420/B, /C and /G have a very similar fuel consumption, the /T consumes about 0.3 l/PAX/100 km more. At 2,000 km, the /G has an advantage of about 0.1 l/PAX/100 km over the /C, which has a small advantage over the /B. The /T is still somewhat behind, albeit with a much smaller margin. At 3,500 km distance, the advantage of the /G over the /C and /B has slightly grown. The /T is now on par with the /B.

Figure 5.12 shows the fuel savings in % compared to the P-420/B on all mission distances. The P-420/G performs best with an advantage of about 5% to the P-420/C and 10% to the P-420/B and /T at 3,500 km mission distance. The P-420/T lacks behind the P-420/B on all distances. However, the difference gets smaller towards longer mission distances.

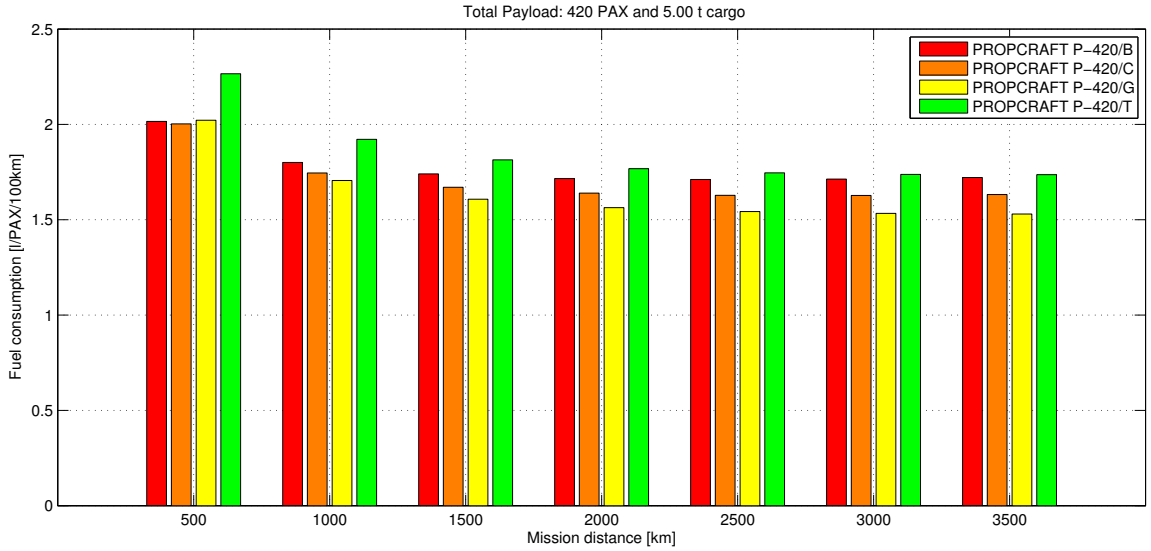

Figure 5.11.: Fuel consumption [l/PAX/100km] for all mission distances and the four P-420 variants with a payload of 420 PAX and 5 t cargo

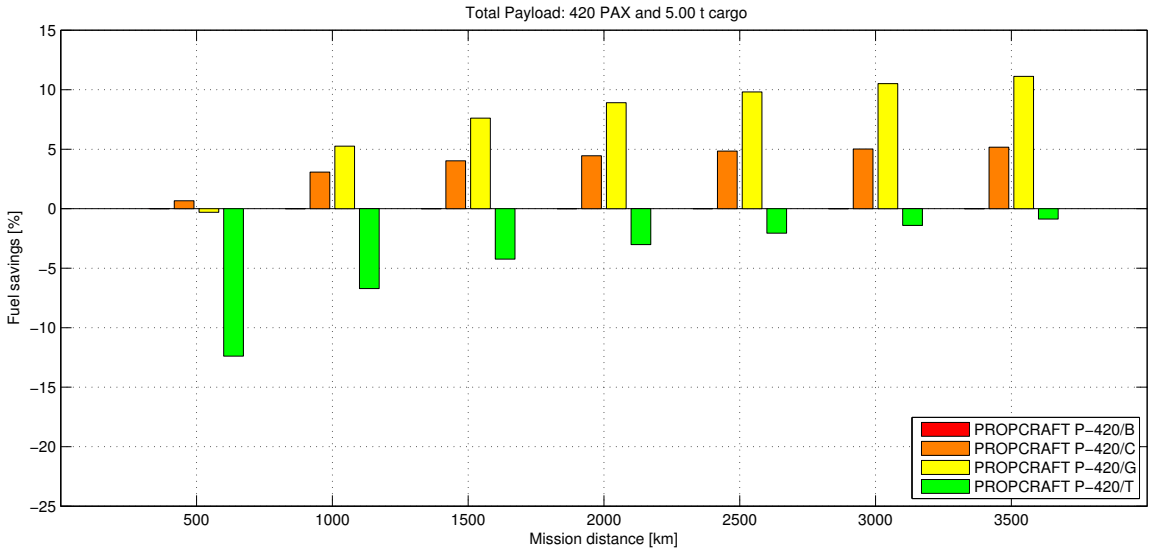

Figure 5.12.: Fuel savings [%] compared to the P-420/B for all mission distances and the four P-420 variants with a payload of 420 PAX and 5 t cargo

With a payload of 315 PAX and 3.75 tons of cargo, figure 5.13 shows a different result. The gaps between the four P-420 versions is similar. In this analysis however, the P-420/T cannot keep up with the values at higher payload and lacks about 4% behind the P-420/B. The P-420/B performs best at a mission distance of 500 km. This result is probably due to an error in the FCECT, which has in some cases issues in iterating the optimal mission mass on very short missions like this. As the P-420/C is basically the same aircraft with lower mass, it should be more efficient on every mission distance compared to the P-420/B. On longer missions, the P-420/C it is outperformed by the P-420/G, which is leading the efficiency scale.

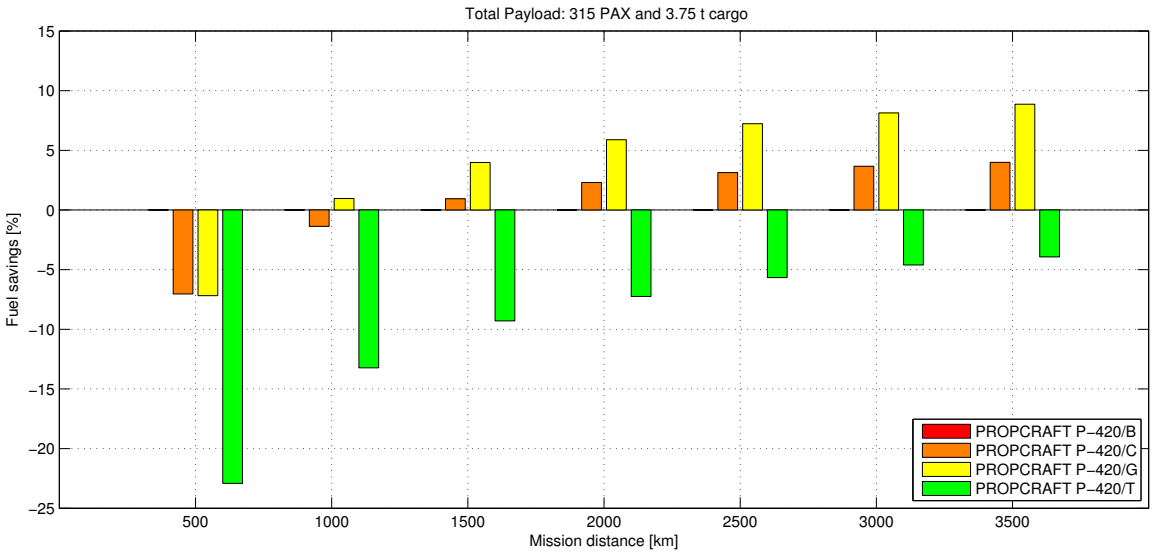

Figure 5.13.: Fuel savings [%] compared to the P-420/B for all mission distances and the four P-420 variants with a payload of 315 PAX and 3.75 t cargo

The analysis shows that the P-420/G is overall the best version of the four P-420 aircraft. It has a slight disadvantage compared to the P-420/C at the mission distance of 500 km. However, the P-420/G outperforms all other versions on all longer mission distances.

5.6.5. Summary

In conclusion, the analysis shows that the ultimate strength of the P-420 is the fuel economy on very short distances. On a mission distance of 500 km, it outperforms all competitors by at least 30%. At 2000 km, this drops to about 7% with the margin getting smaller as the mission distance gets longer.

As the short distances are the strength of the P-420, an example for an optimal mission is the route between Seoul and Jeju in South Korea. As explained in section 5.5.2, 747-400 aircraft are used on this route. The P-420/G could save the remarkable amount of 70 % of fuel per PAX and 100 km compared to the 747-400. On its design mission however, the P-420/G can only save about 5 % compared to the expected performance of the A350-900. In the air transport industry, this is still a non-negligible benefit.

Fuel efficiency is an important factor in the operations of an aircraft, however other operational aspects must not be forgotten. The discussed mission of the 747-400 on the route between Seoul and Jeju is probably a short mission that this aircraft is operated on between long-distance flights to avoid an empty parking of the aircraft. The P-420 must fit into the operations of an airline to actually improve the overall performance of the fleet. Additional factors like maintenance, landing and take-off fees due to the size, noise and weight of an aircraft among many others must be considered. This, however, is not in the scope of this thesis.

CHAPTER 6

Sensitivity Analysis

In this chapter the sensitivity anlysis of the fuel efficiency for chosen parameters is described. First the possible sensitivities in mission definition are identified and described. Afterwards, a detailed analysis and discussion of the fuel efficiency calculations is shown.

6.1. Identification of sensitivities

Possible sensitivities are all parameters that were set as fixed values in the fuel efficiency analysis in section 5.5.2 that can have an impact on the final result. These are the taxi-in and taxi-out times, the initial cruise altitude and the airspeed. For reasons of clarity, not all aircraft were chosen to perform the sensitivity analysis. Aircraft that performed well during the fuel efficiency analysis and where a trustworthy data basis is available were chosen. These are the following:

- Propcraft P-420: /B, /C, /G, /T
- Single-aisle: 737 MAX 9
- Wide-body: A330-900neo, 787-9

6.1.1. Taxi times

The taxi times were initially set to the a total of 26 times, split into 16 minutes of taxi-out and 10 minutes of taxi-in after the ICAO LTO cycle as explained in section 5.5.2. However, taxi times are dependent on airport traffic, layout, weather and more. Thus, different taxi times are entirely possible. As the fuel consumption during taxi is linear with the time spent in taxi, longer taxi times should result in higher mission

fuel consumption. When the taxi-in times after the landing are longer, the aircraft has to transport the additional fuel during the flight, leading to higher fuel consumption. To analyze the impact, the missions described in table 6.1 were calculated using the FCECT.

Parameter	Mission 1	Mission 2
Flight mission distance (FMD) [km]	500 / 3000	
Flight distance inefficiency factor	off	
PAX	420	
Cargo [t]	5	
Initial cruise altitude	optimal	
Step climb	off	
Taxi-out [min]	5	60
Taxi-in [min]	5	60

Table 6.1.: Mission definition summary for sensitivity analysis of taxi times

6.1.2. Initial cruise altitude

In the fuel efficiency analysis carried out in chapter 5, the initial cruise altitude was iterated for every single mission by the algorithm explained in section 5.3.2. This algorithm finds the initial cruise altitude with the lowest fuel consumption to perform a single mission. However, as explained in section 5.5.2, the altitude of the aircraft is dependent on many variables such as traffic and weather. The flight altitude has an impact on lift and drag of the aircraft, resulting in different fuel consumption values. To analyze the sensitivity to altitude changes, the missions described in table 6.2 were calculated using the FCECT. In addition to the optimal initial cruise altitude, the same mission is performed on a 3,000 ft lower cruise altitude to understand the impact of this sensitivity.

Parameter	Mission 1	Mission 2
Flight mission distance (FMD) [km]	500 / 3000	
Flight distance inefficiency factor	off	
PAX	420	
Cargo [t]	5	
Initial cruise altitude	optimal	3000 ft below optimal
Step climb	off	
Taxi-out [min]	16	
Taxi-in [min]	10	

Table 6.2.: Mission definition summary for sensitivity analysis of the initial cruise altitude

6.1.3. Airspeed

The airspeed is not a direct input parameter of the FCECT. However, it uses the values given in the BADA APF for the airspeed of the aircraft. The FCECT assumes that the aircraft always flies at the speed given in the APF. In order to calculate the performance and fuel consumption with a different airspeed, the APF must be changed. For a fair comparison, no new BADA files are generated for the P-420 versions, as it is not possible to create completely new files with aerodynamic, thrust and fuel consumption characteristics for the other aircraft. To analyze the sensitivity to airspeed changes, the missions described in table 6.3 were calculated using the FCECT.

Parameter	Mission 1	Mission 2
Flight mission distance (FMD) [km]	500 / 3000	
Flight distance inefficiency factor	off	
PAX	420	
Cargo [t]	5	
Initial cruise altitude	optimal	
Step climb	off	
Taxi-out [min]	16	
Taxi-in [min]	10	
Airspeed	nominal	Ma = 0.08 below nominal

Table 6.3.: Mission definition summary for sensitivity analysis of the airspeed

6.2. Results

This section shows the results of the sensitivity analysis and a discussion of these results. The results show the expected characteristics, with one exception.

6.2.1. Taxi times

The results of the taxi time calculations show the expected characteristics, especially on the short mission distance of 500 km. The fuel consumption in liter per PAX and 100 km is shown in figure 6.1. Taxi times of 5 min taxi-out and 5 min taxi-in show very little difference to the standard times of 16 min taxi-out and 10 min taxi-in. However, with 60 min for both taxi-out and -in, the fuel consumption rises largely. Figure 6.2 shows the difference in fuel consumption between the standard taxi times and the shorter and longer times respectively for the 500 km mission distance. It is visible that the shorter time saves between 3 and 8 %. At 60 min taxi-out and -in, the P-420/B uses about 12 % more fuel whereas the 737 MAX 9 uses about 45 % more. At this short distance, the time spent taxiing is very high compared to the time spent airborne, largely increasing mission fuel consumption.

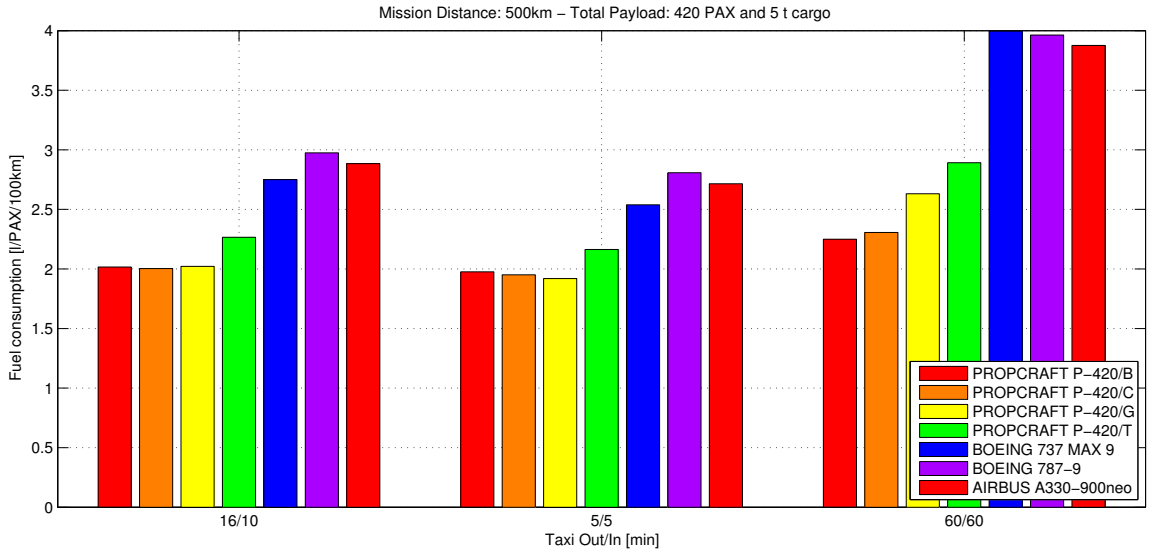

Figure 6.1.: Fuel consumption [l/PAX/100km] for different taxi times at a 500 km mission

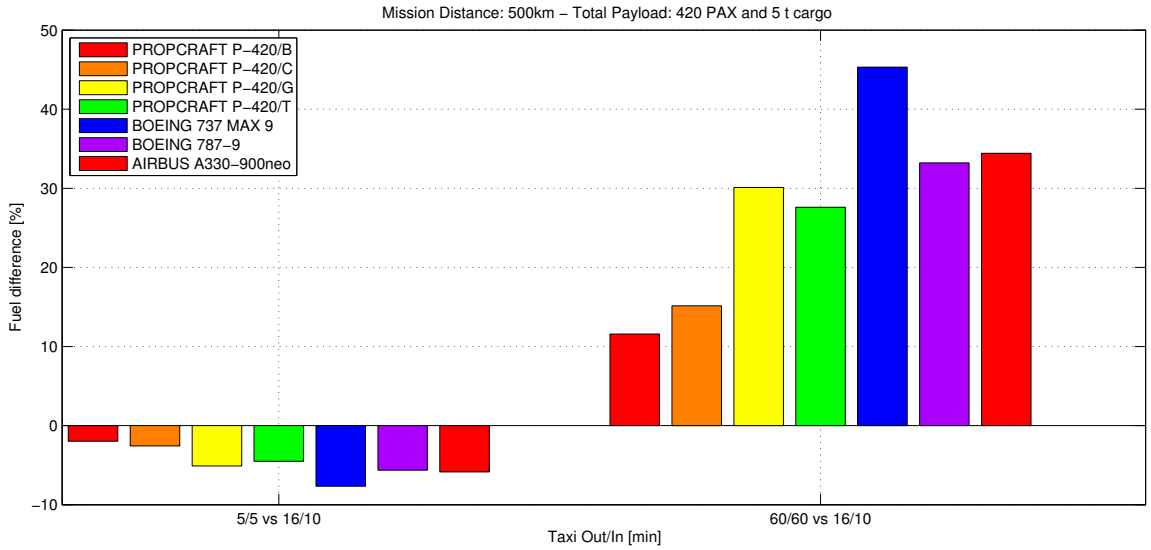

Figure 6.2.: Fuel difference [%] for different taxi times compared to standard taxi times at a 500 km mission

At the longer mission distance of 3000 km, the impact of the time spent taxiing is much smaller, as more time is spent airborne. The savings for this mission at shorter taxi times are 2 % for the 737 MAX 9 and the losses for the longer taxi time account to a maximum of 12 % for the 737 MAX 9, which is shown in figure 6.3.

Generally, the P-420 versions are less impacted by taxi times compared to the other aircraft. The 737 MAX 9 is heavily impacted because the aircraft has to fly two missions to transport the same amount of PAX and cargo. The 787-9 and the A330-900neo are considerably heavier than the P-420 versions, leading to more fuel consumption during taxi.

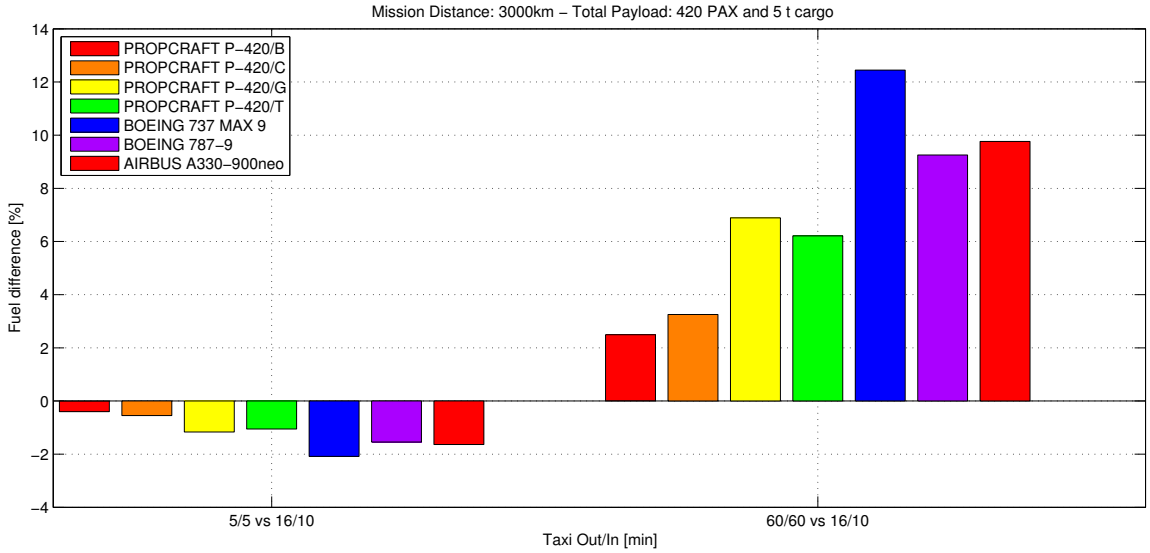

Figure 6.3.: Fuel difference [%] for different taxi times compared to standard taxi times at a 3,000 km mission

6.2.2. Initial cruise altitude

The results of the sensitivity analysis of the initial cruise altitude show the expected results, with fuel consumption rising on non-optimal flight altitudes. However, the differences are rather small, especially at short mission distances.

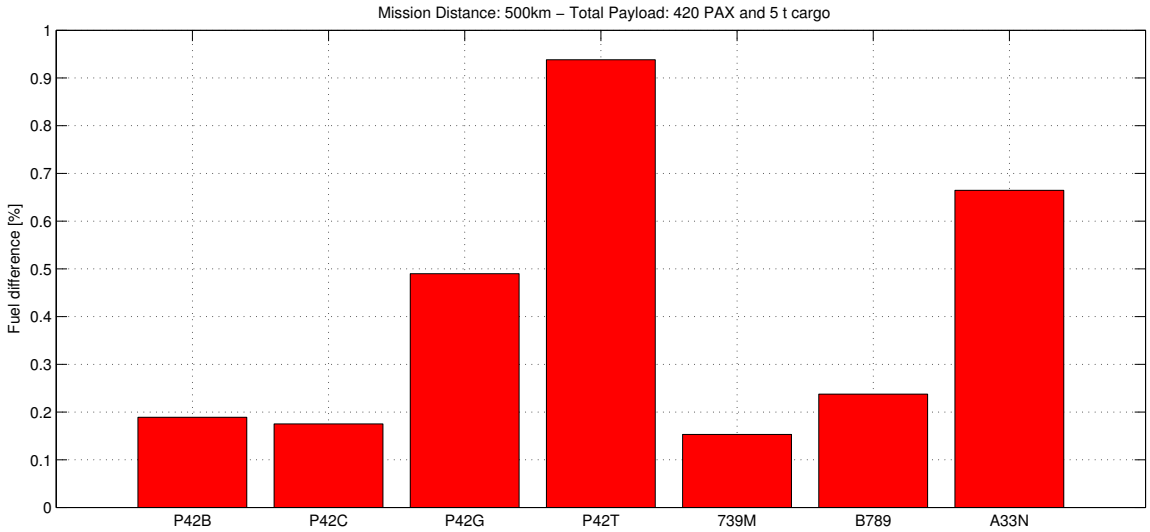

Figure 6.4.: Fuel difference [%] for optimal initial cruise altitude compared to a 3,000 ft lower initial cruise altitude on a 500 km mission

Figure 6.4 shows the fuel difference in percent for optimal initial cruise altitude compared to a 3,000 ft lower initial cruise altitude on a 500 km mission. The mission fuel consumption is up to one percent higher for the P-420/T, with the other aircraft showing even smaller differences. The fuel consumption rises somewhat on the longer

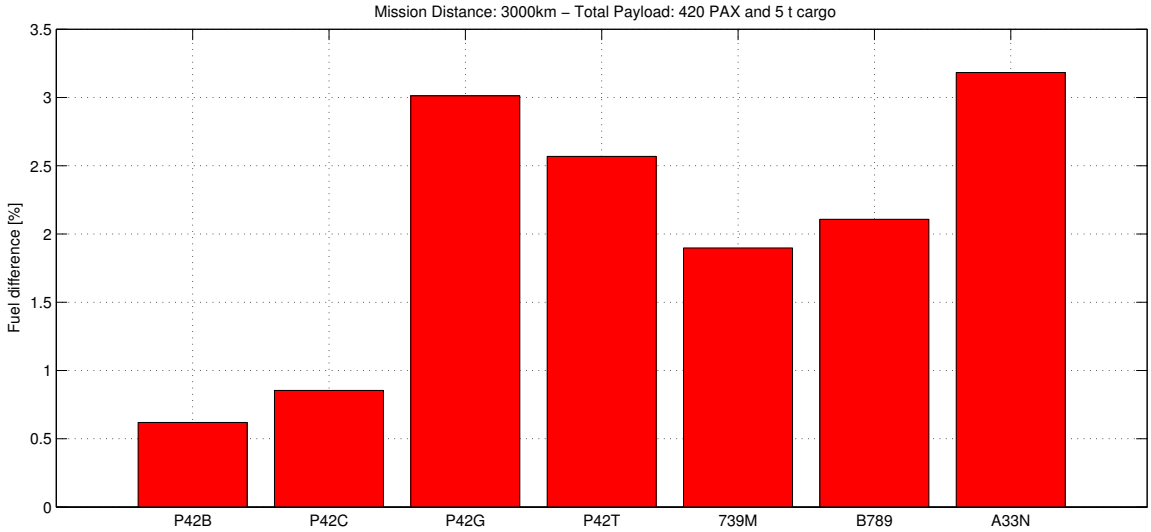

Figure 6.5.: Fuel difference [%] for optimal initial cruise altitude compared to a 3,000 ft lower initial cruise altitude on a 3,000 km mission

mission, as figure 6.5 shows. With up to 3.2 % more fuel consumption for the A330-900neo and about 3 % for the P-420/G, the lower cruise altitude shows a significant impact. The turboprop variants of the P-420 are less impacted by the lower cruise altitude.

6.2.3. Airspeed

The results of the sensitivity analysis of the airspeed show counter-intuitive results, with fuel consumption being lower on short missions and slower airspeed but higher on longer missions with lower airspeed. Figure 6.6 shows the difference in fuel con-

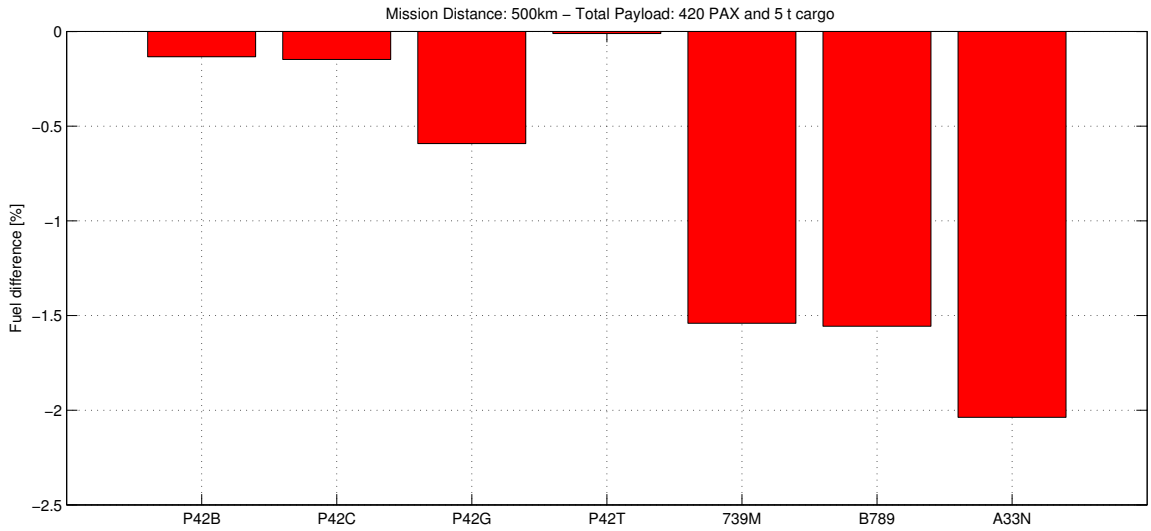

Figure 6.6.: Fuel difference [%] for nominal cruise airspeed compared to a Ma = 0.08 lower cruise airspeed on a 500 km mission

sumption in percent for nominal cruise airspeed compared to a $Ma = 0.08$ lower cruise airspeed on a 500 km mission. Fuel savings account up to 2 % for the A330-900neo on this mission. The P-420 versions show much lower fuel savings of up to 0.7 %. On the longer mission of 3,000 km, the fuel consumption actually rises for all aircraft up to 3.4 %. This is as with the lower airspeed, less lift is produced and thus the aircraft has to fly on a lower cruise altitude which creates more drag. Especially the turboprop versions of the P-420 suffer from the lower altitude as shown in figure 6.7.

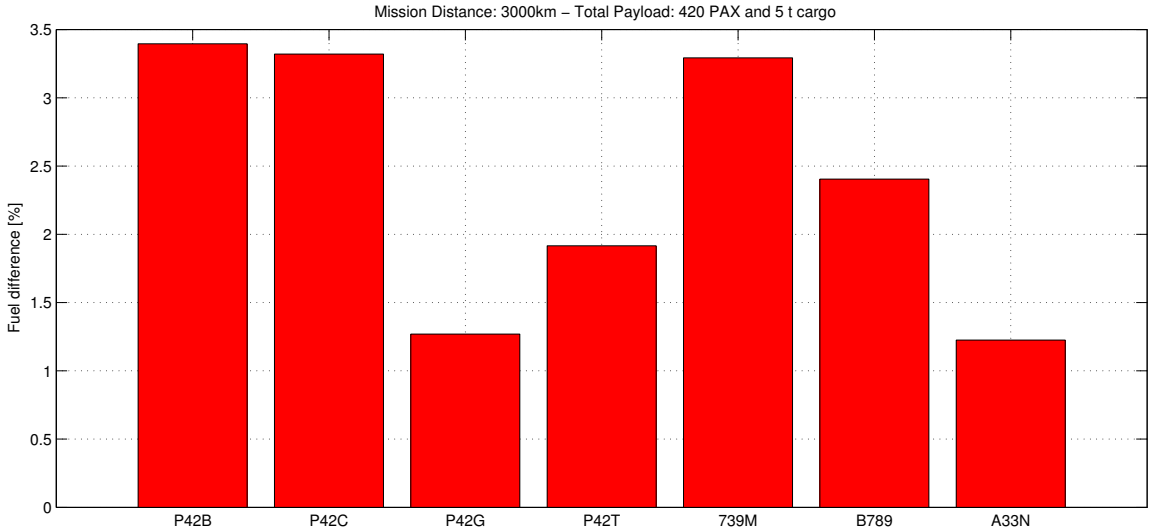

Figure 6.7.: Fuel difference [%] for nominal cruise airspeed compared to a Ma = 0.08 lower cruise airspeed on a 3,000 km mission

6.2.4. Conclusion

In conclusion, the sensitivities show a non-negligible impact on the overall fuel consumption, with different results depending for every aircraft type. While the impact of airspeed and initial cruise altitude is comparatively small on short distances, it can play a significant role on longer missions. Reducing the airspeed shows negative results, however a slight reduction might be beneficial. The taxi times can largely impact the fuel consumption, especially on short mission distances and long taxi times. The P-420 versions show different characteristics to the sensitivities. The turboprop versions are not much affected by taxi times and initial cruise altitude compared to the other aircraft. The advantages and disadvantages of the different aircraft can not be generalized as the results differ for each aircraft and sensitivity.

CHAPTER 7

Integration of the Integrated Design Tool into the Aircraft DEsign BOx

In this chapter, the integration of the IDT into ADEBO is introduced.

7.1. Introduction to the ADEBO

As aircraft development cycles are usually quite long, the use of modeling and calculation tools helps to investigate ideas and varying configurations in order to find the optimal solution. The Institute of Aircraft Design of the Technische Universität München is developing an aircraft development tool box named ADEBO on the basis of ADDAM. ADEBO offers a different tool for fast and simple aircraft development. It is an application-oriented tool which takes little effort to use and generates results of detailed accuracy. This allows for aircraft design in few and simple steps, leading to an overall reduced development time. As ADEBO is MATLAB-based, all of its tools are also developed or integrated into the MATLAB environment. Figure 7.1 shows the workflow and structure of ADEBO and ADDAM for further understanding.

ADDAM is an object-oriented data model for aircraft design purposes was developed. The data model is MATLAB-based and intended to be the basis of a number of aircraft design tools in the ADEBO. Aircraft configurations and further data, e.g. mission parameters, aerodynamics, performance characteristics as well as geometrical definitions of the aircraft and its components are saved in the data model. The data model consists of a number of classes which can be combined and inherited in order to create a representation of the aircraft, which is called 'configuration'. A single ADDAM dataset represents the configuration of an aircraft. The 'artificial engineer' is another part of the ADDAM. It is the interface between the different tools and

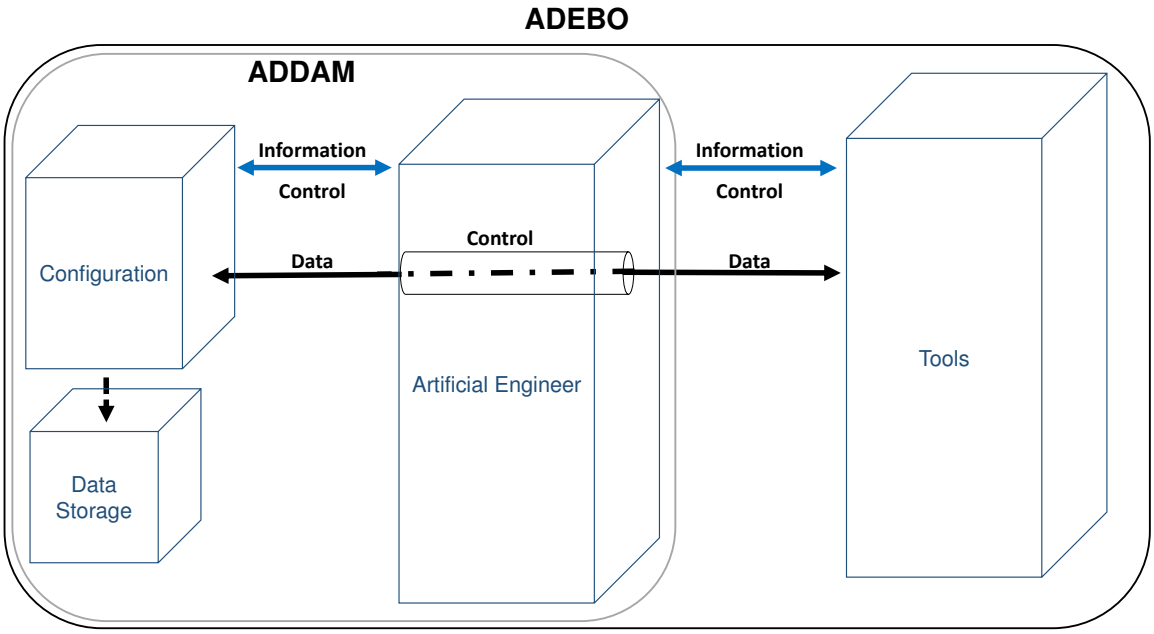

Figure 7.1.: General workflow diagram of ADEBO. Source: LLS (2015)

ADDAM. The artificial engineer manages and analyzes data and ensures consistency before writing it into the 'data storage'. The data storage is the folder in which the configurations are saved. The object structure of an aircraft configuration is shown in figure 7.2.

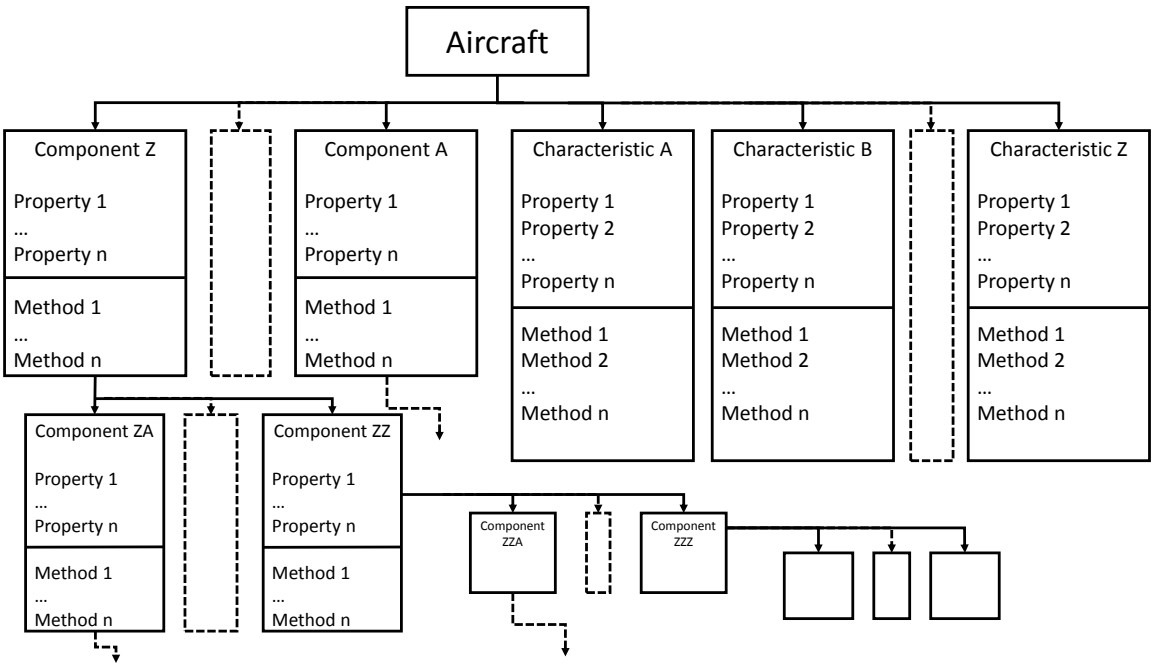

Figure 7.2.: Hierarchic object structure of an aircraft configuration. Source: LLS (2015)

Here, the goal is to integrate the IDT as one of the tools into the ADEBO. In order to do this, ADDAM dataset for the different versions of the P-420 have to be configured according to the ADDAM structure. An input and output wrapper for the IDT have to be created so that the communication of the IDT and the Artificial Engineer is ensured. To fully implement the IDT, a tool-specific class has to be created for ADDAM. This has to be done for every tool which is integrated with ADDAM. Additionally, a configuration template is implemented to configure the P-420 datasets. Finally, another function which initially writes the information and parameters defined in the aircraft definition file of the IDT into the dataset is created. This is for an easy setup of the respective P-420 configuration.

7.2. P-420 Configuration

In this section, the ADDAM configuration of the P-420 is described.
The 'aircraft' is an object of the 'configuration' class. The data structure is defined by the properties of the class definition. Here, e.g. the static thrust of an engine is an attribute of the component 'propulsion'. In general, the structure of the dataset is defined by the attributes of the P-420.
The following list shows the general structure of the P-420 configuration.

- Body
  - Fuselage
  - Fuel tanks
- Lifting surfaces
  - Wing
    - Ailerons
    - Slats
    - Flaps
  - Horizontal Tail
    - Elevators
  - Vertical Tail
    - Rudder
- Gears
  - Nose gear
  - Main gear
- Propulsion
  - Engines
- Subsystems
- ...

Every object contains classes or objects to describe weights, aerodynamics, geometry and position, as well as some special classes e.g. for propulsion performance. Additionally, mission parameters can be defined. With these attributes, the aircraft is sufficiently defined.

For easy initialization of this configuration, three configuration templates are cre-

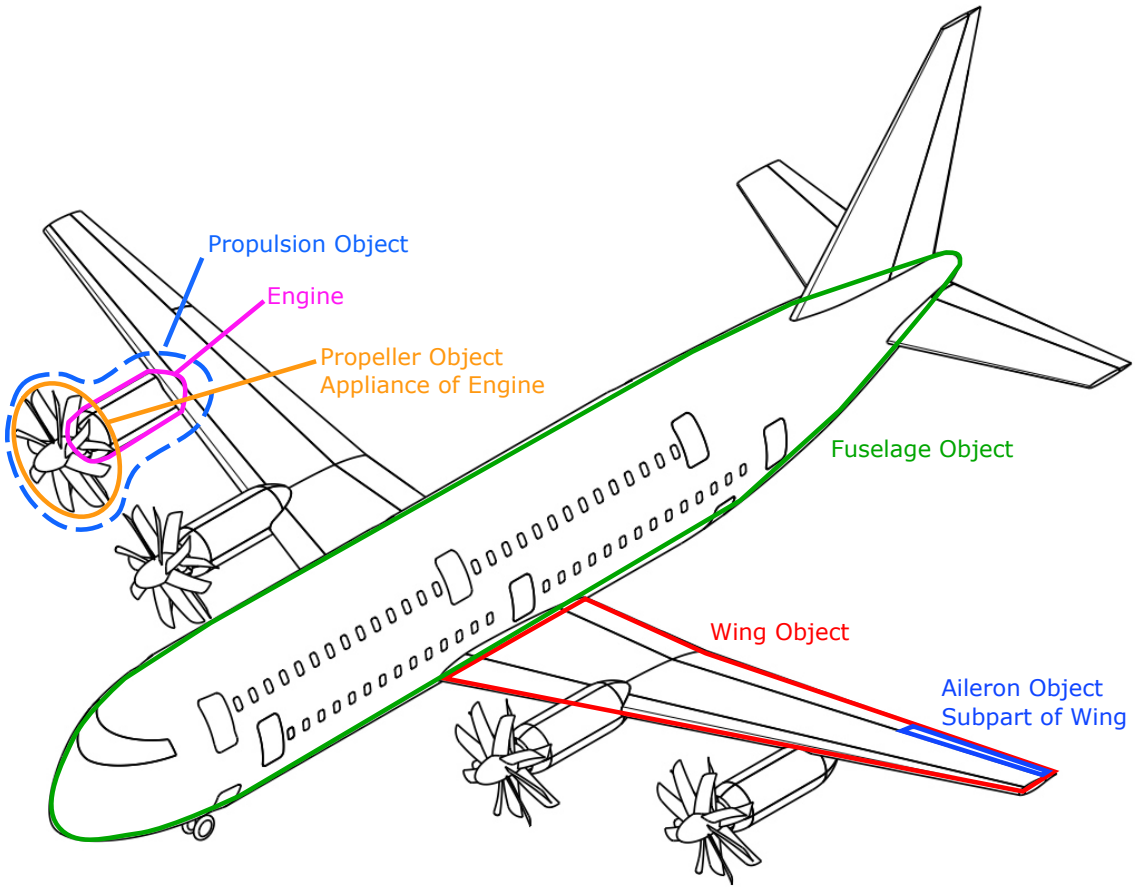

Figure 7.3.: Basic ADDAM structure of the P-420/C. Figure based on: Randt (2014b)

ated, one each for the following P-420 configurations:

- 4 Turboprop engines (e.g. P420/B, /C)
- 4 Jet engines (e.g. P420/G)
- 2 Jet engines (e.g. P420/T)

Additionally, a function is created which calls one of the IDT aircraft definition files and saves the parameters into the correct attributes of the ADDAM configuration. With this, a complete configuration of one of the P-420 models is fully initialized for the use with the IDT.

The full data structure and further information is available from the ADEBO User Manual (LLS, 2015). The structure and hierarchy of ADDAM is available from the ADDAM Folder Hierarchy in appendix A.1. Furthermore, the ADDAM UML is available in appendix A.2.

7.3. Input and output wrapper

The input and output wrapper are functions which connect the IDT and ADDAM. They are responsible to access and save the necessary parameters into the specified variables.
The input wrapper accesses the data in the configuration. All necessary input variables for the successful run of the IDT are loaded and saved with the variable names defined by the IDT.
After the input wrapper successfully loaded all variables, the IDT can be executed as specified in section 7.4.
Finally, some results of the IDT are saved back into the respective attributes of the ADDAM configuration for further use. These are e.g. masses, aerodynamic values and performance parameters.

7.4. Workflow

This section describes the workflow with the ADEBO and the IDT. As an example, the P-420/C is created as a configuration, saved and calculated with the IDT.

To create the new configuration, the following line is executed in MATLAB.

```
aircraft = Configuration_ADDAM('P420C',1)
```

This creates an object of the class 'Configuration_ADDAM' named 'aircraft' with the name 'P420C'. The '1' indicates, that a configuration template is used to initialize the configuration.
A pop-up window appears, and the file 'P420_4_Prop_ConfigurationTemplate.m' is chosen, as the P-420/C is an aircraft with 4 turboprop engines. Now the configuration is correctly initialized.
In order to fill the configuration with the data from the aircraft definition file of the IDT, the function executing this task needs to be called with the following line.

```
ArtificialEngineer_ADDAM.HCACDT_IDT_to_ADDAM(aircraft,'P420C')
```

The function takes the configuration specified in the first input (here: 'aircraft') and fills it with the data from the aircraft identification file with the same name as specified in the second input (here: 'P420C'). All necessary data for the calculations of the IDT are now present in the configuration.
Finally, the configuration can be saved with:

```
aircraft.save('first-calculation')
```

The input (here:'first-calculation') is a descriptive element to distinguish between the different saved configurations and can be specified by the user.

To run the IDT, the following steps have to be performed. It is assumed now that a valid configuration containing all necessary data is available but not currently loaded into MATLAB.
The first step opens a dialog to select and load the saved configuration into MATLAB. This step only has to be performed if no configuration is already loaded into the MATLAB Workspace.

```
loadConfiguration
```

Finally, the IDT is called. For a better understanding, the IDT is called High Capacity Aircraft Design Tool (HCACDT) in ADEBO.

```
ArtificialEngineer_ADDAM.runTool(aircraft,'HCACDT')
```

A short command line dialog is available to chose if the IDT should show graphs, save an output file and create the BADA files. With the confirmation, the IDT as usual. Finally, the configuration can be saved again with the command shown above.

7.5. Conclusion

With the described steps, the IDT is a part of the ADEBO and can be used within the workflow of the aircraft design development environment. However, the IDT was designed for the specific case of the design of a high capacity aircraft. It combines many functions in a highly integrated manner. Many variables are defined directly within the IDT, making the tool apply only for the specific case of this aircraft design problem. Major changes would require changes in the code of the IDT.
For the aircraft design workflow as intended by the ADEBO, it would be very useful to implement tools that have a wide variety of application cases. As an example, the different mass estimation methods carried out by the IDT could be implemented as separate tools. For more application cases, they would require more input variables. However, with this flexibility it could be available to aircraft designers following different aircraft design goals without the need to implement the mass estimation again for their specific case. Furthermore, other parts of the IDT could be separated, rewritten for multipurpose calculation and implemented as separate tools within the ADEBO. An aircraft designer could execute the tools in his workflow to calculate and optimize the aircraft design being worked on, achieving results in a fast and easy manner.

CHAPTER 8

Outlook and conclusion

In this work, the possibility of the P-420 high capacity aircraft powered by modern high bypass ratio turbofans was investigated. In particular, the main goal was to create a derivative of the previous versions while making little changes to the overall aircraft concept. During the course of the thesis, three versions of the P-420 were created, a derivative of the P-420/B, the P-420/C with lower MTOW, a four-engined P-420/G with four geared turbofan engines and a two-engined P-420/T with two large turbofan engines. Both versions were thoroughly analyzed and the advantages and disadvantages were discussed. Both versions are deemed feasible within the given requirements. While the four-engined version proved better performance and fuel consumption, the two-engined version may be more favorable from an operational standpoint.

The turboprop and turbofan versions of the P-420 were implemented into the FCECT in order to assess their performance in regards to fuel consumption to existing or announced competitor airplanes. The analysis showed that the P-420 have a leading fuel efficiency especially on short missions between 500 and 2,000 km. On longer mission distances, their fuel efficiency is on par with the expected performance of the announced Airbus A350-900 aircraft.

The overall performance and fuel consumption of the new turbofan versions of the P-420 are superior to that of the turboprop P-420 versions within the given requirements and calculation methods. Operational aspects were discussed. However they were not deeply analyzed.

The implementation of the IDT into the ADEBO of the Institute of Aircraft Design enables the further development of the P-420 aircraft concept in an aircraft design development environment in collaboration with other tools. To fully embrace the potential of the ADEBO, the IDT could be used as a basis to develop more flexible tools for the design of various aircraft models and configruations.

During the course of the thesis, some aspects of the concept aircraft were identified that were out of the scope of this work but must be incorporated in the aircraft design. The initially performed trade studies showed that larger wing span and subsequently optimized aerodynamics of the aircraft could reduce drag and thus power demand, which could lead to a downsizing of the aircraft engines and mass. As the P-420 configuration currently does not include winglets or even foldable wing tips, this is a proposed topic of research to further optimize the performance of the concept. Additionally, operational aspects are other proposed topics of research, as the customers want an aircraft which perfectly fits their needs.

In conclusion, the enhanced IDT enables a detailed projection of the performance of the P-420 concept aircraft with both turbofan and turboprop engines. The integrated BADA file generator allows for fast and simple fuel efficiency and performance calculation with the FCECT. The simulated performance of the P-420 is outstanding especially on short ranges, where the concept aircraft beats all existing aircraft. With these tools at hand, further development and analysis of the P-420 and comparison of fuel efficiency are possible in an optimized process.

Bibliography

Aerosila. SV-27 propfan and RSV-27 governor, 2005. URL http://en.aerosila.ru/index.php?actions=main_content&id=32.

AIRBUS. Airbus' newest A330 version: 'The right aircraft, right now' for domestic and regional operations, 2013. URL http://www.airbus.com/newsevents/news-events-single/detail/airbus-newest-a330-version-the-right-aircraft-right-now-for-domestic-and-regional-operati/.

Airbus. Airbus announces lower weight A330 for regional & domestic operations, 2013. URL http://www.airbus.com/presscentre/pressreleases/press-release-detail/detail/airbus-announces-lower-weight-a330-for-regional-domestic-operations/.

AIRBUS. A321/A321NEO AIRCRAFT CHARACTERISTICS AIRPORT AND MAINTENANCE PLANNING, 2014a.

AIRBUS. A380 AIRCRAFT CHARACTERISTICS AIRPORT AND MAINTENANCE PLANNING, 2014b.

AIRBUS. Flying on demand 2014-2033, Global Market Forecast, 2014c.

Airbus. A330neo: Powering into the next decade, 2014a. URL http://www.airbus.com/newsevents/news-events-single/detail/farnborough-airshow-2014/.

Airbus. A350-900 specs, 2014b. URL http://www.a350xwb.com/technical-specifications/.

AIRBUS. Airbus offers added seating capacity for the A320 Family while retaining modern comfort standards, 2014. URL http://www.airbus.com/newsevents/news-events-single/detail/airbus-offers-added-seating-capacity-for-the-a320-family-while-retaining-modern-comfort-standards/.

Airbus. A330 AIRCRAFT CHARACTERISTICS AIRPORT AND MAINTENANCE PLANNING, 2014.

AIRBUS. A321 Dimensions & key data, 2015a. URL http://www.airbus.com/aircraftfamilies/passengeraircraft/a320family/a321/specifications/.

AIRBUS. A350-900 AIRCRAFT CHARACTERISTICS AIRPORT AND MAINTENANCE PLANNING, 2015b.

Airbus. A330-300 Dimensions & Key Data, 2015a. URL http://www.airbus.com/aircraftfamilies/passengeraircraft/a330family/a330-300/specifications/.

Airbus. A330-200 Dimensions & Key Data, 2015b. URL http://www.airbus.com/aircraftfamilies/passengeraircraft/a330family/a330-200/specifications/.

James A Albright. Takeoff Climb Gradient Requirements, 2015. URL http://code7700.com/takeoff_climb_gradient.html.

Amadeus. 300 world 'super routes' attract 20% of all air travel, Amadeus reveals in new analysis of global trends, 2013. URL http://www.amadeus.com/web/amadeus/en_1A-corporate/Amadeus-Home/News-and-events/News/2013_04_17_300-world-super-routes-attract/1319560217161-Page-AMAD_DetailPpal?assetid=1319526516400&assettype=PressRelease_C#_ftn1.

Asiana Airlines. Aircraft Information, 2015a. URL http://us.flyasiana.com/C/en/homepage.do?menuId=003009001000000&menuType=CMS.

Asiana Airlines. Flight Schedule, 2015b. URL https://us.flyasiana.com/I/en/DefaultFlightScheduleSearch.do?menuId=001007001000000&menuType=LINK.

ATR. 600 Series - The latest generation turboprop, 2014a.

ATR. ATR 72-600, 2014b.

Raffi Babikian, Stephen P. Lukachko, and Ian a. Waitz. The historical fuel efficiency characteristics of regional aircraft from technological, operational, and cost perspectives. *Journal of Air Transport Management*, 8(6):389–400, 2002. ISSN 09696997. doi: 10.1016/S0969-6997(02)00020-0.

Matthias Bartel and Trevor Young. Simplified Thrust and SFC Calculations of Modern Two-Shaft Turbofan Engines for Preliminary Aircraft Design. In *7th AIAA ATIO Conf, 2nd CEIAT Int'l Conf on Innov and Integr in Aero Sciences, 17th LTA Systems Tech Conf; followed by 2nd TEOS Forum*, 2007.

BDL. Fluglärmreport 2015. Technical report, Bundesverband der Deutschen Luftverkehrswirtschaft, 2015.

Vinay Bhaskara. Analysis: Airbus Launches Lower Weight A330 For Regional Operations, 2014. URL http://airwaysnews.com/blog/2013/09/25/analysis-airbus-launches-lower-weight-a330-for-regional-operations/.

Boeing. 777-200/300 Airplane Characteristics for Airport Planning, 1998.

Boeing. 747-400 Airplane Characteristics for Airport planning, 2002.

Boeing. 767 Airplane characteristics for airport planning, 2005.

Boeing. 777-200LR/-300ER/-Freighter Airplane Characteristics for Airport Planning, 2009.

Boeing. 787 Airplane Characteristics for Airport Planning, 2011.

Boeing. 747-8 Airplane characteristics for airport planning, 2012.

Boeing. 777X Airport Compatibility, 2013a.

Boeing. 737 Airplane Characteristics for Airport Planning, 2013b.

Boeing. Airport Compatibility Brochure - 787, 2013c.

Boeing. Boeing Launches 737 MAX 200 with Ryanair, 2014a. URL http://boeing.mediaroom.com/2014-09-08-Boeing-Launches-737-MAX-200-with-Ryanair.

Boeing. Boeing Receives 330-Minute ETOPS Certification for 787s, 2014b. URL http://boeing.mediaroom.com/2014-05-28-Boeing-Receives-330-Minute-ETOPS-Certification-for-787s.

Boeing. Airport Compatibility Brochure - 737 MAX, 2014c.

Bombardier. Q400 NextGen, 2014a.

Bombardier. Q400 NextGen Factsheet, 2014b.

Willy J.G. Bräunling. *Flugzeugtriebwerke*. Springer, Hamburg, Germany, 3rd edition, 2009. ISBN 978-3-540-76368-0. doi: 10.1007/978-3-540-76370-3.

Rudolf Brockhaus, Wolfgang Alles, and Robert Luckner. *Flugregelung*. Springer-Verlag, 2011. ISBN 3642014437.

Brian J. Cantwell. The GE90 - An Introduction, 2010.

CAPA. Lufthansas new widebody order sends signals to rivals and to manufacturers, 2013. URL http://centreforaviation.com/analysis/lufthansas-new-widebody-order-sends-signals-to-rivals-and-to-manufacturers-130448.

CFM International. The CFM56-5B Turbofan Engine, 2015. URL http://www.cfmaeroengines.com/engines/cfm56-5b.

Deagel. D-27, 2015. URL http://www.deagel.com/Turboprop-Aircraft-Engines/D-27_a000902001.aspx.

Jeremy Dwyer-Lindgren. Boeing To Expand 737 MAX Capacity to 200, 2014. URL http://airwaysnews.com/blog/2014/07/13/boeing-to-expand-737-max-capacity-to-200/.

EASA. EASA Type-Certificat Data Sheet Ratier-Figeac FH385/FH386 series propeller, 2012.

Christoph Engelke. *Erweiterung eines Programmes zur Flugleistungsrechnung für die emissionsbezogene Bewertung moderner Flugzeugkonzepte und -technologien.* Semesterarbeit, Technical University Munich, 2015.

Martin E Eshelby. *Aircraft performance: theory and practice.* American Institute of Aeronautics and Astronautics, 2000. ISBN 034075897X.

EUROCONTROL. Base Of Aircraft Data (BADA) Aircraft Performance Modelling Report, 2009.

EUROCONTROL. USER MANUAL FOR THE BASE OF AIRCRAFT DATA (BADA) REVISION 4, 2012.

EUROCONTROL. USER MANUAL FOR THE BASE OF AIRCRAFT DATA (BADA) REVISION 3.12, 2014.

European Aviation Safety Agency. EASA Type Certificate Data Sheet GEnx Series Engines, 2013.

EUROPROP International. TP400-D6 Brochure, 2011.

FAA. Guide Specification for Aircraft Rescue and Fire Fighting (ARFF) Vehicles, 2011.

FAA. TYPE CERTIFICATE DATA SHEET T00021SE, 2014.

Federal Aviation Administration. 14 CFR 25, Title 14: Aeronautics and Space, Airworthiness Standards: Transport Category Airplanes, 2015.

Paul Finkenstein. PUREPOWER PW1000G GEARED TURBOFAN ENGINE, 2013.

GE Aviation. GEnx high bypass turbofan engines, 2004.

Scott Hamilton. Analyzing the Airbus plan to offer A350, A330 "Regional" aircraft - Leeham News and Comment, 2013. URL http://leehamnews.com/2013/07/29/analyzing-the-airbus-plan-to-offer-a350-a330-regional-aircraft/.

Scott Hamilton. Airbus critiques the Boeing 737 MAX 200 - Leeham News and Comment, 2014. URL http://leehamnews.com/2014/09/21/airbus-critiques-the-boeing-737-max-200/.

Rupa Haria. Airlines Rationalize Revenue Potential Of Airbus A340, 2014. URL http://aviationweek.com/awin-only/airlines-rationalize-revenue-potential-airbus-a340.

Sebastian Herbst. ADDAM UML Version 1.0, 2015a.

Sebastian Herbst. ADDAM Folder Hierarchy v0.7, 2015b.

Hessischer Rundfunk. Neue Entgeltordnung am Flughafen: Laute Flugzeuge werden immer teurer, 2015. URL `http://www.hr-online.de/website/rubriken/nachrichten/index.jsp?rubrik=71831&key=standard_document_54024009`.

Denis Howe. *Aircraft Conceptual Design Synthesis*. Professional Engineering Publishing Limited, London and Bury St Edmunds, UK, 2000. ISBN 1 86058 301 6 A.

ICAO. Forecasts of Scheduled Passenger and Freight Traffic, 2013a. URL `http://www.icao.int/sustainability/pages/eap_fp_forecastmed.aspx`.

ICAO. Aerodromes, Annex 14 to the Convention on International Civil Aviation, 2013b.

International Civil Aviation Organization. Standards and Recommended Practices, Environmental Protection Annex 16, Volume II Aircraft Engine Emissions, 2008. ISSN 0090-0036.

Jonas Ittel. *Developing a software tool for comprehensive flight performance and mission analyses in the context of the assessment of a novel turboprop transport aircraft concept Jonas*. Master thesis, Technical University Munich, 2014.

Michael Iwanizki. *Vorentwurf einer schweren, Propellerturbinengetriebenen Verkehrsflugzeugkonfiguration für den Einsatz auf hochfrequentierten Kurz- und Mittelstrecken*. Master thesis, Technical University of Munich, 2014.

Michael Iwanizki, Niclas Randt, and Sky Sartorius. Preliminary Design of a Heavy Short-and Medium-Haul Turboprop-Powered Transport Aircraft. *AIAA SciTech - 52nd Aerospace Sciences Meeting*, pages 1–11, 2014.

Japan Airlines. JAL Boeing 777-300, 2015a. URL `http://www.jal.co.jp/en/aircraft/conf/773.html`.

Japan Airlines. Domestic Flights Timetable, 2015b. URL `http://www.jal.co.jp/en/dom/time/`.

David Kaminski-Morrow. BA A350 pact seals 747-400 retirement plan, 2013. URL `http://www.flightglobal.com/news/articles/ba-a350-pact-seals-747-400-retirement-plan-385021/`.

David Kaminski-Morrow. FARNBOROUGH: Airbus lays out A330neo specifications, 2014. URL `http://www.flightglobal.com/news/articles/farnborough-airbus-lays-out-a330neo-specifications-401421/`.

Max Kingsley-Jones. Airbus's A350 vision takes shape - Flight takes an in-depth look at the new twinjet, 2006. URL http://www.flightglobal.com/news/articles/airbus39s-a350-vision-takes-shape-flight-takes-an-in-depth-look-at-the-new-211028/.

Korean Air. Korean Air Fleet, 2015a. URL https://www.koreanair.com/global/en/traveling/fleet-info.html.

Korean Air. Passenger Timetable, 2015b.

Martin Enno Kügler. *Development of a Parametric Aircraft Design Tool for Design Iterations of a High-Capacity Turboprop Transport Aircraft*. Master thesis, Technical University Munich, 2014.

John Leahy. The A330neo, 2014.

LLS. Manual ADEBO, 2015.

Chris Markou, Geraldine Cros, Adrian Cioranu, and Eunsuk Yang. Airline Maintenance Cost: Executive Commentary, 2011.

Nathan Meier. Civil Turbojet/Turbofan Specifications, 2005. URL http://www.jet-engine.net/civtfspec.html.

MTU Aero Engines. PurePower PW1000G Engine, 2014.

MTU Aero Engines AG. GEnx turbofan engine - The next generation turbofan, 2014.

OAG. Worldwide Direct Flights Comprehensive Schedule Data, 2014. URL http://www.oag.com/Flight-Schedules/WDF.

S. K. Ojha. *Flight Performance of Aircraft*. American Institute of Aeronautics and Astronautics, 1995.

Pratt & Whitney. PurePower Engine Family Specs Chart, 2014.

N P Randt. Propcraft P-420/A Baseline Technical Report, 2014a.

N P Randt. Propcraft P-420/B Revised Aircraft Concept Technical Report, 2014b.

Daniel P Raymer. *Aircraft design: a conceptual approach*. American Institute of Aeronautics and Astronautics Inc., Washington, DC, USA, second edi edition, 1992. ISBN 0930403517.

Yevgeniy Riftin and Sean Hart. GEnx : THE ENGINE OF INNOVATION. In *Eleventh Annual Freshman Conference 7*, Pittsburgh, 2011. Swanson School of Engineering.

Alberto Riva. Boeing 747 On Deathwatch: How Boeings New 777X Will Kill Its Jumbo Jet Predecessor, Once The Queen Of The Skies, 2013. URL http://www.ibtimes.com/boeing-747-deathwatch-how-boeings-new-777x-will-kill-its-jumbo-jet-predecessor-once-queen-skies.

Jayant Sabnis and Christian Winkler. THE PW1000G PURE POWER NEW ENGINE CONCEPT AND ITS IMPACT ON MRO, 2010.

Singapore Airlines. Timetable, 2015a.

Singapore Airlines. Singapore Airlines' passenger fleet, 2015b. URL http://www.singaporeair.com/en_UK/flying-with-us/ouraircraft/.

Sebastian Steinke. Liebherr liefert Klappflügel für die Boeing 777X, 2015. URL http://www.aero.de/news-21599/Liebherr-liefert-Klappflueel-fuer-die-Boeing-777X.html.

Egbert Torenbeek. *Synthesis of subsonic airplane design: an introduction to the preliminary design of subsonic general aviation and transport aircraft, with emphasis on layout, aerodynamic design, propulsion and performance*. Springer Science & Business Media, 1982. ISBN 9024727243.

Egbert Torenbeek. *Advanced Aircraft Design: Conceptual Design, Technology and Optimization of Subsonic Civil Airplanes*. John Wiley & Sons, Ltd., Delft, The Netherlands, 2013. ISBN 9781118568118.

Stephen Trimble. FARNBOROUGH: Boeing defines the 737 Max, 2012. URL http://www.flightglobal.com/blogs/flightblogger/2012/07/farnborough_boeing_defines_the/.

Daniel Tsang. New Boeing 777X likely to be a highly efficient derivative, 2011. URL http://www.aspireaviation.com/2011/09/14/new-boeing-777x-likely-to-be-a-highly-efficient-derivative/.

United States Department of Transportation. Instrument Flying Handbook. *Federal Aviation Administration, Airman Testing Standards Branch, AFS-630*, 2008.

USAF Test Pilot School. Aero Propulsion. In *Performance flight testing phase*, chapter Aero Propu. USAF Test Pilot School, 1991.

Wikipedia User 'Aainsquatsi'. Schematic diagram of a high-bypass turbofan engine, 2008. URL http://en.wikipedia.org/wiki/Turbofan#/media/File:Turbofan_operation.svg.

Wikipedia User 'M0tty'. Schematic diagram of the operation of a turboprop engine, 2009. URL http://commons.wikimedia.org/wiki/File:Turboprop_operation-en.svg.

APPENDIX A

Appendix

A.1. APF

A.1.1. P-420/B APF file

```
CCCCCCCCCCCCCCCCCCCCCCCCCCCCCCCCCCCCCCCCCCCCCCCC P42B__.APF CCCCCCCCCCCCCCCCCCCCCCCCCCCCCCCCCCCCCCCCCCCCCCCC/
CC                                                                                                                /
CC                 AIRLINES PROCEDURES FILE                                                                       /
CC                                                                                                                /
CC      File_name: P42B__.APF                                                                                     /
CC                                                                                                                /
CC      Creation_date: Apr 03 2015 19:26:45                                                                       /
CC                                                                                                                /
CC                                                                                                                /
CC      Modification_date: Apr 03 2015 19:26:45                                                                   /
CC                                                                                                                /
CC                                                                                                                /
CC                                                                                                                /
CC   LO= 090.94 to ---.--  /  AV= ---.-- to ---.--  /  HI= ---.-- to 165.84                                       /
CC                                                                                                                /
CC================================================================================================================/
CC  COM CO    Company name ------climb-------  --cruise--  -----descent------  --approach-  model- /
CC                    mass  lo  hi              lo  hi         hi  lo            (unused)          /
CC    version engines  ma  cas cas mc xxxx xx  cas cas mc  mc cas cas xxxx xx  xxx xxx xxx  opf___ /
CC===:=======:=======::==::===:===:==:====:==::===:===:==::==:===:===:====:==::===:===:===::======:/
CD  *** **    Default Company                                                                                     /
CD    ----             LO  231 231 58          379 379 64  63 270 270           0   0   0  P42B__ /
CD    ----             AV  231 231 58          379 379 64  63 270 270           0   0   0  P42B__ /
CD    ----             HI  231 231 58          379 379 64  63 270 270           0   0   0  P42B__ /
CC===:=======:=======::==::===:===:==:====:==::===:===:==::==:===:===:====:==::===:===:===::======:/
CC//////////////////////////////////////////////THE END//////////////////////////////////////////////
```

A.1.2. P-420/C APF file

```
CCCCCCCCCCCCCCCCCCCCCCCCCCCCCCCCCCCCCCCCCCCCCCC P42C__.APF CCCCCCCCCCCCCCCCCCCCCCCCCCCCCCCCCCCCCCCCCCCCCC/
CC                                                                                                             /
CC                 AIRLINES PROCEDURES FILE                                                                    /
CC                                                                                                             /
CC      File_name: P42C__.APF                                                                                  /
CC                                                                                                             /
CC      Creation_date: Apr 09 2015 09:47:12                                                                    /
CC                                                                                                             /
CC                                                                                                             /
CC      Modification_date: Apr 09 2015 09:47:12                                                                /
CC                                                                                                             /
CC                                                                                                             /
CC                                                                                                             /
CC   LO= 090.94 to ---.--  /  AV= ---.-- to ---.--  /  HI= ---.-- to 165.84                                    /
CC                                                                                                             /
CC=============================================================================================================/
CC  COM CO    Company name ------climb-------  --cruise--  -----descent------  --approach-  model- /
CC                    mass  lo  hi              lo  hi         hi  lo            (unused)          /
CC    version engines  ma  cas cas mc xxxx xx  cas cas mc  mc cas cas xxxx xx  xxx xxx xxx  opf___ /
CC===:=======:=======::==::===:===:==:====:==::===:===:==::==:===:===:====:==::===:===:===::======:/
CD  *** **    Default Company                                                                           /
CD    ----             LO  231 231 58          379 379 64  63 270 270           0   0   0  P42C__ /
CD    ----             AV  231 231 58          379 379 64  63 270 270           0   0   0  P42C__ /
CD    ----             HI  231 231 58          379 379 64  63 270 270           0   0   0  P42C__ /
CC===:=======:=======::==::===:===:==:====:==::===:===:==::==:===:===:====:==::===:===:===::======:/
CC//////////////////////////////////////////////THE END//////////////////////////////////////////////
```

A.1.3. P-420/G APF file

```
CCCCCCCCCCCCCCCCCCCCCCCCCCCCCCCCCCCCCCCCCCCCCCC P42G__.APF CCCCCCCCCCCCCCCCCCCCCCCCCCCCCCCCCCCCCCCCCCCCCC/
CC                                                                                                             /
CC                 AIRLINES PROCEDURES FILE                                                                    /
CC                                                                                                             /
CC      File_name: P42G__.APF                                                                                  /
CC                                                                                                             /
CC      Creation_date: Apr 08 2015 16:16:22                                                                    /
CC                                                                                                             /
CC                                                                                                             /
CC      Modification_date: Apr 08 2015 16:16:22                                                                /
CC                                                                                                             /
CC                                                                                                             /
CC                                                                                                             /
CC   LO= 090.94 to ---.--  /  AV= ---.-- to ---.--  /  HI= ---.-- to 165.84                                    /
CC                                                                                                             /
CC=============================================================================================================/
CC  COM CO    Company name ------climb-------  --cruise--  -----descent------  --approach-  model- /
CC                    mass  lo  hi              lo  hi         hi  lo            (unused)          /
CC    version engines  ma  cas cas mc xxxx xx  cas cas mc  mc cas cas xxxx xx  xxx xxx xxx  opf___ /
CC===:=======:=======::==::===:===:==:====:==::===:===:==::==:===:===:====:==::===:===:===::======:/
CD  *** **    Default Company                                                                           /
CD    ----             LO  231 231 58          409 409 70  65 292 292           0   0   0  P42G__ /
CD    ----             AV  231 231 58          409 409 70  65 292 292           0   0   0  P42G__ /
CD    ----             HI  231 231 58          409 409 70  65 292 292           0   0   0  P42G__ /
CC===:=======:=======::==::===:===:==:====:==::===:===:==::==:===:===:====:==::===:===:===::======:/
CC//////////////////////////////////////////////THE END//////////////////////////////////////////////
```

A.1.4. P-420/T APF file

```
CCCCCCCCCCCCCCCCCCCCCCCCCCCCCCCCCCCCCCCCCCCCCCC P42T__.APF CCCCCCCCCCCCCCCCCCCCCCCCCCCCCCCCCCCCCCCCCCCCCC/
CC                                                                                                             /
CC                  AIRLINES PROCEDURES FILE                                                                   /
CC                                                                                                             /
CC      File_name: P42T__.APF                                                                                  /
CC                                                                                                             /
CC      Creation_date: Apr 08 2015 16:36:51                                                                    /
CC                                                                                                             /
CC                                                                                                             /
CC      Modification_date: Apr 08 2015 16:36:51                                                                /
CC                                                                                                             /
CC                                                                                                             /
CC                                                                                                             /
CC   LO= 090.94 to ---.--  /  AV= ---.-- to ---.--  /  HI= ---.-- to 165.84                                    /
CC                                                                                                             /
CC=============================================================================================================/
CC  COM CO    Company name ------climb-------  --cruise--  -----descent------  --approach-  model- /
CC                    mass  lo  hi              lo  hi         hi  lo            (unused)          /
CC    version engines  ma  cas cas mc xxxx xx  cas cas mc  mc cas cas xxxx xx  xxx xxx xxx  opf___ /
CC===:=======:=======:::==::===:===:==:====:==::===:===:==::==:===:===:====:==::===:===:===::======:/
CD  *** **    Default Company                                                                           /
CD    ----             LO  231 231 58          409 409 70  65 292 292           0   0   0  P42T__ /
CD    ----             AV  231 231 58          409 409 70  65 292 292           0   0   0  P42T__ /
CD    ----             HI  231 231 58          409 409 70  65 292 292           0   0   0  P42T__ /
CC===:=======:=======:::==::===:===:==:====:==::===:===:==::==:===:===:====:==::===:===:===::======:/
CC//////////////////////////////////////////////THE END//////////////////////////////////////////////
```

A.2. OPF

A.2.1. P-420/B OPF file

```
CCCCCCCCCCCCCCCCCCCCCCCCCCCCCCC P42B__.OPF CCCCCCCCCCCCCCCCCCCCCCCCCCCCC/
CC                                                                      /
CC               AIRCRAFT PERFORMANCE OPERATIONAL FILE                  /
CC                                                                      /
CC                                                                      /
CC      File_name: P42B__.OPF                                           /
CC                                                                      /
CC      Creation_date: Apr 03 2015 19:26:45                             /
CC                                                                      /
CC      Modification_date: Apr 03 2015 19:26:45                         /
CC                                                                      /
CC                                                                      /
CC====== Actype ========================================================/
CD   P42B__          4 engines    Turboprop                  H          /
CC  P-420B   with Generic                  wake        /
CC                                                                      /
CC====== Mass (t) ======================================================/
CC    reference      minimum      maximum     max payload  mass grad  /
CD     .16755E+03   .97326E+02   .17255E+03   .52000E+02   .00000E+00 /
CC====== Flight envelope ===============================================/
CC     VMO(KCAS)       MMO        Max.Alt       Hmax       temp grad  /
CD     .30908E+03   .75000E+00   .32000E+05   .30400E+05   .00000E+00 /
CC====== Aerodynamics ==================================================/
CC Wing Area and Buffet coefficients (SIM)                              /
CCndrst Surf(m2)     Clbo(M=0)       k           CM16                   /
CD 5   .25000E+03   .00000E+00   .00000E+00   .00000E+00                /
CC   Configuration characteristics                                      /
CC n Phase  Name    Vstall(KCAS)    CD0          CD2         unused     /
CD 1 CR   Clean     .16537E+03   .19604E-01   .37287E-01   .00000E+00 /
CD 2 IC   FL50p     .15048E+03   .92103E-01   .43273E-01   .00000E+00 /
CD 3 TO   FL50p     .15048E+03   .92103E-01   .25069E-01   .00000E+00 /
CD 4 AP   FL100p    .11670E+03   .19604E-01   .37287E-01   .00000E+00 /
CD 5 LD   FL100p    .11670E+03   .16463E+00   .26934E-01   .00000E+00 /
CC   Spoiler                                                            /
CD 1      RET                                                           /
CD 2      EXT                                 .00000E+00   .00000E+00 /
CC   Gear                                                               /
CD 1      UP                                                            /
CD 2      DOWN                   .27283E-01   .00000E+00   .00000E+00 /
CC   Brakes                                                             /
CD 1      OFF                                                           /
CD 2      ON                                  .00000E+00   .00000E+00 /
CC====== Engine Thrust =================================================/
CC         Max climb thrust coefficients (SIM)                          /
CD     .14239E+08   .66049E+04   .24285E+06   .00000E+00   .00000E-00 /
CC     Desc(low)    Desc(high)   Desc level   Desc(app)     Desc(ld)  /
CD     .45303E-01   .26573E-01   .24500E+05   .44643E-01   .42734E+00 /
CC     Desc CAS     Desc Mach     unused       unused       unused    /
CD     .13890E+03   .63000E+00   .00000E+00   .00000E+00   .00000E+00 /
CC====== Fuel Consumption ==============================================/
CC   Thrust Specific Fuel Consumption Coefficients                      /
CD     .29064E+01   .13198E+04                                         /
CC   Descent Fuel Flow Coefficients                                     /
CD     .42268E+01   .20516E+06                                         /
CC   Cruise Corr.     unused       unused       unused       unused    /
CD     .10000E+01   .00000E+00   .00000E+00   .00000E+00   .00000E+00 /
CC====== Ground ========================================================/
CC        TOL          LDL         span         length       unused    /
CD     .21479E+04   .23324E+04   .51650E+02   .47700E+02   .00000E+00 /
CC======================================================================/
FI                                                                      /
```

A.2.2. P-420/C OPF file

```
CCCCCCCCCCCCCCCCCCCCCCCCCCCCCCC P42C__.OPF CCCCCCCCCCCCCCCCCCCCCCCCCCCCC/
CC                                                                      /
CC               AIRCRAFT PERFORMANCE OPERATIONAL FILE                  /
CC                                                                      /
CC                                                                      /
CC      File_name: P42C__.OPF                                           /
CC                                                                      /
CC      Creation_date: Apr 09 2015 09:47:12                             /
CC                                                                      /
CC      Modification_date: Apr 09 2015 09:47:12                         /
CC                                                                      /
CC                                                                      /
CC====== Actype ========================================================/
CD   P42C__          4 engines    Turboprop                  H          /
CC  P-420C   with Generic                  wake        /
CC                                                                      /
CC====== Mass (t) ======================================================/
CC    reference      minimum      maximum     max payload  mass grad   /
CD     .15264E+03   .88355E+02   .15764E+03   .52000E+02   .00000E+00 /
CC====== Flight envelope ===============================================/
CC     VMO(KCAS)       MMO        Max.Alt       Hmax        temp grad   /
CD     .32731E+03   .77000E+00   .32000E+05   .32000E+05   .00000E+00 /
CC====== Aerodynamics ==================================================/
CC Wing Area and Buffet coefficients (SIM)                              /
CCndrst Surf(m2)     Clbo(M=0)       k          CM16                    /
CD 5   .25000E+03   .00000E+00   .00000E+00   .00000E+00                /
CC   Configuration characteristics                                      /
CC n Phase  Name    Vstall(KCAS)    CD0          CD2         unused     /
CD 1 CR   Clean     .15806E+03   .19604E-01   .37287E-01   .00000E+00 /
CD 2 IC   FL50p     .14383E+03   .92103E-01   .43273E-01   .00000E+00 /
CD 3 TO   FL50p     .14383E+03   .92103E-01   .25069E-01   .00000E+00 /
CD 4 AP   FL100p    .11155E+03   .19604E-01   .37287E-01   .00000E+00 /
CD 5 LD   FL100p    .11155E+03   .16463E+00   .26934E-01   .00000E+00 /
CC   Spoiler                                                            /
CD 1      RET                                                           /
CD 2      EXT                                .00000E+00   .00000E+00 /
CC   Gear                                                               /
CD 1      UP                                                            /
CD 2      DOWN                  .27283E-01   .00000E+00   .00000E+00 /
CC   Brakes                                                             /
CD 1      OFF                                                           /
CD 2      ON                                 .00000E+00   .00000E+00 /
CC====== Engine Thrust =================================================/
CC         Max climb thrust coefficients (SIM)                          /
CD     .72370E+08   .80964E+05   -.2827E+05   .00000E+00   .00000E-00 /
CC     Desc(low)    Desc(high)   Desc level   Desc(app)     Desc(ld)   /
CD     .59532E-01   .31613E-01   .24500E+05   .58618E-01   .37646E+00 /
CC     Desc CAS     Desc Mach     unused       unused       unused     /
CD     .13890E+03   .63000E+00   .00000E+00   .00000E+00   .00000E+00 /
CC====== Fuel Consumption ==============================================/
CC   Thrust Specific Fuel Consumption Coefficients                      /
CD     .29064E+01   .13198E+04                                         /
CC   Descent Fuel Flow Coefficients                                     /
CD     .54539E+01   .22943E+06                                         /
CC   Cruise Corr.     unused       unused       unused       unused     /
CD     .10000E+01   .00000E+00   .00000E+00   .00000E+00   .00000E+00 /
CC====== Ground ========================================================/
CC         TOL          LDL         span         length       unused     /
CD     .16699E+04   .21568E+04   .51650E+02   .47700E+02   .00000E+00 /
CC=====================================================================/
FI                                                                      /
```

A.2.3. P-420/G OPF file

```
CCCCCCCCCCCCCCCCCCCCCCCCCCCCCCC P42G__.OPF CCCCCCCCCCCCCCCCCCCCCCCCCCCCC/
CC                                                                      /
CC               AIRCRAFT PERFORMANCE OPERATIONAL FILE                  /
CC                                                                      /
CC                                                                      /
CC      File_name: P42G__.OPF                                           /
CC                                                                      /
CC      Creation_date: Apr 08 2015 16:16:22                             /
CC                                                                      /
CC      Modification_date: Apr 08 2015 16:16:22                         /
CC                                                                      /
CC                                                                      /
CC====== Actype ========================================================/
CD   P42G__         4 engines    Jet                        H           /
CC  P-420GTF   with PW1127G                 wake        /
CC                                                                      /
CC====== Mass (t) ======================================================/
CC    reference      minimum      maximum     max payload  mass grad   /
CD     .14971E+03   .84186E+02   .15471E+03   .52000E+02   .00000E+00 /
CC====== Flight envelope ===============================================/
CC     VMO(KCAS)       MMO        Max.Alt       Hmax        temp grad   /
CD     .29443E+03   .90000E+00   .32000E+05   .32000E+05   .00000E+00 /
CC====== Aerodynamics ==================================================/
CC Wing Area and Buffet coefficients (SIM)                              /
CCndrst Surf(m2)     Clbo(M=0)       k          CM16                    /
CD 5   .25000E+03   .00000E+00   .00000E+00   .00000E+00                /
CC   Configuration characteristics                                      /
CC n Phase  Name    Vstall(KCAS)    CD0          CD2         unused     /
CD 1 CR   Clean     .15659E+03   .20342E-01   .37287E-01   .00000E+00 /
CD 2 IC   FL50p     .14249E+03   .92872E-01   .43273E-01   .00000E+00 /
CD 3 TO   FL50p     .14249E+03   .92872E-01   .25069E-01   .00000E+00 /
CD 4 AP   FL100p    .11051E+03   .20342E-01   .37287E-01   .00000E+00 /
CD 5 LD   FL100p    .11051E+03   .16540E+00   .26934E-01   .00000E+00 /
CC   Spoiler                                                            /
CD 1      RET                                                           /
CD 2      EXT                                .00000E+00   .00000E+00 /
CC   Gear                                                               /
CD 1      UP                                                            /
CD 2      DOWN                  .27283E-01   .00000E+00   .00000E+00 /
CC   Brakes                                                             /
CD 1      OFF                                                           /
CD 2      ON                                 .00000E+00   .00000E+00 /
CC====== Engine Thrust =================================================/
CC         Max climb thrust coefficients (SIM)                          /
CD     .34947E+06   .29724E+05   .38128E-09   .00000E+00   .00000E-00 /
CC     Desc(low)    Desc(high)   Desc level   Desc(app)     Desc(ld)   /
CD     .58670E-01   .40397E-01   .22500E+05   .55429E-01   .51195E+00 /
CC     Desc CAS     Desc Mach     unused       unused       unused     /
CD     .15000E+03   .65000E+00   .00000E+00   .00000E+00   .00000E+00 /
CC====== Fuel Consumption ==============================================/
CC   Thrust Specific Fuel Consumption Coefficients                      /
CD     .25958E+00   .20360E+03                                         /
CC   Descent Fuel Flow Coefficients                                     /
CD     .10999E+02   .89358E+05                                         /
CC   Cruise Corr.     unused       unused       unused       unused     /
CD     .10000E+01   .00000E+00   .00000E+00   .00000E+00   .00000E+00 /
CC====== Ground ========================================================/
CC         TOL          LDL         span         length       unused     /
CD     .22325E+04   .21201E+04   .51650E+02   .47700E+02   .00000E+00 /
CC======================================================================/
FI                                                                      /
```

A.2.4. P-420/T OPF file

```
CCCCCCCCCCCCCCCCCCCCCCCCCCCCCCC P42T__.OPF CCCCCCCCCCCCCCCCCCCCCCCCCCCCC/
CC                                                                      /
CC               AIRCRAFT PERFORMANCE OPERATIONAL FILE                  /
CC                                                                      /
CC                                                                      /
CC      File_name: P42T__.OPF                                           /
CC                                                                      /
CC      Creation_date: Apr 08 2015 16:36:51                             /
CC                                                                      /
CC      Modification_date: Apr 08 2015 16:36:51                         /
CC                                                                      /
CC                                                                      /
CC====== Actype ========================================================/
CD   P42T__          2 engines    Jet                          H         /
CC  P-4202TF    with GEnx-1B74                  wake         /
CC                                                                      /
CC====== Mass (t) ======================================================/
CC    reference      minimum      maximum     max payload  mass grad  /
CD     .15683E+03   .88096E+02   .16183E+03   .52000E+02   .00000E+00 /
CC====== Flight envelope ===============================================/
CC     VMO(KCAS)       MMO         Max.Alt       Hmax        temp grad  /
CD     .24139E+03   .90000E+00   .32000E+05   .32000E+05   .00000E+00 /
CC====== Aerodynamics ==================================================/
CC Wing Area and Buffet coefficients (SIM)                              /
CCndrst Surf(m2)     Clbo(M=0)       k          CM16                    /
CD 5   .25000E+03   .00000E+00   .00000E+00   .00000E+00                /
CC   Configuration characteristics                                      /
CC n Phase  Name    Vstall(KCAS)    CD0          CD2         unused     /
CD 1 CR   Clean     .16015E+03   .20260E-01   .37287E-01   .00000E+00 /
CD 2 IC   FL50p     .14573E+03   .92775E-01   .43273E-01   .00000E+00 /
CD 3 TO   FL50p     .14573E+03   .92775E-01   .25069E-01   .00000E+00 /
CD 4 AP   FL100p    .11302E+03   .20260E-01   .37287E-01   .00000E+00 /
CD 5 LD   FL100p    .11302E+03   .16531E+00   .26934E-01   .00000E+00 /
CC   Spoiler                                                            /
CD 1      RET                                                           /
CD 2      EXT                                .00000E+00   .00000E+00 /
CC   Gear                                                               /
CD 1      UP                                                            /
CD 2      DOWN                  .27283E-01   .00000E+00   .00000E+00 /
CC   Brakes                                                             /
CD 1      OFF                                                           /
CD 2      ON                                 .00000E+00   .00000E+00 /
CC====== Engine Thrust =================================================/
CC         Max climb thrust coefficients (SIM)                          /
CD     .50266E+06   .29724E+05   .38128E-09   .00000E+00   .00000E-00 /
CC     Desc(low)    Desc(high)   Desc level   Desc(app)     Desc(ld)  /
CD     .37681E-01   .26010E-01   .22500E+05   .35623E-01   .37669E+00 /
CC     Desc CAS     Desc Mach     unused       unused       unused    /
CD     .15000E+03   .65000E+00   .00000E+00   .00000E+00   .00000E+00 /
CC====== Fuel Consumption ==============================================/
CC   Thrust Specific Fuel Consumption Coefficients                      /
CD     .28692E+00   .20360E+03                                         /
CC   Descent Fuel Flow Coefficients                                     /
CD     .11266E+02   .84633E+05                                         /
CC   Cruise Corr.    unused       unused       unused       unused    /
CD     .10000E+01   .00000E+00   .00000E+00   .00000E+00   .00000E+00 /
CC====== Ground ========================================================/
CC         TOL          LDL         span         length       unused    /
CD     .15786E+04   .22042E+04   .51650E+02   .47700E+02   .00000E+00 /
CC=====================================================================/
FI                                                                      /
```

A.3. FCECT

A.3.1. FCECT output spreadsheet parameters

Parameter	Unit
Aircraft Type	
Aircraft Type (BADA)	
Engine Type	
Maximum Seats	
Flight Mission Distance	km
PAX to transport	
Cargo to transport	t
Number of flights	
Payload Factor Seats	%
PAX	
Payload Factor Cargo	%
Cargo	t
Payloadfactor total	%
Initial Cruise Altitude	ft
Taxi-out Time	min
Taxi-in Time	min
Step Climb	on/off
Maximum Take-off Weight	kg
Maximum Payload of Aircraft	kg
Operating Mass Empty	kg
Initial Mission Mass	kg
Final Mission Mass	kg
Zero Fuel Mass	kg
Payload	kg
Fuel Consumption Mass Mission	kg
Fuel Consumption Mass Taxi-out	kg
Fuel Consumption Accel. Runway	kg
Fuel Consumption Mass Climb	kg
Fuel Consumption Mass Cruise	kg
Fuel Consumption Mass Descent	kg
Fuel Consumption Mass Taxi-in	kg
Fuel Mass Reserves	kg
Fuel Mass Contingency	kg
Fuel Mass Alternate	kg
Fuel Mass Final Reserve	kg
Fuel Mass Extra Fuel	kg
Fuel Mass Total	kg
Fuel Consumption Mass Mission - all Flights	kg
Fuel per Payload	l/t/km
Fuel per PAX	l/PAX/100 km
Number of Step Climb performed	
Flight Distance	kg
Flight Time	s
Error Message	

Table A.1.: FCECT output spreadsheet parameters. Source: Ittel (2014), Engelke (2015)

A.3.2. FCECT output file parameters

Parameter	Unit
Aircraft Type	
Engine Type	
Payloadfactor	%
Flight Mission Distance	km
Initial Cruise Altitude	ft
Taxi-out Time	min
Taxi-in Time	min
Engine Type	Turboprop / Jet
Maximum Take-off Weight	kg
Maximum Payload of Aircraft	kg
Operating Mass Empty	kg
Initial Mission Mass	kg
Final Mission Mass	kg
Zero Fuel Mass	kg
Payload	kg
Fuel Consumption Mass Mission	kg
Fuel Consumption Mass Taxi-out	kg
Fuel Consumption Accel. Runway	kg
Fuel Consumption Mass Climb	kg
Fuel Consumption Mass Cruise	kg
Fuel Consumption Mass Descent	kg
Fuel Consumption Mass Taxi-in	kg
Fuel Mass Reserves	kg
Fuel Mass Contingency	kg
Fuel Mass Alternate	kg
Fuel Mass Final Reserve	kg
Fuel Mass Extra Fuel	kg
Fuel Mass Total	kg
CO2 Emissions total	kg
H2O Emissions total	kg
CO Emissions total	g
HC Emissions total	g
NOx Emissions total	g
LTO Soot Emissions	g
Flight Distance	kg
Flight Time	s
Leg No.	
Time (for each leg)	min
H_p (for each leg)	ft
Dist (for each leg)	km
v_tas (for each leg)	kts
v_cas (for each leg)	kts
M (for each leg)	
ROCD (for each leg)	ft/min
Thrust (for each leg)	kN
FCM (for each leg)	kg
Fuel Flow (for each leg)	kg/s

Table A.2.: FCECT output file parameters. Source: Ittel (2014), Engelke (2015)

A.4. ADEBO

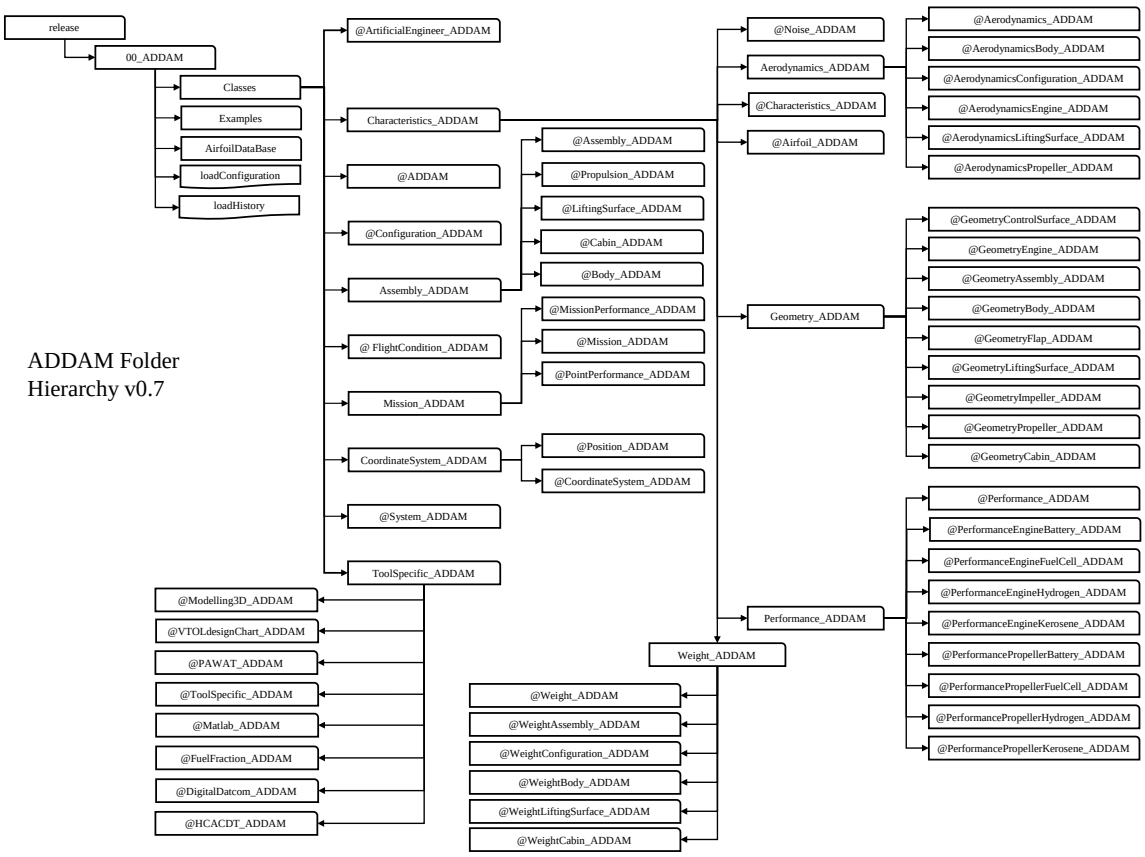

Figure A.1.: ADDAM Folder Hierarchy. Source: Herbst (2015b)

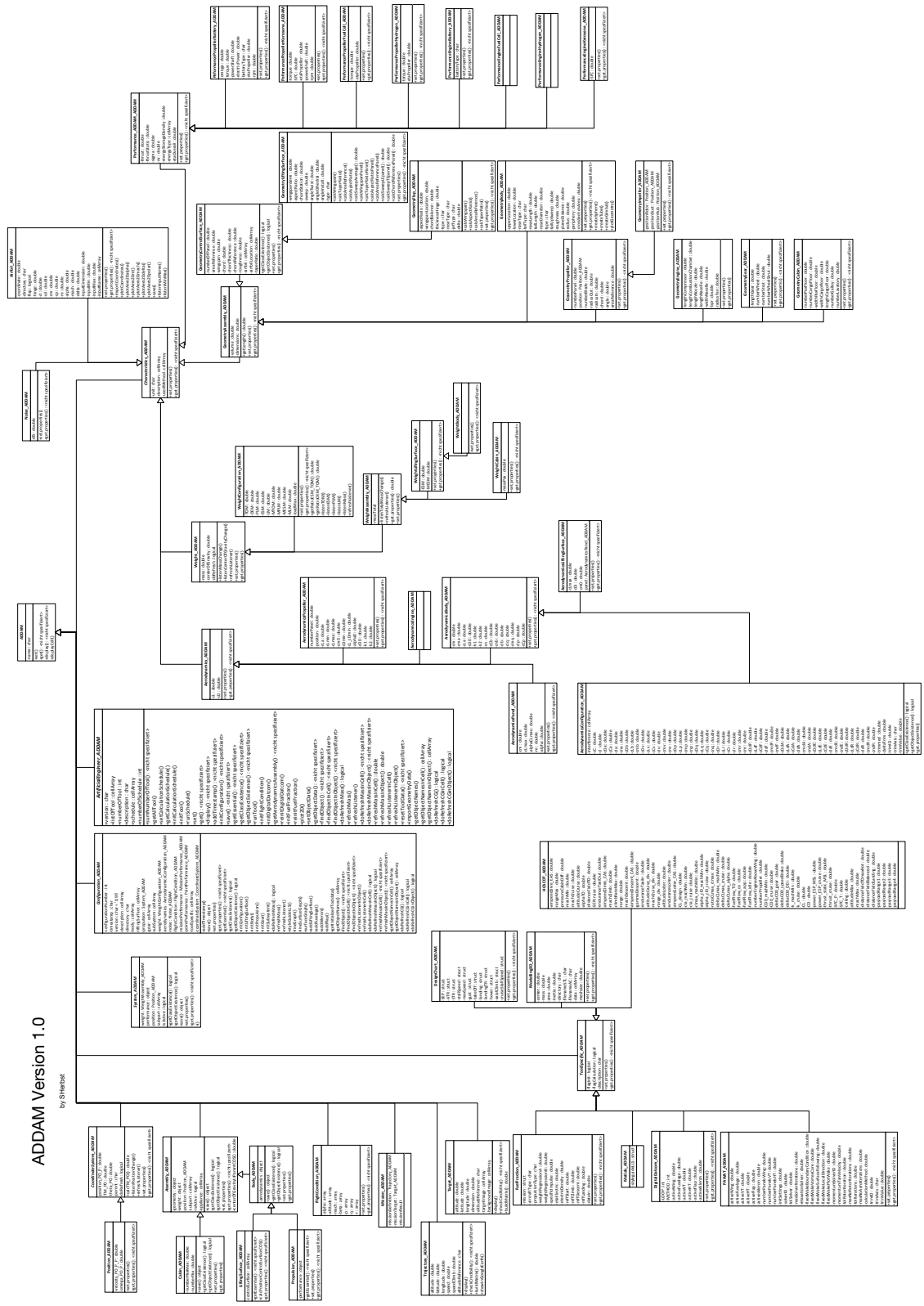

Figure A.2.: ADDAM UML. Source: Herbst (2015a)

Eidesstattliche Versicherung

“Ich versichere, dass ich diese Masterarbeit selbstständig und nur unter Verwendung der angegebenen Hilfsmittel angefertigt und die den benutzten Quellen wörtlich oder inhaltlich entnommenen Stellen als solche kenntlich gemacht habe. Die Arbeit hat in gleicher oder ähnlicher Form noch keiner anderen Prüfungsbehörde vorgelegen.”

Ort und Datum

Unterschrift